CIRCULATION OF COPPER AND COPPER ALLOYS IN HINTERLAND SOURTHERN AFRICA: MATERIAL EVIDENCE FROM GREAT ZIMBABWE (1000-1700CE)

By Bedone Mugabe

Thesis Submitted in partial fulfilment of the requirements for the Degree of Master of Philosophy in the Department of Archaeology

University of Cape Town

Supervisor: Professor Shadreck Chirikure

Co-supervisor: Dr Petrus Le Roux

February 2022

Abstract

This dissertation seeks to establish the possible provenance of copper and copper alloys used at Great Zimbabwe (1000-1700CE) to infer local and regional circulation circuits. It employs archaeological, archival, and geochemical methods to characterize samples of 26 wound wire bracelets, bangles, anklets, necklaces, and other forms of expressive and decorative wear excavated from the southern terrace, (Hill Complex) at Great Zimbabwe. The samples were macroscopically, microscopically, chemically and isotopically characterized to understand the technique of manufacture, chemical composition, lead isotopic ratios and the starting composition of uranium and thorium in relation the model ages. The Pb isotopic data calculated $^{238}U/^{204}Pb$ (μ), $^{232}Th/^{238}U$(κ) ratios and estimated model ages (*T*) were compared with published lead isotopic ratios from various ore samples from central and southern Africa. Within opportunities afforded by the historical record and limitations imposed by small sample sizes especially of the comparative geology, indications are that the studied objects were produced using ores matching the Cu-Ni mineralization at Empress Mine (in Zimbabwe), Cu Ag and Cu Pb Zn Ag mineralization associated with the Kundelungu Plateau (bordering Zambia and Democratic Republic of Congo). This suggests that Great Zimbabwe participated directly and indirectly in the vibrant micro, regional and interregional circulation of copper and other resources. Future work, must however, add more trace element data from the objects and increase the number of samples from ancient mines and other sites to develop a fuller picture of the movement of copper in Iron Age southern Africa through space and time. .

Keywords: copper-alloys, trade and exchange, circulation, geological- mineralization, lead isotope analysis provenance,

Declaration

I Bedone Mugabe hereby declare that the work presented in this dissertation is my own original work and has not been submitted before to any institution. Any information derived from the literature has been acknowledged intext and in the reference list.

Name Surname: Bedone Mugabe

Date: 2022/02/13

Signature: Signed by candidate

Acknowledgements

First and foremost, I would like to thank God almighty for his blessings during this research. I would also want to thank my supervisors Professor Shadreck Chirikure and Dr Petrus Le Roux for their unshaken support, advice and guidance throughout this research. To Professor Shadreck Chirikure, I would like to express my utmost gratitude for making this happen. I am where I am today because you had faith in me and provided the much-needed financial support during my time at the University of Cape Town. I am humbled by your big heart, humbleness, and willingness to attend to my frequent requests be it on Zoom or WhatsApp. Despite your busy schedule and different time zones, you were one call or message away which made my life easy. To Dr Petrus Le Roux, I am exceptionally grateful for the guidance, love, support and encouragement. Your door was always open for me and I will always cherish the stimulating intellectual discussions we had about isotopic geochemistry from day one up to date. I am also indebted to Dr Vincent Hare whose moral support and intellectual input shaped this research. You were my unofficial supervisor and provided the necessary guidance and tools to explore the *Mu-kappa-T* system.

I am also grateful to Professors Ari Sitas and Shadreck Chirikure for facilitating additional funding through the Re-Centering Afro-Asia:Musical and Human Migrations in the Pre-Colonial Period 700-1500 AD post-graduate funding which sustained me between 2020-2021. To Rhoda Issacs and the rest of the Afro Asia research cohort, I am thankful for the numerous academic engagements during our conferences that helped shape this research.

I would also want to thank Dr Robert Nyamushosho for the unwavering support and guidance left, right and centre. Thank you so much for being a mentor, friend, and brother “mukoma”. Drs Mukwende (mukoma), Mtetwa (father), Thondhlana (Mhondoro), Msindo, Sagiya and Machiridza thank you so much for teaching me the basics of archaeology and continued support. Within the National Museums and Monuments of Zimbabwe, I am forever grateful to Mr Chipunza, Mr Mandima and the Southern Region Conservation Department for their support during my post graduate attachee period and my field work.

At UCT, I am indebted to Ms Miranda Waldron for teaching me the basics of SEM, Ms Rene Van De Merwe for the technical support with metallography and Mrs Fayrooza Rawoot for assisting with sample preparation for MC ICP MS. Within the department of archaeology, I would like to thank Associate Professor D. Stynder (HOD Archaeology), Emeritus Associate Professor Simon Hall (Former HOD), Professor Judith Sealy, Dr Julie Luyt, Mrs L. Cable, Mrs

L. Hutten and numerous colleagues for creating a conducive learning environment. Fellow post graduate students Humfrey, Precious, Patricia, Joseph, Malefeu and Hope thank you for the moral and academic support.

Last but not least, to my family and friends, thank you so much for the patience, love and support. To my father 'Gono' thank you so much for being a pillar of strength and introducing me to the world of archaeology, metallurgy and stone-masonry. My siblings Bryn, Nish and Polite (Dzidzai) thank you so much for being a source of inspiration. Dr N. Mnukwana I salute you. To my best friend Kudzai Muchemwa, thank you so much for being a pillar of strength, source of joy and above all for coping in my absence especially when mum passed on. I am forever grateful and indebted to you. Mukoma Mtikani, Khule Harvey,Tatenda, Providence, Kudzwaishe, Thulisile, Zee, Duduzile and Melz thanks so much guys for the support. However, despite the contributions of so many individuals and organisations all errors are solely mine.

Dedication

To my beloved mum who never got a chance to see what her son grew up to be.

Table of Contents

Contents

List of Figures

List of Tables

CHAPTER 1

INTRODUCTION AND LITERATURE REVIEW

1.1 Introduction

The development of metallurgy has been put forward as a trigger that kickstarted and sustained societies in southern and central Africa from the early first millennium CE to the 1900s (Herbert 1984, 2002; Child and Killick 1993; Child and Herbert 2005; Chirikure and Rehren 2006; Chirikure 2007; Chirikure *et al.,* 2013; Chirikure 2015; Thondhlana 2012). This study is alert to the distortion brought about by the drawing of colonial borders at the Berlin Conference of 1884-5. Prior to that the modern-day countries of Zimbabwe, Zambia and among others South Africa did not exist. Rather, the political geography was different with people moving across the landscape, sharing ideas, resources and building communities (Chirikure 2020). My research situates Great Zimbabwe within this wider landscape, unfettered by the coloniality imposed by borders drawn in Berlin. Figure 1 below shows Africa and some of the prominent ancient civilisations (including Great Zimbabwe) before the development of colonial boundaries.

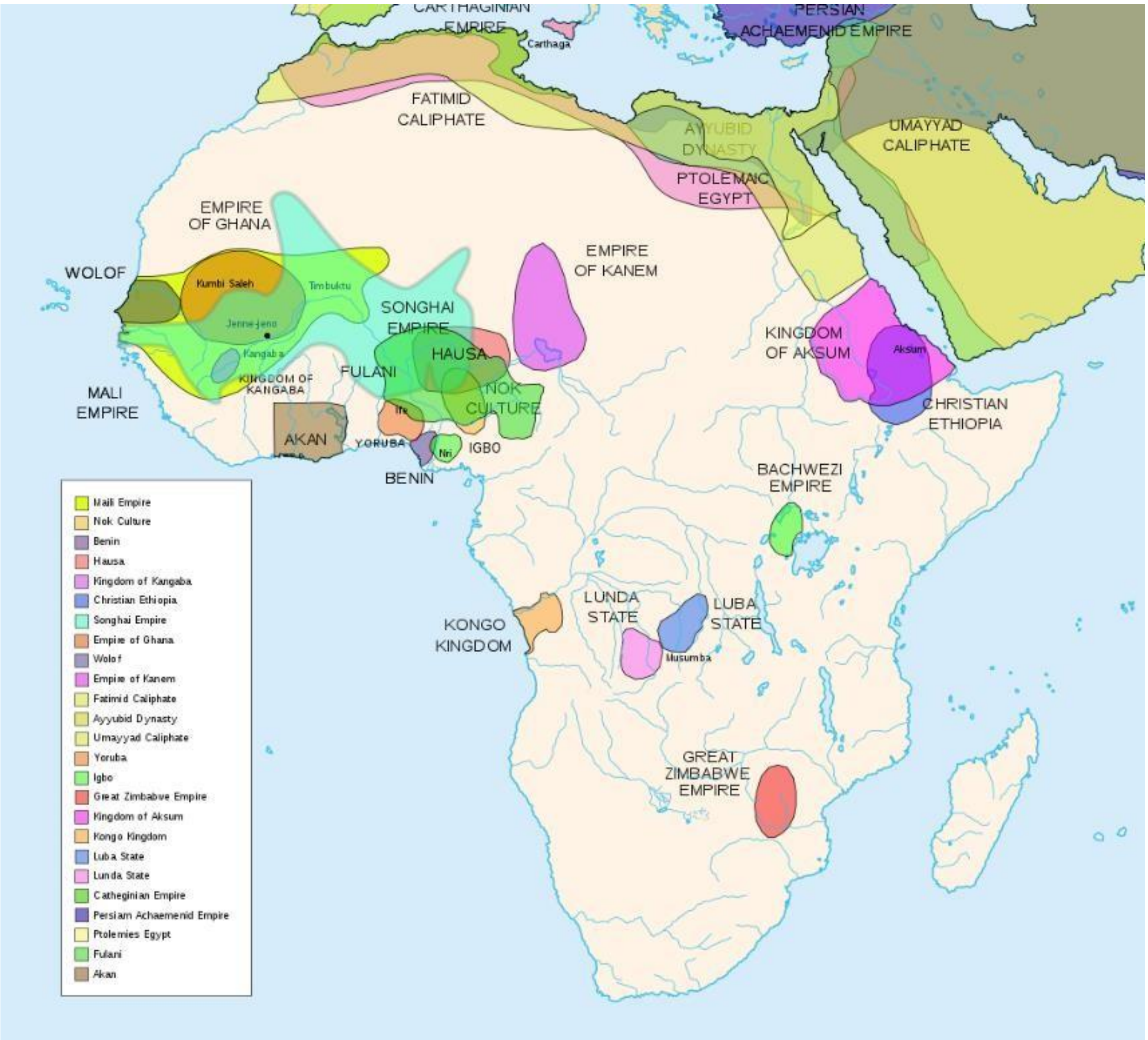

Fig1: Precolonial Map of Africa showing the location of Great Zimbabwe and other ancient civilisations (adopted from Africa before Europe: https://www.chenarch.com/images/arc3313/slides-18/01-03-00-african-empires-anno.jpg)

The history of metallurgy in southern and central Africa began with the working of iron and copper in the early first millennium CE (Miller 2002; Thondhlana 2012 ; Bandama *et al.*, 2015). The copper alloys bronze (Cu and Sn) and brass (Cu and Zn) as well as gold were only worked when southern Africa was incorporated into the Indian Ocean based trade and exchange system (Killick 2009; Moffett and Chirikure 2016). While iron was mostly utilitarian, nonferrous metals and alloys were used for decorative purposes where their physical and aesthetic properties intersected with general ideas about beauty and spirituality (Herbert 1984; Chirikure 2014).

Available evidence suggests that from the early first millennium CE, traces of iron and copper production started to accumulate on the landscape in southern and central Africa. This left distinctive marks in the form of ancient mines in regions such as Phalaborwa and Musina in South Africa (Thondhlana 2012; Moffett 2017), Copper Queen and Hurungwe in Zimbabwe (Swan 2002, 2007), and among others the Copperbelt area of Zambia (Bisson 1974, 2000). Indeed, Summers (1969) developed a comprehensive inventory of ancient copper mines distributed in the Zambezia region of southern Africa. In addition to evidence of mining, there exist a large number of smelting sites where oxide and carbonate ores of copper were reduced to metal and refined in crucibles to produce a wide variety of objects (Thondhlana 2012). Often, copper was hammered into sheets or drawn into wire which was used to manufacture ornamental objects (Miller 1996, 2002). Primary and secondary copper smelting took place near mines such as Copper Queen in Zimbabwe (Swan 2002:74), Dukwe in Botswana, (van Warden 2014), Kafue River campsite near Kansanshi in Zambia (Bisson 1975:258) and other places. Within variation, copper was also worked inside settlements at Phalaborwa, Marathodi, Great Zimbabwe, Khami, Chumnungwa, Mapela and other places (Hall *et al.*, 2006; Anderson 2009; Thondhlana 2012; Moffett 2017; Nyamushosho 2020).

The differential existence in nature of sources of rich copper mineralisation promoted trade and exchange that sustained local, regional, and interregional networks (Herbert 1984; Bisson 2000; Miller 2002; Pikirayi 2006; Thondhlana and Martinon-Torres 2009; Bandama *et al.,* 2018). However, towards the end of the first millennium CE hierarchically organised polities started to emerge in southern Africa (Phillipson 2005). One such polity emerged at Great Zimbabwe flourishing into what is now one of the most famous medieval civilisations in the world (Chirikure 2020). Although the history of archaeological research in Great Zimbabwe started in a context of plunder and illicit export of objects by some antiquarians and even archaeologists as recently as the 1970s, some progress was made towards understanding copper-based metallurgy in this group of settlements.

Apart from abundant copper and bronze objects such as those studied by Stanley (1929) and Miller (2002), ingot moulds and crucibles were also recovered in different areas together with kit for wire drawing and copper working (Bandama *et al.*, 2017). Rescue excavations performed on Mtuzu Hill on the southern edge of Great Zimbabwe recovered a collection of different types of tongs, wire draw plates and pieces of copper metal (Mukwende pers comm 2021). The recovery of tin ingots geochemically provenanced to Rooiberg about 500 kilometers to the south in current day South Africa suggested that metal was moving distances into and perhaps out of

Great Zimbabwe (Grant 1999; Huffman 2007; Molofsky *et al.*, 2014). Similarly, the presence of copper ingots stylistically similar to those produced in Central Africa (Swan 2007) and iron gongs from the same part of the world (Chirikure 2015, 2019) suggest connections between Great Zimbabwe and other areas in the region. New research insights on the political economy of Great Zimbabwe is showing that metal (both ferrous and non-ferrous) production and exchange was decentralized without elite monopoly and formalized distribution centres (Bandama *et al.*, 2016; Mtetwa 2017; Chirikure 2019).

Given these wide networks, the presence of ubiquitous amounts of copper mines recorded by Summers (1969) and copper recovered from different excavations at Great Zimbabwe, the source of copper used at the site and how it was distributed become issues of strong academic interest. This work seeks to contribute to a growing body of literature (e.g Grant 1999; Molofsky *et al.* 2014; Rademakers *et al*. 2019; Stephens *et al.* 2020) aimed at understanding metal circulation in southern and central Africa using combined archaeological and geochemical techniques. It achieves this by characterizing copper and copper-based objects associated with homesteads on the Southern Terraces of the Hill Complex at Great Zimbabwe occupied between 1000-1450 CE (Chirikure 2020). Communities based at Great Zimbabwe and elsewhere exchanged commodities such as copper making it imperative that we apply state of the art archaeological science techniques to explore the circuits of trade and exchange. This directs us to some of the tools used by archaeological scientists to identify movement of ores and metal from geological sources and producer communities to consumers in the past.

1.2. Background to the study - theoretical approaches to metal provenance studies

According to Pollard and Heron (1996), the application of analytical chemistry to identify the source of objects found in the archaeological record can be traced back to the 1840s. However, advances in instrumentation and analytical techniques have made it possible for systematic studies of the source of ores used to make metal objects in the archaeology (Gale and Stos-Gale 1982, 2009; Pernicka 1993, 2014). Provenance studies of copper and copper alloys are premised on the principle that some characteristics of the source raw materials in the form of trace elements or isotopic ratios are present in finished artefacts and can be used to differentiate distinct sources geographically and geologically (Wilson and Pollard 2001). Advances in geochemistry and geostatistics made it possible to apply the technique of lead isotope analysis (LIA) to provenance non-ferrous metallurgical objects in archaeology with contextually mediated degrees of success

(Brill and Wampler 1965; Stacey and Kramer 1975; Gale and Stos-Gale 1982, 2009; Albarede *et al.,* 2012; Baron *et al*. 2014; Artiolii *et al.,* 2020). Lead isotope analysis exploits the differences in the genetic history of stable isotopes of lead ^{204}Pb, ^{206}Pb, ^{207}Pb and ^{208}Pb (Dickins 1995; Faure and Mensing 2009). Three of the four isotopes ^{206}Pb, ^{207}Pb and ^{208}Pb are products of the radioactive decay of uranium and thorium with predictable half-lifes (Doe and Stacey 1974, Dickin 1995, Baron *et al.,* 2014; Faure and Mensing 2005). This makes them time-dependent. By comparison, ^{204}Pb isotope is time-independent (stable), with its abundance being constant since the earth's formation (Albarede *et al.* 2012). The abundance of four Pb isotopes is approximately 52.4%, 22.1%, 24.1% and 1.4% for ^{208}Pb, ^{207}Pb, ^{206}Pb and ^{204}Pb sequentially.

Geochemists have demonstrated that Pb isotopic composition will change over time, with variations across the earth's crust being influenced by various factors namely geological age, style of mineralization and ore type (see Dickin 1995; Baron *et al*., 2014; Pernicka 2014:247, Longman *et al.,* 2018). Such Pb evolution is generally governed by phenomena which geochemists have labelled the single stage and two stage evolution conditions (Doe and Stacey 1974, Stacey and Kramer 1975). In the single stage evolution model, the daughter/parent rock or deposit undergoes normal radioactive decay (no abnormal uranium (U)/ thorium (Th) levels influence) and usually contain Pb ratios within the following range: ^{206}Pb/^{204}Pb=18,5, ^{207}Pb/^{204}Pb=13,3, ^{208}Pb/^{204}Pb= 38,3. (Liu *et al.,* 2014, Doe and Stacey 1974:759). Therefore, mineral resources containing Pb ratios that resulted from single stage evolution are referred to as having 'common lead ratios.' However, ores that went through a two-stage evolution were altered after the formation of the earth and enriched by excess amounts of Th and U, which results in their ^{206}Pb, ^{207}Pb and ^{208}Pb ratios being highly radiogenic or anomalous (see Doe and Stacey 1974, Stacey and Kramer 1975). Notably, the gradual evolution of Pb ratios in deposits due to the decay of U and Th is only limited to the ore formation period, since all deposits will be containing very little or no U/Th to facilitate Pb growth (see Longamn *et al.,* 2018). Thus, Pb ratios in the earth's crust anytime remains equivalent to the amount produced during ore formation or mineralization (Dickins 1995; Faure and Mensing 2009; Albarede *et al.,* 2012). Pb isotopes do not fractionate during smelting ensuring that Pb isotopic ratios from metalliferous ores are passed onto finished metallic artefacts (Stos-Gale and Gale 2009; Pernicka 2014), providing a powerful tool for metal artefacts provenance analysis in archaeology (Albarede et *al.,* 2012; Baron *et al.,* 2014; Pollard *et al.,* 2018; Balliana *et al.,* 2014: 2974, Stephens *et al.,* 2020).

The pioneering approach for provenance analysis using lead isotopes was spurred from Europe resulting in the establishment of research groups in Germany (Heidelberg and Mainz) and the United Kingdom (University of Oxford). The application of lead isotope analysis contributed towards provenancing silver, copper and bronze objects in the Mediterranean and resulted in the production of huge databases offering contrasting opportunities and constraints (see Stos-Gale and Gale 2009). However, the application of lead isotopes in archaeology raised significant points of controversy regarding some of the factors complicating the utility of the technique. Some of the hotly debated issues included the effects of human activities on Pb isotopic ratios in metals, (Budd et al 1995, Mc Gill *et al*., 1999), display and interpretation of Pb data (Budd *et al.,* 1995, Gale 1997) and magnitude to which sources should be assigned based on bivariate plots (See detailed review by Pollard 2009). Additional factors include the small geological samples, poor understanding of the economic geology and mineralisation of ore deposits worked in ancient times and the mixing and recycling of metals from different sources (see Pollard 2009: Pollard *et al.,* 2018). These factors required acknowledgement when provenancing metal objects in archaeology using lead isotope analysis. Some of this criticism resulted in more consideration being given to geological parameters resulting in the identification of sources of copper in Cyprus and other regions (Stos-Gale and Gale 2009; Albarede *et al.,* 2012; Baron *et al.,* 2014). Also, it was acknowledged that lead isotope analysis must be supplemented with trace element analyses to build a robust approach (Pernicka 1993; 2014). That lead isotope analysis has come of age is shown by the fact that the technique is now being widely applied in different parts of the world with differing rates of success (see Killick *et al.,* 2020 for a detailed review).

As lead isotopes became more widely applied to address archaeological questions, one significant caveat was the unqualified assumption that the circulation of metals in ancient societies followed a simplified linear trajectory from source, use and discard (Pollard *et al.,* 2018:45). However, such linearity which is preferentially geologically tailored ignores the complex nature associated with the dynamic circulation of copper and fundamental human interactions shaping the production, consumption, and distribution of objects. Therefore, Bray *et al.,* (2015: 204) caution researchers not to fall into the trap of assuming a linear hereditary trajectory from geological source to the artefact because the trajectory of copper in circulation is not only dependent on place, time and social context alone but its mutability and resistance to corrosion, which lends it a long and complex life cycle through time. Human behaviour-driven methodological and theoretical trends in provenance studies now favour the complex biographies or multiple approaches which assume that the isotopic and chemical composition of objects do not simply reveal the birthplace of copper objects but offer a window into their life histories (Pollard and Bray 2015; Bray *et al.*,2015; Pollard *et al.*,2018; Rawson and Pollard 2018). This enables researchers to pinpoint the parent metalliferous deposit, model the flow of metals and identify the mixing or recycling of copper, therefore, providing insight into the technological innovations and cultural choices and constraints that were experienced by past societies as well as the circulation of objects through space and time.

A special issue of the journal *Archaeometry* published in 2020 reviewed the application of lead isotopes in the discipline of archaeology. Dominated by writers with earth science backgrounds of varying forms, the conclusion reached in most of the papers was that lead isotopes was first and foremost a geological issue. Consequently, an understanding of the geology was paramount to identifying sources of copper, tin, silver and other non-ferrous metals used in the past (see for example Killick *et al.*, 2020; Artioli *et al.*, 2020 and other papers in the Archaeometry 2020 Special Issue). While the significance of geology cannot be doubted, favouring a geological perspective over others is neither helpful nor desirable. For example, it cannot be denied that human behaviour was responsible for mining the ores, smelting, mixing metals and distributing them. Consequently, championing a single parameter over others may not be as robust as required. This produces different patterns of circulation that are beyond the capability of linear approaches that claim to privilege geology. By necessity, it is vital to combine different parameters, approaches and perspectives to think about the dynamics of metal circulation in the world in more nuanced ways (Sainsbury *et al.*, 2021).

One region that has benefited from the windfall of developments associated with lead isotope analysis in archaeology is Africa (Rademakers *et al.*, 2019; Killick *et al*., 2020). The historical linkages between southern and central Africa and the presence of objects such as iron gongs, and copper ingots prompted some researchers to apply lead isotopes to identify possible sources of metal. Stephens *et al.*, (2020) suggested that the copper used to make objects from Nqoma and Divuyu in Botswana matched the trace element and isotopic signatures of the Copper Belt region in Central Africa. Rademakers *et al.*, (2019) studied the circulation of copper in central Africa and used the presence of stylistically shaped ingots (Katanga crosses) to support the movement of copper into southern Africa. Earlier studies such as Molofsky *et al.,* (2014) applied lead isotopes to confirm Grant (1999)'s suggestion that the tin ingots excavated by Huffman from Great Zimbabwe were sourced from Rooiberg. It can be concluded that the provenance studies of metals in southern and central Africa have been limited to the study of tin and copper within a simplistic linear model aimed at pinpointing the geological source used to make artefacts (Grant 1999; Molofosky 2009; Molofosky *et al.*, 2014; Rademakers *et al.*, 2019; Stephens *et al.*, 2020). This has been achieved at the expense of the layers of human behavioural and environmental realities behind the chemical and isotopic composition of the samples studied. The provenance results, however, despite revealing the possible birthplace of some of the objects, remain devoid of the ideology and social context of the objects, which influenced the type of ore exploited, metal and alloy manufactured, kept and exchanged locally, regionally and internationally.

Based on these early studies, what new information do we get if we apply lead isotope and chemical analyses, in conjunction with historical sources to study copper circulation in Great Zimbabwe? This provides the motivation for this research.

1.3. Aims of the Study

The main objective of this research is to evaluate the viability of provenancing copper and copper alloy objects sampled from materials excavated from the Southern Terraces of the Hill Complex at Great Zimbabwe in 2018. The following sub-aims apply:

- What were the fabrication and alloying techniques employed by metallurgists at Great Zimbabwe and are there any variations through space and time?
- What was the source of copper used to fabricate objects excavated from the Southern Terraces at Great Zimbabwe?
- What are the dynamics of copper and copper alloys circulation in and around Great Zimbabwe?

These research questions will be pursued using an integrated approach which combines optical, chemical and isotopic analyses with historical information. This will pay attention to geological, geochemical, and historical and sociological parameters.

1.4. **Literature Review: Review of Provenance Studies in southern Africa**

Archaeometallurgy is an interdisciplinary method of studying past remains of metal production and use (Killick 2012; Chirikure 2015). In southern Africa, the study of indigenous metallurgy developed through different research pulses (Miller 2002; Thondhlana 2012; Thondhlana *et al.*, 2016). The earliest work was focused on reconstructing iron-smelting technologies using waste materials from production and embedded anthropological factors (Childs 1991; Ndoro 1991; 1994; Collett 1993; Chirikure 2013; 2015; Mtetwa 2011; 2017). Other archaeometallurgical interests focused on ancient mining (Summers 1969; Swan 1994; Swan 2002,2007; Chirikure 2010). Research interests in copper metallurgy also followed (see Swan 2003; Thondhlana 2007, Thondhlana and Martinon-Torres 2009; Bandama *et al.,* 2016, 2017, 2018). These studies applied routine metallography to try and understand the chemical composition of copper-based artefacts and fabrication techniques employed by ancient metallurgists of copper and copper alloys at various sites across southern Africa.

Most studies of copper metallurgy in southern African archaeology were aimed at understanding technologies behind copper extraction, alloying and fabrication, as well as the value of copper and its alloys within the socio-economic and political spheres of Iron Age societies (Herbert 1984; Herbert 1996; Swan 2007). This gave rise to metallographic studies of copper and copper alloys from the legacy collections in various institutions across southern Africa (see Childs 1993; Miller 1996, 2002; Thondhlana 2007; Thondhlana and Martinon-Torres 2009). Such studies provided essential information about the nature of fabrication technology associated with copper and its alloys in the Iron Age period of southern Africa with Great Zimbabwe included. However, most of the samples analysed lacked accurate contextual information from the sites they were excavated. Some of the results produced were highly technical and lacked cultural context as they were simply descriptions of the fabrication technology reinforced with the chemical composition of samples under study. Routine metallographic studies seem to be the trend in archaeometallurgical research in southern Africa. Chirikure (2010; 2014) cautions researchers against the prioritization of sophisticated geochemical techniques at the expense of context (both cultural and location). Privileging technological parameters promotes the reconstruction of a partially reconstructed past where technology is seen as a monolithic force divorced from human behaviour and society.

The quest for provenance analysis in southern African archaeology can be traced back to earlier studies in archaeology and metallurgy that tried to understand the source and flow of goods to elite centres within southern Africa and abroad (Huffman 1974; Swan 2002; Killick 2009). In traditional archaeological research, the assumption was that the political economy of elite centres such as Great Zimbabwe thrived on their ability to control the exploitation and exchange of mineral resources such as gold, iron, copper and tin within their territories and beyond. However, this may have not been always the case, since the political power of some elite cultural centres such as Great Zimbabwe was not always materialised in distant rich mineral resource areas such as Phalaborwa and Rooiberg in northern South Africa where metals such as copper and tin are thought to have been extracted (Thondhlana 2012; Bandama *et al.,* 2015; Moffet 2017). This realisation, therefore, validates Chirikure's (2007:117)'s opinion that managing access to resources in southern Africa was reliant on the interaction of multiple factors such as the socio-economic and the cultural.

New insights on the political economy of Great Zimbabwe show that it was based on ephemeral production and decentralized circulation involving a vibrant internal circulation and exchange routes, and not fixed redistribution centres (Bandama *et al.,* 2016; Chirikure 2019). This view seems to find support in the absence of any large-scale metal production evidence at the site of Great Zimbabwe. Most large-scale evidence appears to be in metal production landscapes and not in any centres of states (Chirikure 2018). All preliminary research surveys point towards household-based production dominated by copper and tin bronzes among other cuprous alloys (Bandama *et al.,* 2016, 2017). The surveys have at least provided comprehensive research coverage of the site, illuminating on cuprous metallurgy consumption and distribution of objects across Great Zimbabwe. This opens possibilities for asking bigger questions about copper and metal circulation in southern Africa and beyond using the example of samples from Great Zimbabwe. An appraisal of possible sources of copper and tin directs the spotlight to deposits that are located at varying distances in southern Africa. Some of these such as Bikita, Shamva, Concurpia, Kamativi, Umkondo, Mashava, Makati-Makaha and Kalunda pegmatites with documented evidence of tin exploitation within the vicinity of Great Zimbabwe as documented by Summers (1969).

Mike Grant employed the trace element analysis approach to analyse and provenance tin (*hereafter* Sn) ingots (lerale, musuku, bun and rod) from various archaeological sites and places across Southern Africa (Great Zimbabwe, Messina, Thabazimbi, Rooiberg etc) housed in museums, universities and private collections (Grant 1999). The sample trace elemental composition were compared with ores, slag and cassiterite from modern Rooiberg mine and based on similarities in the amounts of heavy elements (tantalum, arsenic and scandium) with Rooiberg most of the artefacts were attributed to have been sourced from Rooiberg which had unquestionable tin working in precolonial times (Grant 1999). However, the technique employed (Neutron Activation Analysis) can easily identify heavy elements with lighter elements such as bellium and lithium being undetectable and overlooked despite them being essential discriminators or indicators of certain ore deposits. Furthermore, ingot 2030 BD1 from Great Zimbabwe among Grant's samples contained tungsten but lacked arsenic to match it with Rooiberg cassiterite as its possible cradle, thus suggesting that Rooiberg was not the only source of tin at Great Zimbabwe. It is possible, therefore, that less studied casserite deposits in Zimbabwe such as Bikita, Kamativi and Corncupia might have been exploited by the inhabitants of Great Zimbabwe for tin. For instance, geochemical studies of casserite from Bikita shows that the deposit is a Sn-Ta rich pegmatite (Melcher *et al.*, 2015; Kinaird *et al*., 2016) hence due to its proximity and ample evidence of pre-European working there is a possibility that the tin (Sn) used in the manufacturing of the ingots might have been sourced from the pegmatite.

Furthermore, Lisa Molofosky and colleagues employed the Pb isochrone dating technique, which matched most tin ingots and tin bronzes artefacts from across southern African archaeological sites (including Great Zimbabwe)'s isotopic ratios to the isochrone model age of 2057 ± 3a Ma associated with the cassiterite deposits of Rooiberg in the Lebowa Granite Suite (Molofosky 2009; Molofosky *et al*., 2014). The research also showed that even after being mixed with copper to manufacture tin bronzes, tin and tin-bronzes could still be provenanced to its cassiterite ore. However, despite showing that Rooiberg was indeed one of the sources of tin for southern African societies before the 1900s, the provenance of four bronze artefacts (two from Great Zimbabwe and two from Thulamela) could not be established. The lead isotopic ratios of these four artefacts showed that they were not from the Lebowa Granite Suite. This calls for more research - trace elemental and lead isotopic ratios of artefacts from different candidate sources such as the Zaaiplaats, which are part of the Legbowa Granite Suite that showed distinctive evidence of independent ancient working (see Chirikure 2010).

Unlike tin, copper from ancient southern African sites have been linked with the Copper-belt region of Zambia and the Democratic Republic of Congo. X-shaped moulds retrieved at Great Zimbabwe were typologically analysed and linked to northern Zimbabwe, Ingombe Illede and Lumbumbashi's HIH stylized ingots (Swan 2007). It was established that the HIH croisettes from the Copper Belt dated from the ninth to the fourteenth century (Swan 2007; Killick 2017; Nikis and Livingstone 2017). However, it is puzzling that the HXR stylized ingots and moulds that followed from the fourteenth to the seventeenth century (Nikis and Livingstone 2017), are limited to Ingombe llede and northern Zimbabwe sites. Killick's (2017) suggestion that the absence of HXR stylized ingots and moulds at Great Zimbabwe is because their production period postdates Great Zimbabwe lacks merit. Killick overlooks new insights and evidence from

Great Zimbabwe that suggests that the site did not decline around the fourteenth century but flourished into the 16th and 17th centuries (Huffman 2007; Bandama *et al.,* 2016; Chirikure et al., 2018). A more plausible suggestion is that of changing sources of copper at different times during the flourishing of Great Zimbabwe. Also, just speculating that similar styled artefacts originated from one area in a unidirectional way without thinking of whether the distribution was direct or indirect creates conceptual barriers that hinder a decent understanding of copper circulation in southern and central Africa. Also, central Africa was not the only source of copper as Summers (1969) has shown. This motivates nuanced ways of using integrated techniques to think about copper circulation in our region and beyond.

Rademakers *et al.,* (2019) carried out trace elemental analysis and lead isotope analysis of X-shaped croisettes from Upemba burials and concluded that they were smelted from certain sources within the Copperbelt. However, the researchers did not characterize and isotopically analyse HIH croisettes from Great Zimbabwe but simply added them based on similarity to widen the geographical and typological scope of their research. Thus, it remains to be proven scientifically if Great Zimbabwe, just like the Upemba Depression inhabitants, sourced their copper from the Katanga Copperbelt, or they simply served as imported templates to manufacture moulds for casting copper from local deposits (Stephens *et al.,* 2020). Furthermore, since there is ample evidence of copper exploitation in various deposits across southern Africa (Summers 1969) there is a possibility that copper might have been sourced from the Zimbabwean or Kaapvaal Craton associated deposits and nearby orogenic deposits surrounding the major cratons-based sources.

New insights on provenance studies elsewhere in southern Africa also emphasise the role of the Copperbelt as the maiden source of copper during the Iron Age period. According to Stephens *et al.,* (2020), cobalt-nickel ratios and the radiogenic lead isotopic ratios of artefacts from Tsodilo (Divuyu and Ngoma sites) are compatible with the Katanga Copperbelt's Copper Cobalt mineralization at Musoshi and Dikulushi. However, two samples (D24 and 106) had low radiogenic ratios. They were assumed to have been sourced from one of the nearest deposits in northern South Africa (Limpopo Mobile Belt and Bushman Shear Zone) and Kundulengu Plateau. Their alternative suggestions dismissed other possible sources of copper like the Namaqualand deposits of South African and Central Namibian deposits based on distance and gruesome environmental conditions. Furthermore, deposits within the Zimbabwe craton were dismissed on the basis of being Precambrian derived, thus distinctive metalliferrous deposits within the country with documented evidence of ancient copper exploitation (Summers 1969), were assumed to be characterised by invariable high Pb ratios. This is despite evidence various techno-thermal events in distinctive deposits such as the Zambezi belt, Makati Makaha, Kamativi and Chiwore (Goscombr *et al.,* 2000, Moore *et al.,* 2009) which points towards post-cratonization, mineralization and low Pb ratios. Therefore, there is a higher probability thatsamples D24 and D104's copper ore could have been sourced from the aforementioned young deposits within the Zimbabwean craton, transported or exchanged until they eventually reached Tsodilo Hill settlements.

Moreover, copper deposits like the Boseto in Botswana are classified as sedimentary rocks that share the same geochemical similarities with Kupferschiefer deposits (in Poland and Germany) and the Central African Copperbelt in Zambia and the Democratic Republic of Congo (Hitzmann *et al.,* 2005; Hall 2013). Given their proximity to Tsodilo sites, evidence of ancient mining and geochemical similarities to the Copperbelt, there is a higher probability that the deposit might have been exploited by the Tsodilo inhabitants and circulated across southern Africa.

This brief literature review has shown that little has been done archaeologically in Southern Africa concerning the use of lead isotope analysis in the sourcing of copper and illuminating the various trade networks that existed between southern Africa and the coastal areas. There is an observable lack of appreciation in previous literature of the diversity of copper and tin mines within Precambrian southern Africa. The assumption in these earlier studies that copper was only mined in the copper-belt region and northern South Africa and that Rooiberg was the only unquestionable source of tin in precolonial southern Africa serve to highlight an incomplete geological knowledge of southern Africa. According to Killick *et al.,* (2020), southern Africa is a promising area for the provenance of copper, tin and bronze due to the large differences in ages of the deposits. Therefore, there is a need for research that explores the diversity and variability of copper and tin deposits within southern Africa that were exploited in a wide range of socio-economic and political contexts of the region's dynamic history.

1.5. Gap identification

Recent interest has developed around the identification of sources of copper and copper alloys circulated across southern Africa (Bisson 2000; Swan 2007; Killick 2017; Rademakers *et al.*

2019). Notwithstanding the above-mentioned studies, the lack of geoarchaeological and archaeomining studies of copper-rich geological deposits, cassiterite and ancient copper mines within southern Africa has imposed some limitations that constrain the utility of provenance studies in the region. While historical and archival sources suggest the existence of multiple ancient copper mines in southern Africa, the mineralogical, geochemical and formation history of some of the mines is not known. Killick *et al.* (2020) suggested that because ore deposits in southern and central Africa formed at different times spanning a large part of the geological history of the subcontinent, it is possible to separate metal smelted from old and young ore mineralisation. While attractive as a proposition, very little is known about the mineralisation of ancient mines where no lead isotopic values are known. Furthermore, geological histories often dictate that some deposits are comprised of primary and secondary mineralisation of different ages. The assumption that most of the copper deposits in parts of southern Africa such as the Zimbabwean craton are generally Precambrian age with the same lead isotopic ratios as the rest of Southern African sources, in the absence of definitive evidence based on assessment of ore mineralisation is a limitation. It is possible that the top sections mined by ancient peoples might be young while the older and deeper sections of the same mines exploited by modern mining might be older giving different estimated ages. Of course, trace elements are a powerful way of discriminating sources but as with Pb isotope signatures, the trace element geochemistry of large numbers of mines worked historically is unknown. This means that any indications of sources is only at best suggestive but is not conclusive. What is required is enlarging the number of observations based on different parts of the sub-continent to avoid generalised reconstructions of copper circulation across southern Africa. Historical models such as those by Mudenge (1988) and Beach (1974) suggests that communities exploited nearby and distant resources raising interesting possibilities for provenance studies to identify metal from different areas. Equally, it will be interesting to establish if some of the copper from south of the Zambezi ended up north of the Zambezi. The limited number of observations used to make inferences about provenance motivates for the evaluation of the applicability of studies aimed at exploring the sources of copper from networking hubs such as Great Zimbabwe which is the primary goal of this thesis.

1.6 Thesis outline

The thesis is divided into five (5) chapters. The current introductory and literature review chapter is followed by chapter two (2) which focuses on the background to Great Zimbabwe, its immediate environment and the wider region. The chapter explores the density of metallurgy at

Great Zimbabwe and the various rich metalliferous deposits within the vicinity of Great Zimbabwe that were exploited by the inhabitants of the site. Chapter three (3) provides brief a overview of the archaeological context where the copper and bronze objects were recovered. Reinforced by a detailed insight into the systematic analytical procedures employed from preliminary macroscopic sorting of material in the field to metallographic and isotopic examination in the laboratory. This is followed by Chapter Four (4) where material analysis and lead isotopic results will be presented and interpreted in various forms. which comprises data collection procedures during the fieldwork and in the laboratory. In chapter four (4) the collected and analysed data will be comprehensively presented and interpreted in various forms. In this chapter compositional, microstructural, and fabrication data, alongside characterized lead isotopic ratios from copper and bronze samples from Great Zimbabwe and legacy metalliferous Pb data will be discussed in detail to assess the nature of cuprous metallurgy at Great Zimbabwe and hinterland south-central Africa. Finally, Chapter six (6) wraps up the dissertation with a discussion of some observation and make recommendations for future provenance studies in archaeology.

CHAPTER 2

BACKGROUND TO GREAT ZIMBABWE & THE WIDER REGION

2.1. Introduction

Great Zimbabwe is one of the largest precolonial structure in sub-Saharan Africa (Pikirayi 2002; Ndoro 2001; Huffman 2007; Chirikure 2021). It is one of the various polities that thrived in the second millennium CE, with evidence of greater social complexity, urbanism, and statehood. The site is located 27km southeast of the present-day town of Masvingo and it covers an area that is approximately 720 hectares (Sinclair *et al.,* 1993). It is characterized by an array of impressive architecture that constitutes the three main zones namely the Hill Complex, Great Enclosure and Valley Enclosures, and the unwalled areas in between and surrounding the architectural constituencies of the site (Garlake 1973, Chirikure *et al.,* 2017). The Hill complex is located at the summit of a steep whaleback to the north of the site (Chipunza 1994), with the Great Enclosure located to the southern part of the Hill complex slightly conterminous with the Valley Enclosures. The valley enclosures are situated between the Great Enclosure and the Hill Complex. All the three major architectural zones are made up of various enclosures, that are believed to have served special purposes but chief among them was to accommodate the elites who ruled Great Zimbabwe from 900-1700CE (Chirikure and Pikirayi 2008, Chirikure et *al.*,2013).After many decades of archaeological work and various dating systems from classical architectural and structural dating, radiometric dating and the comprehensive Bayesian modelling, it has been suggested that the construction and occupation of the site was gradual with the Hill complex and its associated terraces being occupied first followed concurrently by the Great Enclosure and some parts of the Valley Enclosure. Before the site expanded to areas beyond the outer perimeter wall (see Summers *et al.,* 1961; Collett 1992; Chipunza 1994; Ndoro 2001; Chirikure *et al.,* 2013; Huffman 2020).

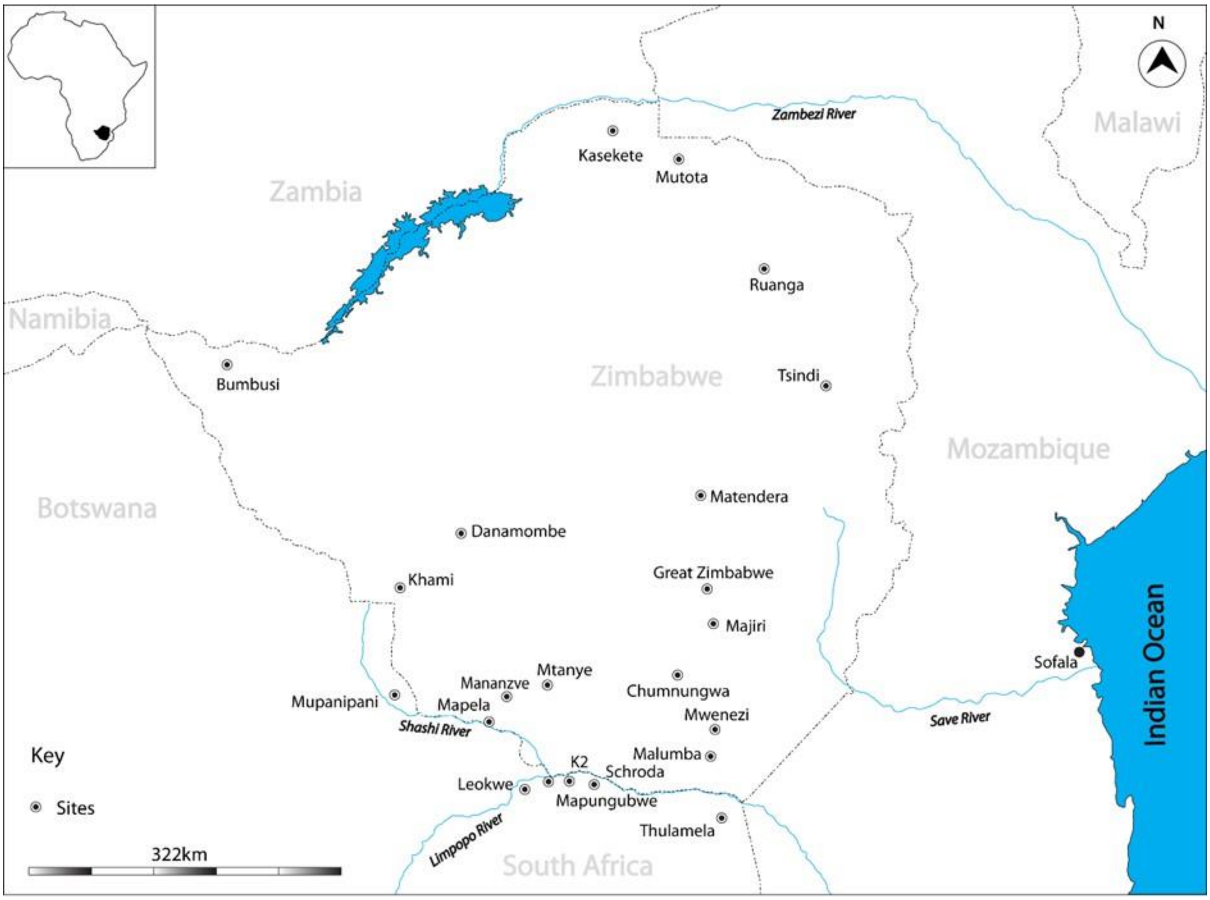

Fig 2: Map showing the location of Great Zimbabwe and other Zimbabwe Culture sites (drawn by Dr Robert Nyamushosho)

Notably the contemporary architecture that only stretches over 720 hectares, is believed to be a brainchild of the formalised heritage management system, which created arbitrary boundaries to a capital of a powerful kingdom whose influence stretched far and wide across south-central Africa (Garlake 1982; Pikirayi 2001, 2013; Chirikure 2019, 2020). However, during its time Great Zimbabwe's influence and monopoly stretched from the elite capital at Great Zimbabwe in present-day Masvingo, Zimbabwe to the north of the Zambezi River (modern-day Zambia), south of the Limpopo River (present-day South Africa), present-day north-western Botswana and the Swahili Coast (contemporary Mozambique and Tanzania Indian Ocean coast). The inhabitants of Great Zimbabwe (both elite and commoners) practised in regional, interregional and intercontinental commerce. This is evidenced by an array of artefacts retrieved across the site's various contexts such as croisettes ingots, double-edged iron gongs, imported porcelain, ceramic ware, stone ware glass beads, a copper coin with Arabic inscriptions, cowrie sea-shells, cornus shell, zinc or brass (Pikirayi 2001; Swan 2002; Bandama *et al.*, 2016; Chirikure

2017,2019; Bisson 1982; Moffet and Hall 2019; Moffet *et al.,* 2021). In exchange, Great Zimbabwe exported gold, ivory and skin to the coastal entrepôts of Kilwa and Sofala (Beach 1974; Pikirayi 2001; Huffman 2007). Both imported and locally produced goods were exchanged and circulated across hinterland south-central African polities contemporary to Great Zimbabwe. However, it should be noted that despite most imported goods being an essential part of an expansive exchange system, they were mainly luxurious goods that had local replacements and minimum impact on the political economy of hinterland polities such as Great Zimbabwe (Mudenge 1974, 1988; Garlake 1978, 1982; Beach 1974; Bhila 1992; Pikarayi 2001,2013; Chirikure 2019, 2020). According to Pikarayi (2001), coastal trade became part of an exchange system practised by already thriving states in south-central Africa. Thus, essential goods that sustained Great Zimbabwe state and its neighbouring polities were locally produced and sourced within hinterland southcentral Africa. Such goods included agro-based produces (grain, cattle, sheep, goat, poultry), metallurgical based commodities (metals such as copper, tin, iron, bronze and metalliferous ores), salt, timber, bush meat and skin (Beach 1974, Garlake 1982). See Fig. 5 simplified map further below that presents the distribution of essential resources within the territory of Great Zimbabwe State.

Fig 3: The Hill Complex at Great Zimbabwe, Photo credit author

Fig.4: The Valley Enclosure and Great Enclosure (big circular structure in the background) photo was adopted from Getty Images

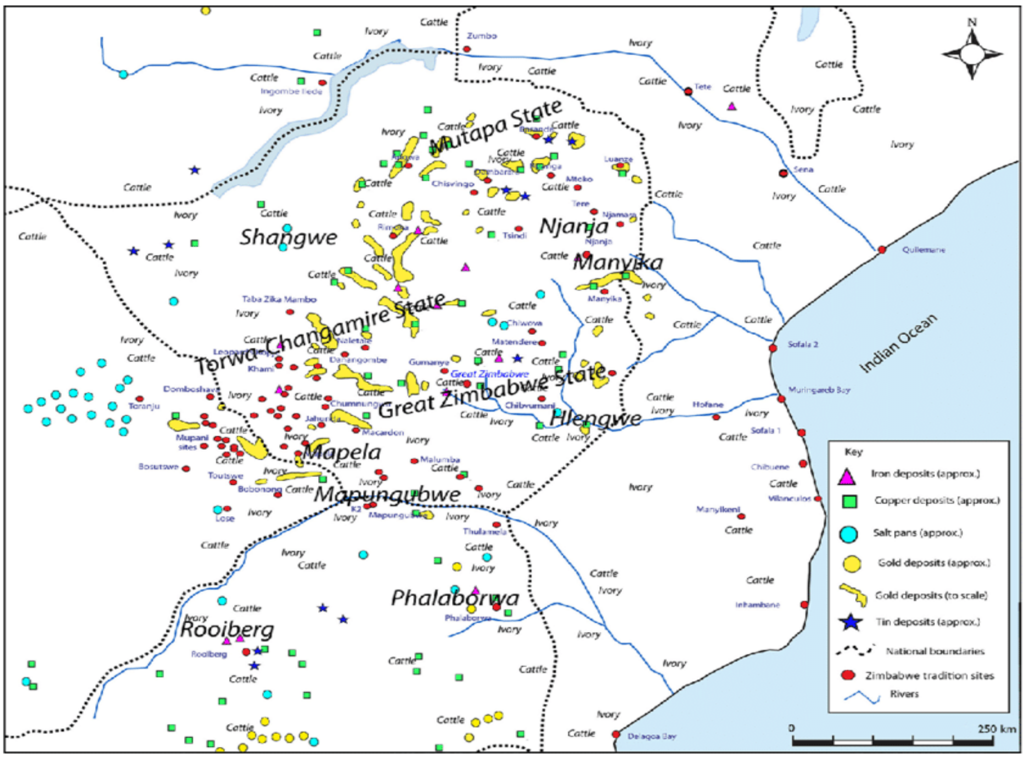

Fig 5: Map of the distribution of essential resources that sustained Great Zimbabwe (First drawn by Bandama 2013 and adopted from Chirikure 2020:153)

2.2. The metal economy of Great Zimbabwe

Despite the importance of various goods in the political economy of Great Zimbabwe as emph asized above, scholars appear to agree that metals were important in sustaining the socio-political economy of Great Zimbabwe by providing metal tools in crop cultivation, mining, wa rfare, symbolism, and that could be exchanged over short and long distances between Great Zi mbabwe, coastal and hinterland southcentral Africa (Herbert 1996; Bisson 2000, Chirikure 2007; Bandama *et al.,* 2016, Moffet 2017). Archaeological excavations at Great Zimbabwe over the past centuries have documented unquestionable evidence of primary and secondary production of both ferrous and non-ferrous metals at the site's various constituents. For instance, ferrous metallurgical production debris and objects in the form of furnace remains, slag, tuyeres, even haematite ore, tongs, pincers, draw plates, spears and arrowheads, hoes, rods, bangles and wire fragments were excavated in elite domains such as the Hill Complex, Valley Structures and the Great Enclosure (Caton-Thompson 1931; Robinson 1961; Summers 1961; Collett *et al* 1992; Herbert 1996; Chirikure 2007; Bandama *et al.,* 2016, 2018).

The availability of ferrous material evidence within walled areas across the site suggests that iron production at the site might have been partially regulated by elites and that it was household-based (Herbert 1996; Chirikure 2007). According to Chirikure (2007), given the nature and the extent of the territory the lack of mass production debris at the site, suggest that iron was produced and siphoned from nearby chiefdoms under the control of the king at Great Zimbabwe and attached specialist which was a common feature in precolonial south-central Africa. The above observation is supported by evidence of intensive iron production debris and finished objects within areas around Great Zimbabwe such as Hlambamlonga, Chigaramboni, Mashava and Mtevedzi (Swan 2002, Mtetwa 2011, 2017), thus these areas might have produced iron for the elite inhabitants of Great Zimbabwe and sustained ferrous-metal circulation between Great Zimbabwe and other polities across hinterland southcentral Africa.

In addition, just like ferrous metals, non-ferrous metallurgical evidence has been found in reasonable quantities across all occupational areas at Great Zimbabwe. Notably much of the gold evidence at Great Zimbabwe is fragmentary since it suffered from looting by antiquarians during the early 1900s (Garlake 1982; Miller 2001). However, there has been documented evidence of gold ornaments, wire, pellets, foils, nails and gold melting crucibles from the Hill Complex, Valley Enclosures and the Great Enclosure (Stanley 1931, Carton Thompson 1931, Garlake 1973, Collett *et al.*, 1992; Chirikure and Pikirayi 2008). There seems to be a consensus among most scholars that most of the gold mined and produced in hinterland southern Africa was exported through Swahili entrepôts (Summers 1969; Phimister 1974; Huffman 1974, 2007; Garlake 1974; Swan 1994; Kusimba *et al.,* 1994; Bisson 2000; Miller 2002; Bandama *et al.*, 2016, 2017, 2018), with its use at elite sites such as Great Zimbabwe being attributed to the adoption of foreign ideologies associated with Arabic and Swahili merchants (Herbert 1984; Killick 2009).

However, regardless of the influence of foreign ideology on hinterland elite settlements such as Great Zimbabwe, it is believed that gold never attained the same status given to copper within local southcentral African societies (see Herbert 1984; Bisson 2000). Therefore, unlike gold, copper and its alloys are ubiquitous at Great Zimbabwe's walled and unwalled areas dating from CE 1000- 1700 (see Garlake 1973; Bandama *et al.*,2016, 2017 and references therein). Over the years archaeologists and archaeometallurgists have documented ample evidence of cuprous metallurgy at the site such as crucibles (specialised and non-specialised), refractories, ingot moulds, wound copper, bronze and brass wire fragments, beads, spears, Sn ingots and Pb-pewter ingots, showing that copper and its alloys were melted, remelted, cast and alloyed within and outside walls Great Zimbabwe (see Stanley 1931, Carton Thompson 1931, Miller 2002; Thondhlana 2007; Chirikure 2015,2020,2021;Bandama *et al.,* 2016, 2017).

Preliminary studies of some of the crucibles and moulds at the site have shown that bronze, brass and gold were melted in both specialised and non-specialised crucibles (Bandama *et al* 2017), with specialised crucible technology believed to be cascading from coastal Swahili and Arabic traders, whilst non-specialised crucibles were drawn from the domestic pool of pottery (Kusimba 2009; Bandama *et al.,* 2016, 2017). In addition, the X shaped ingot mould (HIA type) retrieved at Great Zimbabwe is stylistically associated with the northern Zimbabwe sites, northern Zambezi and Copperbelt region (Swan 2007; Killick 2009; Nikis and Livingston 2017, Rademakers *et al.,* 2019; Chirikure 2019). Notably despite contact, diffusion of ideas, technological concepts and raw materials such as zinc or finished alloys such as brass or gunmetal from the coastal region, cuprous metallurgy across most African capitals such as Great Zimbabwe and its nearby polities remained purely African (see Miller 2002; Bandama *et al.*, 2016; Chirikure *et al.,* 2017 Moffett *et al.,* 2020).

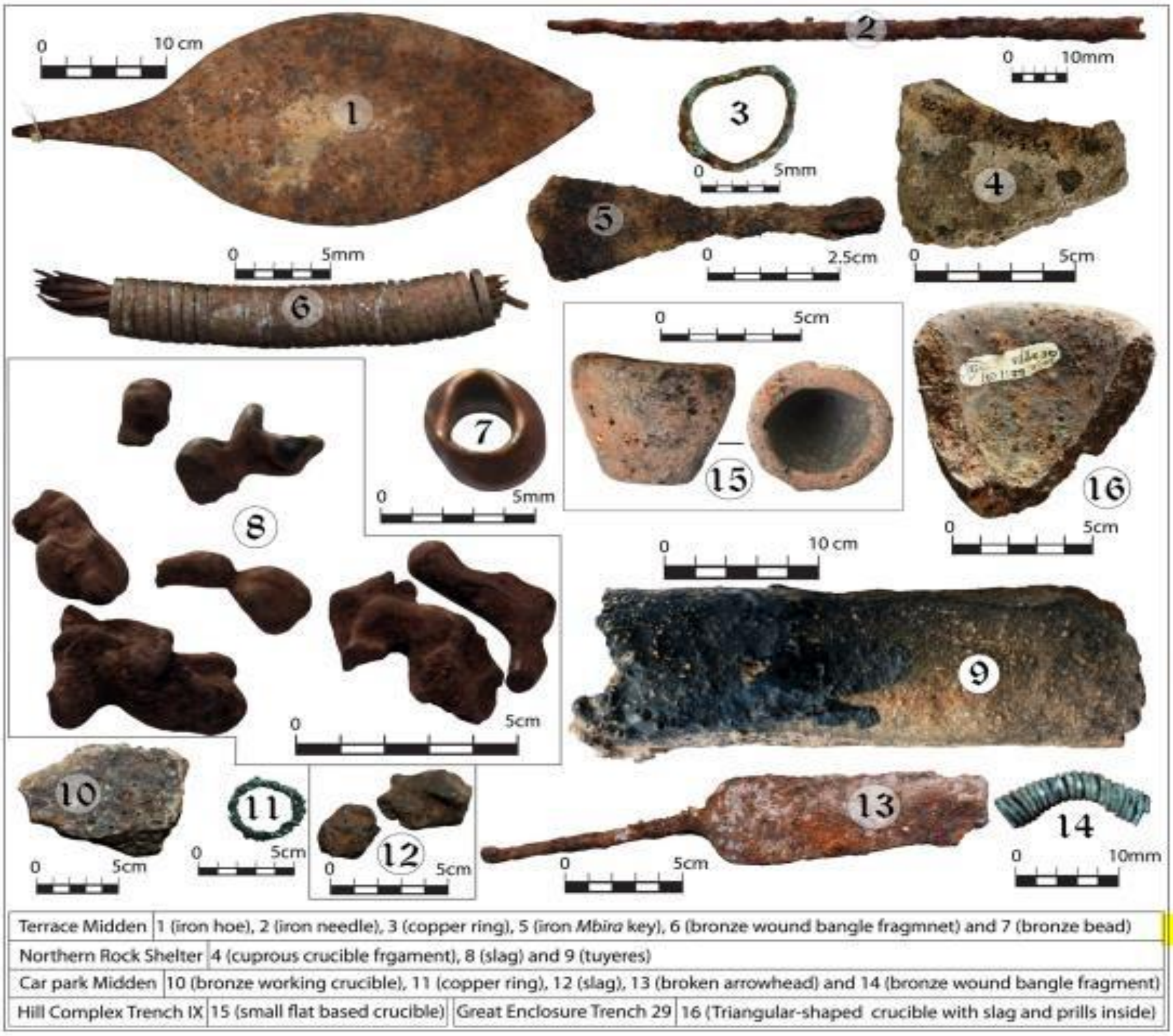

Fig 6: Metals, crucibles, slag and tuyeres from Hill Complex, Great Enclosure (walled areas) and Car Park Midden (unwalled area) photo adopted from Bandama et al., (2016:5)

Fig 7: Evidence of draw plates, nail, tongs and copper bar from Mtuzu Hill adjacent to the Hill Complex (Photo Credit Dr Mukwende)

The omnipresence and high density of cuprous metallurgy across the site is testimony to the importance of copper among the inhabitants of Great Zimbabwe. Just like other polities across south-central Africa, copper and its alloys were revered by both elite and commoners at the site and was part of a multi-complex system whereby it was used as the medium of exchange, adornment, symbol of power, kingship, status, age, gender, office and within medicinal anthropology or ethnopharmacology (Herbert 1984,1996; Bisson 2000, Bvocho 2005, Thondhlana 2007,2012; Bandama *et al.*,2016). Such importance and relevancy of copper in mundane activities ensured that it was widely circulated across individual households at the capital, within the territorial state of Great Zimbabwe and beyond with its neighbouring communities scattered all-over south-central Africa. Recent insights on the political economy of Great Zimbabwe shows that circulation and exchange of copper were based on reciprocity and was achieved through various mechanisms imbedded in the socio-ideological lifeways of the inhabitants of Great Zimbabwe such as gifts, marriage alliances, trade, taxation, tokens of appreciation, wages, raiding and even distribution of inheritance among relatives (Chirikure 2019, 2020). Therefore, this shows that circulation and exchange of copper, bronze, brass and zinc were not done only when there was excess but was a way of life, hence why cuprous metallurgical material culture is evenly distributed across Great Zimbabwe's walled and unwalled areas.

In conclusion, the density of traces of metallurgical debris, technical ceramics and finished objects insitu, documented and excavated at Great Zimbabwe's walled and unwalled contexts attest to the richness and accessibility of various metalliferous deposits within the site's (Great Zimbabwe) vicinity and distant wider landscape. It is important to note that despite the metal economy of Great Zimbabwe being the bedrock of a strong political economy an array of resources embedded within the immediate geophysical environment kept the political economy of the state vibrant. In general, the Great Zimbabwe state's natural environment was characterised by an array of resources that ranged from quality pastures, timber, fertile arable land, perennial water sources, hunting grounds, various rocks (granite and serpentinite), firewood and clay minerals which were all important in the socio-economic and political setup of Great Zimbabwe. However, in this study, the researcher is going to explore the various geological deposits that were exploited by the inhabitants of Great Zimbabwe and their neighbours across south Central Africa for various ores used to manufacture metallic objects that were circulated from household-level up to intercontinental level.

2.3. Geology and Mineral Wealth Around Great Zimbabwe and Beyond

The geology of Zimbabwe is tectonically divided into two main parts which are the Zimbabwean Archaeon Craton and three mobile belts (Zhao *et al.,* 2014). The country's central part is characterised by the Zimbabwean Archaeon Craton and surrounded by rift valleys in the north/north-west (Zambezi valley) that forms the Zambezi Belt, the Mozambiquan Belt to the east and the Limpopo Belt to the south (Wilson and Nutt 1988; Vinyu 1996; Dirks *et al.,* 1998; Jordon 1990; Zhao *et al.,* 2014; Dittrich *et al.,* 2019). According to Rollison and Whitehouse (2011), the Zambezi and Limpopo Mobile belts represent the Neo-Archean Mobile belt accreted or fused to the Zimbabwean Craton between 2700-2600 Ma.

Stratigraphically the Zimbabwean craton is further subdivided into three distinctive granitic groups namely the Sebakwian Group (3600-3000 Ma), Bulawayan Group (3100-2900 Ma) and Shamvaian Group (2700-2600 Ma). According to Wilson (1972: 391), the Sebakwian-Bulawayian and Shamvaian granitic terrain/groups (previously known as systems) constitute the oldest greenstone belts in the Zimbabwean Craton. The Sebakwian Group covers most of South-central Zimbabwe, with the rock types being predominantly mafic to ultramafic, volcanic and metasedimentary generally covered by ironstones (see Wilson and Nutt 1988:558; Dittrich *et al*., 2009:23 and references therein). The Bulawayan Group is subdivided into two major groups the Lower and Upper sections (Ranganai *et al*., 2008:259); however, both are characterized by volcaniclastic rocks, komatiitic basalts with interbedded ironstones and polymict (conglomerates) clastic sediments (Wilson 1991). The difference between the two aforementioned sections is based on the tectonic setting of the sequence, with the lower Bulawayan Archaean Group (Greenstone Belts) being characterized by an extensive basaltic unit (platform type) whereas the upper section is dominated by a bimodal unit of mafic felsic rocks overlain by calc-alkaline rock series dominated by andesites (Wilson 1981; Wilson and Nutt 1988:560-61). The separation is simply based on geologically unconformity and deformation (see Wilson 1981; Talyor *et al.,* 1998). According to Dittrich *et al.,* (2009) the 'geological period predominated by mafic volcanism associated with Bulawayian super group was superseded by the accumulation of felsic volcanism.' The thick volcanoclastic sedimentaries make up the Shamvaian group. The Shamvaian intrusions overlie the upper Bulawayian group. It was also accompanied by the geological emplacement of tonalites and granodiorites of the Weda and Sisombo suites between 2700-2690 Ma (Wilson 1988; Dirks and Jelsma 1998). The Bulawayian and Shamvaian granitic groups are the most extensivegreenstone belts in the Zimbabwean Craton (Wilson *et al.,* 1995). The events were followed by tectonic movements to the south of the Zimbabwean Craton and the Limpopo Greenstone belt resulting in the granitoid developments in the upper and middle Zimbabwe craton (see Rollison and Whitehouse 2011). The intrusion and formation of the Chilimanzi (*Chirumanzi*) granite suite and Bikita igneous complex are assigned to this period of 2650-2600 Ma (Wilson and Nutt 1979; Jelsma and Dirks 2002; Melcher *et al.,* 2015). Notably, the formation of the three main greenstone belts was concurrent with the formations of various igneous complexes, pegmatites, alluvial ore deposits and above all greenstone belts of significance in this research such as the Harare-Shamva, Masvingo, Belingwe (*Mberengwa*), Odzi-Mutare-Manica, Shamva, Midlands and Tati. In total, the Zimbabwean Craton comprises twenty-six (26) greenstone belts with most of them constituting twenty percent (20%) of the craton whilst the rest is characterized by mineral-endowed granite-gneiss complexes (see Jelsma and Dirks 2002 and references therein).

Furthermore, various geochronology and lithographical studies carried out across the Zimbabwe craton concluded that the tectonic movements and intrusion of mafic to ultramafic swarms on the Zimbabwean craton around 2575 Ma resulted in the emplacement of the Great Dyke which cuts across the Zimbabwean Craton in a slightly north-south direction (Wilson and Nutt 1988:580; Wilson 1996:388: Obertheur *et al.,* 2002; Mackintosh *et al.*, 2017; Dittrich *et al*., 2019:25). The Great Dyke is an essential formation since it is one of the richest mineral deposits within the Zimbabwean Craton and it is currently one of the largest chromite and Platinum group minerals (PGM) sources in southern Africa (Taylor *et al.,* 2005:36,108). There is also evidence of the Magondi Belt (Supergroup) characterized mainly by metasedimentary succession, limited mafic and felsic metavolcanic (Master 1996:22; Master *et al.,*2010). The Magondi belt is hypothesised to have been formed after the western edge of the Zimbabwean craton collided with an unknown continental terrain to the west which resulted in the development of the high-grade Magondi belt (see Master *et al.,* 2010; Glynn *et al.,* 2020). The belt is lithostratigraphically divided into the three main supergroups namely the Lomagundi, Dewera and Piriwiri which are characterised by various mineral deposits (Stagman *et al.,*1978; Woldai *et al.,* 2014). In general, the Lomangundi and Dewera supergroups are endowed with various minerals and polymetallic deposits which played an essential role in metallurgy during precolonial times (Summers 1969) and is also a modern source of copper, tin, nickel, gold, and industrial minerals such as graphite and kyanite (see Master 1996; Master *et al.,* 2010 and references therein).

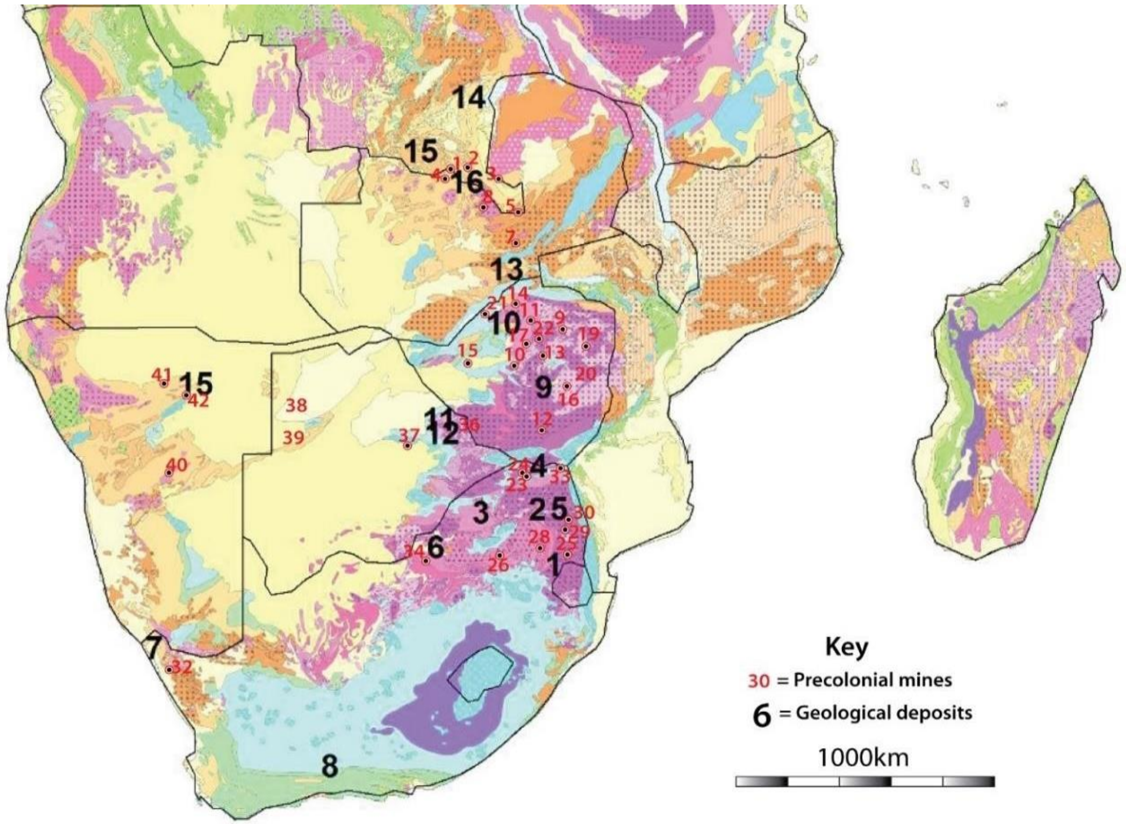

Fig 8: Map of southern Africa with deposits mentioned in this study. Modified from Stephens et al., 2020 and references therein (drawn by Dr Robert Nyamushosho)

Table 1: Detailed key of mines presented in Fig 8

Number assigned in this study	Stephens *et al.*, 2020 assigned N[0/]	Name of deposits	Name of ancient mine	coordinates		Country
1	16	Copperbelt	Lumbumbashi (general area)	11°41'14.28"S	27°30'8.04"E	DRC
2	16	Copperbelt	Kipushi Mine	11°46'14.38"S	27°14'12.29"E	
3	16	Copperbelt (Katanga region)	Musoshi	12°15'1.18"S	27°38'47.11"E	
4	15	Kanshansi (Zambian Cu Belt : ZCB)	Kanshansi	12° 5'31.91"S	26°25'58.50"E	Zambia
5	13	Copperbelt (ZCB)	Bwana Mkubwa	13° 1'10.49"S	28°40'54.19"E	
6		Kitumba Deposits (ZCB)	Kitumba Hills area			
7	13	Zambian (Copper-belt)Katanga Deposit	Broken Hill (Now Kabwe)	14°25'56.12"S	28°27'1.49"E	
8	13	Copperbelt (ZCB)	Ndola	12°59'26.31"S	28°38'59.33"E	
9	9	Mangondi Copperbelt	Mhangura	16°53'10.43"S	30° 9'58.77"E	Zimbabwe
10	10	Shamvaian Greenstone Belt)	Sanyati	17°57'5.84"S	29°18'16.93"E	
11	9	Mangondi belt	Nora copper (Miriam Mine)	16°55'59.02"S	30° 8'60.00"E	
12	9	Umkondo Basin	Umkondo Copper Mine	20°19'3.78"S	32°12'38.79"E	
13	9	Mangondi Belt	Alaska copper mine	17°22'36.52"S	30° 3'54.06"E	
14	9	Mangondi Belt	Shamrocke copper mine	16°27'37.01"S	29°53'50.03"E	
15		Bulawayan Greenstone Belt	Gwaai River Copper Mine	18°27'38.38"S	27°10'8.00"E	
16		Masvingo Greenstone Belt (Bikita Pegmetite)	Bikita	19°57'40.27"S	31°25'40.98"E	
17	9	Piwiriri Mineral Belt	Copper Queen mine	17°31'0.01"S	29°19'59.01"E	
18	9	Hydrothermal Deposits Au, Cu Ag: Archaean greean Stone Belt (MGB)	Inyati Mine	18°13'5.18"S	32°14'43.93"E	

19	9	Masvingo Green Stone Belt	Sviba area	20°57'8.99"S	30° 8'37.00"E	
20	9	Dorowa Complex, Save Catchment Area Phosphate Hill	Save Catchment (Dorowa Complex)	19° 4'5.91"S	31°46'4.98"E	
21	9	Piriwiri Mineral Belt	Copper King Mine	17°34'59.01"S	29°16'0.01"E	
22	9	Lomangundi Mineral Belt	Alaska Mine	17°22'32.96"S	30° 4'8.03"E	
		Bulawayo greenstone belt	Empress Mine	18°28'8.51"S	29°26'38.70"E	
23	4	Limpopo MobileBelt Central Zone	Mussina Copper Deposits (Mussina Copper Mine)	22°19'27.77"S	30° 3'13.39"E	South Africa
24	4	Limpopo Mobile Belt Central Zone	Artonvilla Copper Mine	22°18'25.85"S	30° 5'1.62"E	
25	5	Phalaborwa Igneous Complex	Phalaborwa	23°58'7.58"S	31° 8'29.97"E	
26		Kraaipan Greenstone Belt (Kaapvaal Craton	Harmony Mine	26°10'52.53"S	27°42'51.60"E	
27	5	Phalaborwa Igneous Complex	Lowle Hill			
28	5	Phalaborwa Igneous Complex	Murchison Mine	23°53'31.21"S	30°41'50.83"E	
29	2	Murchison Greenstone Belt	Kasteelkoppies	23°51'10.00"S	30°47'20.00"E	
30	2	Murchison Greenstone Belt	Monarch Kop	23°54'19.82"S	30°41'2.54"E	
31	2	Murchison Greenstone Belt	Solomon Mine			
32	7	Namaqualand (O'okiep Copper District)	O'Okiep Mine	29°35'48.47"S	17°52'43.30"E	
33	4	Pafuri Nickel Deposit	Pafuri Area	22°19'59.99"S	31° 0'0.00"E	
34	6	Bushman Shear Zone	Abjeterskop Area (Close to Botswana)	24°48'59.01"S	26° 9'56.00"E	
35		Tati Green Stone Belt	Selkirk Mine			Botswana

36	12	Tati Green Stone Belt	Phoenix Nickel Mine	21°14'48.12"S	27°45'31.53"E	
37	11	Bushman Shear Zone	Dukwe mines (Southen and North)	20°37'22.92"S	26°25'9.96"E	
38	11	Kalahari Copper Belt Deposit	Khoemacau Copper Mine - Boseto Site	20°20'52.62"S	22°58'46.16"E	
39	12	Matsitama Greenstone Belt	Thakadu Mines	21°44'21.44"S	21°40'42.93"E	
40	15	Southern Zone of the Damara Orogen	Otjihase Area close to Onganja	22°26'20.02"S	17°10'22.16"E	Namibia
41	15	Southern Zone of the Damara Orogen	Ongeama Area close to Ongumba	18°43'50.62"S	17° 2'55.59"E	
42		Upper Damara Orogen Supergroup	Tsumebi	19°13'56.53"S	17°42'34.19"E	

The geochemical studies of the aforementioned geological features across the Zimbabwean plateau and adjacent landscapes revealed that most of the deposits are polymetallic with evidence of various metals (Zhao *et al.*, 2014). Most mineral deposits in Zimbabwe are confined to the various greenstone belts, the Great Dyke and adjacent mobile belts. They are dominated by a great deal of diverse minerals, such as silver, diamonds, zinc, gold, iron, copper, nickel, lead, nickel, and tin, with the gold, iron, tin, and copper being the ones exploited since the early second millennium AD up to colonial period.

Great Zimbabwe is situated on the southern edge of the Zimbabwean Plateau within the Archaean complex of greenstone, mafic, ultramafic rock, gneisses, migmatites and late intrusive granites that make up the Masvingo greenstone belt (Gwavava and Ranganai 2009:278). The Masvingo greenstone belt dominates the south-central and eastern part of the Zimbabwean craton. It covers an area that encompasses various distinctive geological areas like the Mashava Ultramafic Complex (MUC), Buhwa Green Belt (BGB), Mushandike Igneous Complex, Bikita Pegmatite Deposits, Charumbira, Chivi, Sviba and Chikwanda Pluton. (Dodson *et al.*,2001; Prendergast and Wingate 2007; Gwavava and Ranganai 2009). All these deposits are rich in various minerals such as tin, copper, gold and iron which formed part of the most exploited and circulated metals across the hinterland and coastal Southern African gradient from 900-1700CE.

2.3.1. Gold and iron occurrences around Great Zimbabwe

According to Mtetwa (2017), the geographical location and environmental features around the site played an essential role in the sustenance of the inhabitants of Great Zimbabwe. Geologically the site is characterised by various mineral occurrences in the form of reefs, alluvial and complex deposits of gold, iron, tin and copper within its immediate and distant locality. For instance, the nearest occurrence of gold placer deposits with evidence of pre-European working was documented 10 km to the west of Great Zimbabwe within the Bhani area (Summers 1969; Phimister 1974) and 15 km northwest within the Bondolfi area (Mtetwa 2017). According to Chirikure (2019) there is a possibility of the exploitation of gold deposits at the Mashava Ultramafic Complex situated 50 km west of Great Zimbabwe, the Mberengwa greenstone belt deposits (previously documented as Belingwe greenstone belt) approximately 150 km southwest of the site and Renco area within the northern marginal zone of the Limpopo Mobile Belt

70 km south-east of the site. There is also evidence of gold lodes along the south-eastern section of the Masvingo Greenstone Belt, Mushandike Granitic Areas (possibly the area currently called Nyanda) and Tokwe-Mukosi Gneiss area (see Blenkinsop 1991). Phimister (1974:236) documents evidence of placer deposits around the Shurugwi area (formerly known as Selukwe) situated 130 km from Great Zimbabwe and Wadanda area (formerly Fern Spruit) near the Providential Pass along the Masvingo-Beitbridge highway. In addition to the above, there is a possibility that alluvial gold nuggets were panned from various rivers that drained the various Zimbabwean greenstone belts since they eroded the primary gold belts and gold-bearing auriferous veins and created placer deposits in rivers such as Munyati, Mazoe, Odzi and Save which were all panned for gold in precolonial times (Summers 1969; Beach 1998; Miller *et al.*, 2000).

The availability of gold is simultaneous with the ample evidence of hematite ore (iron) in the Precambrian rocks that constitute Chigaramboni, Nyanda (Mushandike Igneous Complex), Nyuni, Charumbira and Beza mountain ranges near Great Zimbabwe (Gwavava and Ranganai 2009). Blenskisop (1991) showed that much of the gold lodes in the Masvingo Greenstone Belt occur concurrently with iron, in various polymetallic deposits, igneous complexes and granitic landscapes. The mountains mentioned above (Chigaramboni, Charumbira, Nyanda and Beza) are within a 20 km radius of the site of Great Zimbabwe and dotted with evidence of precolonial or ancient iron exploitation and working within their neighbourhood (Ndoro 1994; Mtetwa 2017). In addition to the above, there is evidence of gangue materials from iron smelting sites in the ultramafic zones of Mashava in the form of vitrified single and multiple fused tuyeres, furnace walls, quarries of iron, and dense chunks of slag (Mtetwa 2011). In addition to the above, Swan (2007) documented evidence of extensive ironworking industries in the Mhangura and suggested that they provided iron to Great Zimbabwe. The area is approximately 400 km to the north of Great Zimbabwe.

2.3.2. Tin occurrences around Great Zimbabwe

However, unlike gold and iron which were ubiquitous within a short distance of Great Zimbabwe, the nearest evidence of tin deposits with evidence of ancient working is at Bikita pegmatite field, located on the eastern edge of the Masvingo green belt, approximately 100 km from the Great Zimbabwe site (Carton-Thompson 1931; Stagman *et al.*,1978:41; Kinnaird *et al.*, 2016; Chirikure 2019). The Bikita complex is dominated by cassiterite, tantalite and minor microlite rare elements with the earliest colonial documentation of tin production being around the early 1900s, it was prospected and pegged based on the evidence of remnants of ancient mining and limited to eluvial deposits mining at Bikita and Ruengwe Tin mines (Tyndale-Biscoe 1951; Hunter and Lenthal 1971; Jordon 1990; Dittrich *et al.*, 2019). The Ta-rich pegmatites at Bikita Mine yielded an Archaean age of 2617 ± 1 Ma (Melcher *et al.*, 2015; Kinnaird *et al.*, 2016) and are also characterised by pollucite mineralization (Dittrich *et al.*, 2019:8).

In addition, other stannic pegmatitic deposits with evidence of ancient working occur in the south-western portion of Mutare (formerly Umtali) schist belt in Rusape at Cornucopia (Tyndale-Biscoe 1951; Summers 1969:112; Kritzinger 2012). The place is located within the east Mutare-Odzi-Rusape Greenstone Belt dominated by dolerite igneous rocks that are rich in tin, copper, cobalt and nickel. According to Hunter and Lenthal (1971) tin in the Rusape greenstone belt area occurs in the form of quartz veins, pegmatitic quartz veins and lepidolite grains. Furthermore, there is also a probability of the exploitation of various deposits situated in the north-eastern section of the country within Shamvaian-deposits, places where old or colonial period tin mines such as Rusambo, Sutwe and Shamva were located (Hunter and Lenthal 1971; Kinniard *et al.,* 2016). The pegmatite deposits located in eastern Harare towards Shamva Area are within the Harare-Shamva Greenstone Belt, which is polymetallic pegmatite deposits dominated by cassiterite, tantalite, scheelite, stibiotantalite and simpsonote microlite with tin, iron, copper, and uranium evidence (Robertson 1973).

Furthermore, there is also the Makati-Makaha pegmatites located in the north-eastern section of the country, which is rich in coltan, manganotantalite and microlite (Barton *et al.*,1991; Kinnaird *et al.*, 2016). The Makati-Makaha pegmatite deposit is associated with the Benson, Gooday and Jordwyitt Mines whose pegmatite geochemistry shows that they all contain ample evidence of amblygonite, cassiterite beryl, lepidolite and spodumene (Ackermann *et al.*, 1968). The area is located within the Mudzi and Mutoko area. There are also other areas with notable pegmatites with evidence of tin deposits such as Sandawana located in the Mberengwa Greenstone Belt, Beryl Rose and Bepe Hills (Buhera area) that fall within the main economically exploitable pegmatites deposits in Zimbabwe (Kusky *et al.,* 19921; Dittrich *et al.,* 2019).

In addition to the above, there is evidence of tin deposits at Kamativi situated within the Hwange (previously documented as Wankie) area which falls under the northern section of the Magondi belt (Hunter and Lenthal 1971; Master *et al.,* 2010; Zhao *et al.,* 2014). The Kamativi pegmatite deposit located in the Dete-Kamativi Inlier is one of the largest is LCT (Lithium-Caesium-Tantalum)-type pegmatites (Shaw *et al.,* 2019:791) which is a predominantly Sn-Ta-W rich pegmatite deposit characterized by varying detectable amounts of monazite, zircon and tapiolite that intruded the Kamativi Schist Belt. The deposit was formed around 900-1100 Ma (Molofosky 2009:17, Molofosky *et al.,* 2014). Within the same area, 40 km from the Kamativi pegmatite deposit is the Kalinda pegmatite, however, unlike the Kamativi deposit the latter (Kalinda pegmatite) is characterized by casserite and other CGM mineralization (columbite-group mineralization) with no evidence of lithium (Kinnaird *et al.,* 2016; Shaw *et al.,* 2019). The area is in the north-western part of the country and is located approximately 494 km from the site of Great Zimbabwe. Despite no documented evidence of ancient working around the Kamativi tin mine or within its vicinity due to the lack of systematic archaeological studies around the region, the area is believed to be one of the ancient historical sources of tin within southern Africa (Kinnaird *et al.,* 2016).

Moreso, the Rooiberg valley in the Limpopo region within the Bushveld Geological Complex in modern-day South Africa has a well-documented and vibrant precolonial tin industry that was smelted at Smelterskop and Elandsberg (Chirikure *et al.,* 2010; Bandama *et al.,* 2015; Kinnaird *et al.,* 2016). The area has for long been viewed as one of the main and only unquestionable sources of tin in precolonial southern Africa (Friede and Steel 1976; Grant 1999; Miller and Hall 2008; Molofosky *et al.,* 2009; Miller 2010; Bandama 2013; Bandama *et al.,* 2015). According to Bandama *et al.,* (2016) Rooiberg is located 300 km south of Great Zimbabwe. It (Rooiberg tin field) is characterised by an array of tin deposits situated at various farms namely Leeuwport 554 KQ, Vellefontein 517KQ, Onverwacht 486 KQ, Hartebeesvley 510 KQ, Weynek 505KQ, Hartebeesfontein 511 KQ and Olievenbosch 506 KQ where there is extensive evidence of ancient tin working (Cairncross and Dixon 1995:95). Evidence from the ancient mines at Rooiberg and its vicinity especially smelting areas such as Rhenosterkloof 3 shows that the exploitation of tin started from 1100 to 1900 CE (see Bandama *et al.,* 2015:91; Chirikure *et al.,* 2015:63; Chirikure 2018). Thus, tin mined at Rooiberg was cast into various ingots and alloyed with copper to manufacture an array of materials that were circulated across southern African sites and beyond via the Indian ocean (Miller 2001:20; Bandama *et al.,* 2015; Moffett *et al.,* 2019). However, there is a probability that raw tin ore was also sourced from this region to Great Zimbabwe.

Furthermore, there is evidence of tin mineralization within the locality of Rooiberg in places such as the red granite of Zaaiplaats, Granophyre Suites (Stavoren), Union Tin Mine, Elands, Moloto and Olifants (Cairncross and Dixon 1995; Chirikure 2014; Hunt *et al.,* 2017). Noteworthy all these places are tin deposits or fields located in the Bushman Igneous Complex. The Zaaiplaats tin field is characterized by various pegmatite zones in the Groenvlei 224KR, Roodepoort 222KR, Salomons Temple 2030KR and Groenfontein 227KR farms whereas the deposits of Stavoren Suites are well developed and exposed at Stavoren 676KS area in Waterberg District (Cairncross and Dixon 1995: 100-101). The Union Tin mine situated in Mookgophong is a predominantly crystallized casserite deposit that was exploited during antiquity and might have added to the tin already circulation across southern Africa (Kinnaird *et al.,*2016). Furthermore, there is casserite mineralization at areas like Eland, Moloto and Olifants within the Lebowa Granite Suite rocks however, just like most deposits within the Bushveld Igneous complex these pegmatites are mainly characterized by polymetallic mineralization (see Lenthal and Hunt 1972; Croker *et al.,* 2001; Hunt *et al.,* 2017).

Moreover, various deposits occur within the tin-bearing pegmatite that extends southeast from the South African border to central Eswatini (formerly Swaziland) around the Sanceni area and to the north-western section of the country in the vicinity of Mbabane and Ezulwini Valley (Trumbull 1995; Kinnaird *et al.,* 2016). Notable deposits are in areas such as Makwame, Tokwane, Lupholo and Mantega near the contact area between Mpuluzi and Ancient Complex (Scott 1950). There is ample and documented evidence of shallow ancient mines within the Au Sn (gold-tin) rich deposits of the Forbes schist belt. The tin provinces in Eswatini, are characterized by a predominance of cassiterite bearing quartz pegmatites in association with muscovite, magnetite, garnet, tourmaline, biotite and rare Nb-Ta oxides (Kinnard *et al.,* 2016). Finally, there are concentrations of zinc and tin in quartz veins of the Damaran Orogen located in Namibia.

2.3.3. Copper occurrences around Great Zimbabwe

Copper deposits with evidence of ancient working also occur within the Bikita geological complex and the Umkondo Basin (reef) adjacent to the Ndanga District in Zaka (see Summers 1969:89; Kritzinger 2012; Chirikure 2019). According to Chaúque *et al.,* (2017) the Umkondo Basin is in the south-eastern part of the Zimbabwe Craton and is dominated by the Nyanga facies along its eastern margin (covering an area within parts modern-day Masvingo and Chipinge). According to Summers (1969) ancient mining within the Umkondo Basin was visible and documented at various areas such as Hotsprings, Chipinge, Nyanyadzi, Save Valley and the main Umkondo Mine. The area was documented and defined as a series of mines characterised by rich upper quartzite-shale, with an array of malachite-rich nodules, veins of chalcopyrite, magnetite, diamond and gold mineralization.

There is also evidence of Cu-Ni deposits at the Mundonguara deposits located in the easternmost part of the Mutare Greenstone belt (Zimbabwe Craton) and the southwestern part of the Mozambique (Manica) greenstone belt (Chaúque *et al.,*2017). According to Forster (1996) despite the general area that make up the Mutare-Odzi-Rusape greenstone belts being historically known for ancient gold mining as documented by the Portuguese around the 1559 -1878 CE, there is ample evidence of some mines that are located with chalcopyrite deposits thus they might have been sourced for copper in precolonial times. Summers (1969) documented evidence of ancient copper working within the Mutare-Odzi-Greenstone belt with evidence of shallow ancient copper exploitation being mainly confined to Penhalonga, Upper Sabie (Save) and Odzi rivers areas.

However, it is within the sedimentary basins in the north-western fringe of the plateau within the Dewera, Lomagundi and Piwiri supergroups that form the Magondi Belt upper section where copper deposits are hosted in abundance within the Zimbabwean Craton (Jourdan 1990; Swan 2008; Woldai *et al.,* 2006). The Magondi Belt is surrounded by the Phanerozoic cover, which stretches over an area of some 500 x 150 km, within north-western Zimbabwe. It is generally known as the "Magondi Copper Belt" because it is dominated by an array of copper mines such as Mhangura (Mangula), Miriam, Sanyati, Norah, Hans, Shackleton (within Avondale belt), Angwa and Nora (Woldai *et al.,* 2014). Geochronology, sedimentology and geochemistry of the Magondi belts have shown that the various mines were located on distinctive deposits whose mineralization and sedimentology was influenced by the formation of the three main super groups that make up the Magondi belt (Master 1995,1996). Woldai *et al.,* (2014) show that the Mhangura, Nora, Shackleton and Angwa mines within the Dewera supergroup are dominated by Cu-Ag (Au-Pt-Pd-U) mineralization and Shamrock characterised by Cu-Ag mineralization within the Lomagundi group, whilst the Copper Queen and King Mine are endowed with copper-lead-zinc mineralization (Cu-Pb-Zn).

The area (Magondi belt) is characterised by evidence of ancient, extensive shallow mining targeted at rich deposits, especially at areas such as Copper Queen Mine, dating from 1100-1400 CE (Evers and Van Den Bergt 1974; Swan 2002,2009; Moffet *et al.,* 2020). The contemporaneity of some of the mines (Copper Queen Mine) with Great Zimbabwe and documented evidence of ancient copper reef mining in northern Zimbabwe, resulted in the area being viewed as the cradle of most, if not all the copper found in the archaeological record in Zimbabwe (Garlake 1982; Swan 2002).
In addition, there is a presumed copper deposits 60 km west of the Save-Runde confluence with evidence of ancient copper extraction (Kritzinger 2012). This was confirmed by a survey done by Hall and Neal in the early 1900s around Mashonaland as they noted evidence of extensive ancient copper mining in the northern parts of the Sabi (Save) river basin (Hall and Neal 1904; Hall 1912:139).

The Midlands greenstone belt situated approximately 96 km from Great Zimbabwe is one of the largest gold-bearing areas within Zimbabwe. Despite the general assumption of gold dominance, the central deposit which stretches to the lower part of the deposit is characterised by gold bearing porphyry copper system (Bucholz *et al.,*1998). The area is dominated by gold-copper occurrences and an array of ancient workings. According to Summers (1969:106) evidence of ancient working was documented around the Unicorn Mine (NB currently defunct), situated in Lower Gweru (formerly Lower Gwelo). These polymetallic deposits were exploited for iron and copper alongside gold by the inhabitants of Great Zimbabwe or various sub-groups of the Shona speaking people such as the renowned '*Karanga of Shurugwi'* ancient metallurgist as evidenced by various iron smelting sites around the Tebekwe Mine (Swan 1994, 2008; Chirikure 2006).

Furthermore, there is the Limpopo Belt which is characterised by metamorphic rocks that distinguishes the Zimbabwean and Kaapvaal Cratons (Mason 1973; Taylor et al., 2009). The belt cuts across three countries (Zimbabwe, Botswana and South Africa) and is divided into three main sections namely the Northern Marginal Zone, Central Zone and the Southern Marginal Zone (Wilson and Nutt 1988:557; Dodson *et al.,* 2001; Dittrich *et al.,* 2019). All three zones of the Limpopo Belt were heavily exploited by southern African inhabitants (either those at Great Zimbabwe or their nearby or distant polities) during precolonial times for copper as evidenced by shallow ancient working recorded within a 6 km radius from the Limpopo River in the Northern Maginal Zone (NMZ) at the Bande and Dititi tributaries (Kritzinger 2012). The Bande, Dititi and Limpopo confluence area is associated with the Renco type gold and copper polymetallic deposits (Zhao *et al.,* 2014), in the upper section within the region close to the Zimbabwean Craton boundary along the Nyajena (Jena) area.

There is also an array of documented ancient copper mines in the central and Southern Marginal Zone of the Limpopo Belt (these are areas confined to the Messina area, Kaapvaal Craton and Kalahari Basin boundaries section). Evidence of copper exploitation in the northern part of the Kaapvaal Craton area is believed to have commenced around the late first millennium and was dated to around 1000 CE (Evers and Van Den Bergt 1974; Hammel *et al.,* 2000; Killick *et al.,* 2016). The area is also home to the Phalaborwa Igneous Complex which is one of the richest deposits of copper in the world (Forsyth 1987; Bisson 2000; Taylor 2009; Thondhlana 2012). Mines such as Harmony Mine (1260-1900 CE) and Musina (1700-1900 CE) are contemporary to Great Zimbabwe and were the possible sources of copper in form of finished artefacts or ingots (lerale, musuku or convex shaped), circulated across southern African trade network that included Great Zimbabwe (Thondhlana 2012; Thondhlana and Martinon-Torress 2009; Thondhlana *et al.,* 2016; Killick *et al.,* 2016; Moffet *et al.,* 2020).

Furthermore, the Murchison Deposits or greenstone belt are located in the northern section of the Kaapvaal Deposit between the Drakensberg escarpment in the west and Kruger national park in the east, in South Africa. The belt is characterized by an array of minerals and base metals due to its distinctive mineralization, dominated by beryl-emerald confined to the southern section, Sb and Au mineralization on the Antimony Line located on the central part and Cu-Zn mineralization in the northern section of the deposit (Jaguin *et al.,* 2012:1-2; Cairncross and Dixon 1995: 9). Most of the copper-zinc deposits are found in felsic schists, where their ancient working evidence was documented for instance at the contemporary Maranda mine area (Cairncross and Dixon 1995).

The Barberton greenstone belt located on the eastern edge of the Kaapvaal Craton is a polymetallic deposit dominated by gold mineralization and a few copper occurrences. It is predominantly a gold-pyrite-arseno-pyrite mineralization (Cairncross and Dixon 1995:16). The area had evidence of ancient mining, especially on gold deposits where some of the earliest modern mines, from around 1885 CE, such as Sheba were located.
More so, the polymetallic deposits of the Bushman Igneous Complex, within the Rooiberg area have ample evidence of copper deposits. According to Cairncross and Dickson (1995:96) evidence of the earliest mining from Rooiberg is of malachite, cuprite and native copper surface exploitation and working (smelting) at Blaauwbank between 1100-1200 CE. The area is dominated by Cu-Pb mineralization, with some areas especially the western section being dominated by iron oxide copper gold mineralization (IOCG), thus it is indeed a polymetallic deposit that was sourced during the precolonial era mainly for copper, gold and tin.

There is also a possibility that copper deposits in Botswana, such as the hydrothermal copper, lead and zinc mineralization at the Bushman shear zone where the Dukwe mines are located, Matsitama Greenstone Belt (Thakadu Mines) and Tati Green Stone belt (Selkirk Mine and Phoenix Nickel Mine), were sourced for copper by societies in Zimbabwe, Botswana and South Africa (Summers 1969:112; Huffman *et al.,*1995; van Waarden 2012: 230-33). Places where modern/colonial mines such as Selkirk, Dukwe, Molokojwe and Thakadu were located, had ample traces of ancient mining and have visible evidence of metallurgical debris in their vicinity (Summers 1969; Huffman *et al.,*1995; Kinnaird *et al*.,2016). According to van Waarden (2014:13) Dukwe mines yielded dates ranging from 1460-1680 CE which are contemporary to Great Zimbabwe. Therefore, copper from the mine might have been exchanged directly or indirectly via Khami, until it eventually reached Great Zimbabwe (Huffman et al 1995; van Warden 2012).

Furthermore, there is ubiquitous evidence of precolonial copper exploitation across Zambia where some of the remnants of old precolonial mines were documented in the Kansashi, Kabwe and Bwana Mkubwa areas (Bisson 1974; Robertson 2013). Dated evidence from the mines, smelting sites and occupational areas within the vicinity of the Kansashi area show that copper was exploited from around 400-1700 CE (see Bisson

1974,2000). Given the proximity of the Zambian Copper Belt and Great Zimbabwe, there is a possibility that some of the copper ore that was used to manufacture an array of cuprous expressive ware at Great Zimbabwe was sourced in its raw or processed form from these copper provinces.

Namibian deposits are dotted with evidence of ancient mining and smelting within the vicinity, especially at sites such as the Drieriver smelting sites approximately 15 km of the Swartmodder geological deposit (Miller *et al.,* 2005). This is reinforced with evidence across the Damara orogen characterised by heavy concentration of copper, zinc and tin, with noticeable copper deposits concentrated at Otjhase and Onganga mines (Killick 2000; Moore 2010).

This section gave an overview of various geological deposits with evidence of ancient (precolonial) extraction within the neighbourhood of Great Zimbabwe and beyond. Most of the copper and tin mines are contemporary to Great Zimbabwe and various other polities across the landscape, which points towards circulation of the resources from one polity to the other, from copper or tin rich areas to areas without copper and tin through various forms of exchange, until it eventually reached the coastal towns of Kilwa and Sofala on the Indian Ocean coast. It was also highlighted that most modern mines established during the colonial period usually followed deposits with evidence of ancient exploitation.

2.3.4 Discussion

The above sections have shown that both ferrous and non- ferrous metals played an important role in the socio-political and economic setup of the Great Zimbabwe State. The omnipresence of metalliferous ores, primary and secondary production debris and finished objects in-situ across the capital's walled and unwalled areas is testimony to the importance of the metals at the site, unregulated access to metals and household-based production. Given the territory controlled by the Great Zimbabwe state and the documented small-scale production as evidenced by production debris at the site (see Chirikure 2007; Bandama *et al.,* 2016), suggest that most of the metals were siphoned from nearby or distant chiefdoms, attached specialist and polities under the influence of the state. Geologically, south-central Africa is characterized by an array of rich metalliferous deposits with abundant Fe, Cu, Au, Sn, Ni, Pb Zn, with some of the being polymetallic and having undisputable evidence of ancient working as documented by Summers (1969). It is important to note that some deposits fall within the domain of the Great Zimbabwe state while other deposits such as those in northern Zambezi and southern Limpopo regions as well northwestern Botswana were beyond the political monopoly of the Great Zimbabwe elite. For instance, iron and gold usually occurred simultaneously within nearby localities polymetallic deposits such as Renco Mine, Bhani, Mushandike, Charumbira, Chigaramboni, Mashava, Shurugwi, Tokwe Mukosi and Mberengwa (Phiminister 1974; Blenkinskop 1991; Buchholz *et al.*, 1993; Zhao *et al.*, 2014). Therefore, due to their proximity to the capital there is a higher probability that were mined by elites residing at the capital and subjects within the state. In addition, iron might have been sourced in distant deposits such as the Wedza mountains where the well-known Njanja iron specialist sourced their iron ore (Chirikure 2007) and south-eastern Zimbabwe in the Hlambamolonga area (Swan 2007) presentday Malilangwe Conservancy in Chiredzi approximately 100km from the site (Mtetwa 2017). Gold was also mined from distant alluvial reefs during winter season and panned in rivers as far as Odzi-Save, Runde, Sanyati, Runde, Munyati and even Mazowe (Phiminister 1974) before being exchanged across the landscape to Great Zimbabwe and the coastal region (Bhila 1982) and circulated to Great Zimbabwe, across hinterland south-central Africa and the coastal region.

Copper and tin were sourced from diverse deposits and cassiterites within Great Zimbabwe's wider landscapes respectively. The two core cuprous metals (Cu and Sn) were mined from the Zimbabwean and Kaapvaal Cratons, adjacent Mobile belts across south central Africa (namely Zambezi, Limpopo, Mozambique), Katanga and Copperbelt deposits (see Summers 1969; Caimcross and Dixon 1995; Bisson 2000, Kinnard *et al.,* 2014). Thus, copper and tin are believed to have been circulated between inhabitants of Great Zimbabwe capital, subjects within the state and independent polities that resided in these areas either directly or indirectly through attached or non-attached specialist, as gifts, tribute or even marriage alliances. However, the most notable and unquestionable sources of Cu and Sn within southcentral Africa were Rooiberg for Sn (Grant 1999, Molofosky *et al.,*2009,2014, Bandama 2013), and Messina and Phalaborwa (Thondhlana 2012, Moffet 2017), Hurungwe area (Swan 2002, 2007) and the Copperbelt region for Cu (Bisson 2000, Rademakers *et al.,* 2017,2019; Niki and Livingstone 2017) for Cu. Furthermore, Summers (1969)'s detailed documentation of archaeomining evidence across south central Africa (modern day Zimbabwe, South Africa, and Botswana) demonstrates an array of copper, tin, gold and iron mines within Great Zimbabwe's wider landscape. Based on such evidence it is indeed crystal clear that both ferrous and nonferrous metals were exploited within these mines during precolonial times and circulated multi-directional from mining sites, markets, households, villages and capitals of polities such as Great Zimbabwe state across hinterland, and coastal south-central Africa. Despite the above knowledge, there is very little evidence from stratified Great Zimbabwe contexts that have been characterised isotopically, compared with the current Pb isotopes database from various metalliferous deposits and mines across southcentral Africa and legacy data to try and suggest possible mines that were mined for copper by the inhabitants of Great Zimbabwe, hence the major aim of this research. Notably the researcher bears in mind that there are very few radiometric dates from most of mines within southcentral Africa and that most of the deposits are not characterised, which makes this research a bit challenging but a worthwhile adventure. The reason being the current research will assess the effectiveness of using LIA to provenance copper and tin bronzes from the stratified Great Zimbabwe contexts, with the help of the available metalliferous Pb database (see Killick 2021) and archival data. Therefore, laying the foundation for future researchers interested in isotopic geochemistry and provenance studies in south-central Africa.

2.4 Summary

Great Zimbabwe as a state was sustained by trade and exchange from household, village, territorial, and regional to interregional levels. A variety of products were circulated, with metals namely iron, copper, tin, gold, bronze, brass being at the backbone of the metal economy that sustained Great Zimbabwe as a capital and state's socio-economic and political setup. There is indeed undeniable evidence of archaeomining across south central Africa metalliferous deposits (Summers 1969), but little archaeological work has been done to date the mines, understand mining techniques over time and the polities that exploited them. In the absence of such essential archaeological or archaeomining work and well resolved dating across most of Southern Africa, Pb isotopes has the ability to link archaeological metallic specimens to possible mines, geological provinces (zonal, provincial or regional) and even determine the model ages of mineralisation of the deposits sourced for ore used to manufacture the metallic archaeological objects (see Does and Stacey 1974; Stacey and Krammer 1975; Stos-Gale and Gale 2009; Alabarede *et al.*, 2012, Pernicka 2014; Baron *et al.*, 2014; Longman *et al.*, 2018). The next chapter describes samples and data collection procedures employed in this study.

CHAPTER 3

DATA COLLECTION AND ANALYTICAL PROCEDURES

3.1. Introduction

This objects-based research examines copper (4 samples) and tin bronze (22 samples) retrieved during an excavation held at Great Zimbabwe Hill Complex's Southern Terraces (see Chirikure 2020 for details). Great Zimbabwe is comprised of two types of dry-stone walls: freestanding walls and retaining walls. The retaining walls are on the western side (Watergate Path) and the southern side overlooking the Camp Ruins and Curio Shop. There has been a bias in favour of freestanding walls in studies of Great Zimbabwe (see Chipunza 1994; Ndoro 2001). This is despite the presence of massive retaining walls such as Wall 55 on the southern slopes of the Hill Complex.-Part of this wall was restored in 1987 by a team led by David Collett an archaeologist and former conservator with the National Museums and Monuments of Zimbabwe.

In 2018, a decision was made to restore a major collapse on the eastern end of Wall 55 as part of a collaboration between the National Museums and Monuments of Zimbabwe and the University of Cape Town. Wall 55 is situated on the southern slopes of the Hill Complex and is a very long retaining wall that created space for multiple houses to be built on top. The processes of wall restoration were preceded and accompanied by detailed documentation. Thereafter, excavations were performed to the wall foundation to address causes of structural collapse. At the foundation level, a decision was taken to excavate a midden that lay underneath the wall. This yielded copper-based objects, Garden Roller beads, soapstone fragments and animal bone, local pottery and a Chinese celadon fragment. For control purposes, a decision was made to excavate a trench on the Upper Terrace due east of Wall 55. The Upper Southern Terrace Midden was very prolific in terms of copper-based objects, gold foil, glass beads, soapstone, figurines and Chinese apple green celadon. The Wall 55 Trench and Upper Southern Terrace Midden Trench were dated from the 12th centuries to the 15th centuries (see Chirikure 2020). The copper-based objects from the excavations were studied macroscopically at the Great Zimbabwe Conservation Centre and sub sampled for detailed laboratory investigations in Cape Town. The permission to export and conduct invasive archaeometallurgical analysis on the samples at the UCT was granted by the National Museums and Monuments of

Zimbabwe (*hereafter* NMMZ) in Form E permit number 24/10/2019. This chapter presents the analytical procedures adopted in the study.

3.2. Analytical Procedures

3.2.1. Sampling and microscopic analysis

Preliminary analyses started during fieldwork with the separation, bagging and labelling of copper and copper-based artefacts and all metallurgical remains. The nonferrous objects were sorted based on their contexts which were the trenches they were retrieved from namely USTM, Wall 55 Test Pit and Southern Terrace Middens. This was followed by a comprehensive macroscopic and visual analysis that was done at the Great Zimbabwe Conservation Centre Laboratory. Twenty-six (26) nonferrous objects were selected for further studies (see Fig 9 below for the selected objects). Based on macroscopic evidence, the selected copper-based coiled wire objects were mainly wound on a vegetable core and were a mixture of either rounded or rectangular shaped specimens as illustrated by Foreman Bandama and colleagues (consult Bandama 2018 for a detailed distinction between the two typologies). During the macroscopic analyses, various attributes such as decoration and technique of the manufacture, degree of corrosion and the stability of the objects under study were documented and considered before sample selection for further geochemical analysis at the University of Cape Town (UCT *henceforth).* This resulted in the sampling and collection of 26 less elaborate, partially corroded, fragmented and stable copper-based specimens

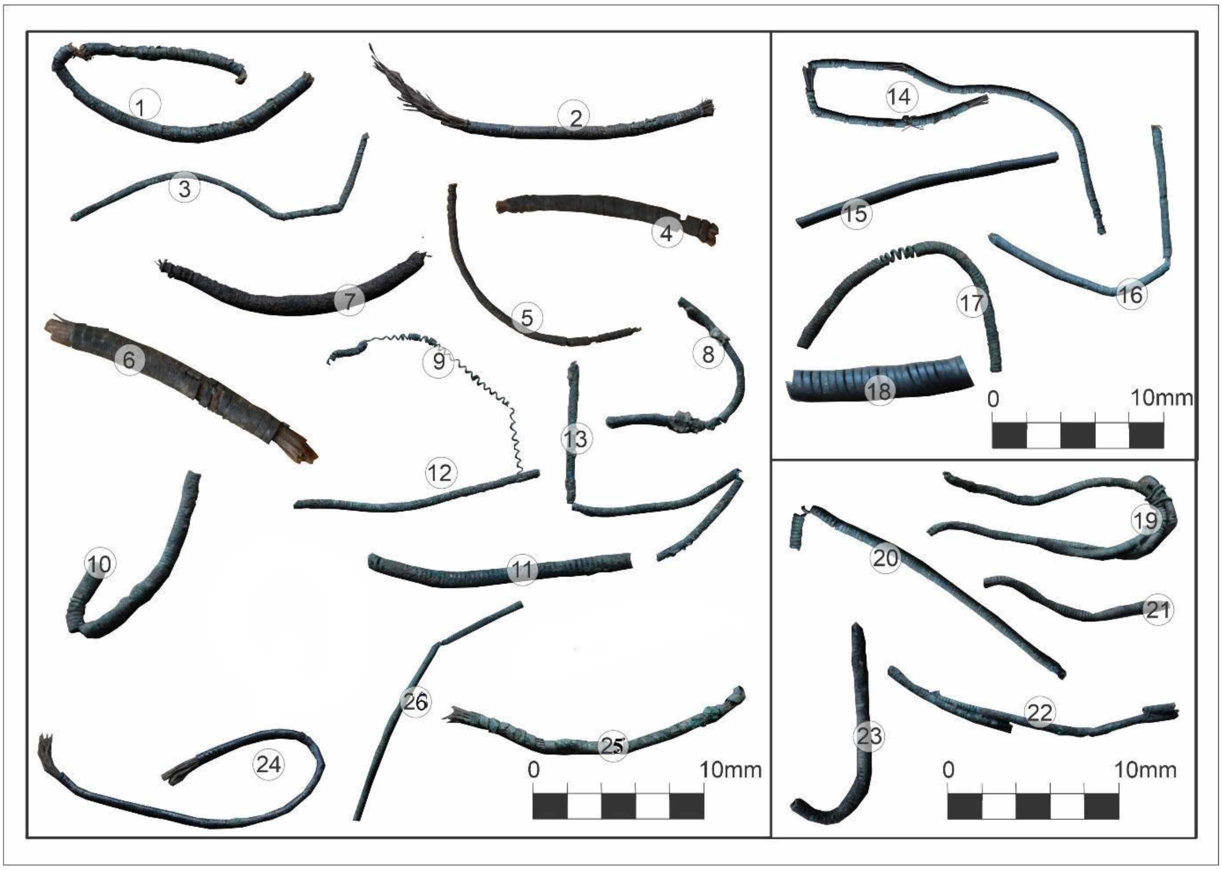

Fig 9: List of samples from USTM and Wall 55 TP1 that were sampled and analysed in this study. Numbers correspond to Table 2 below.

3.2.2. Initial Sample Preparation for Laboratory Techniques

The section gives an overview of the systematic metallographic protocols that were employed during sample preparation and examination at the University of Cape Town's Materials Laboratory (Department of Archaeology), Thin Section Laboratory, MC-ICP-MS Facility (Department of Geological Science) and Electron Microscope Unit. The whole process commenced with assigning name tags based on context and level, and unique laboratory codes for easy identification. The process was done concurrently with documentation of every sample by photographs, which are presented above in Fig 9. Since the samples were going to be examined by Optical Microscopy (OM *hereafte*r), Scanning Electron Microscope Energy Dispersive X-ray Spectrometry (SEM-EDS) and Multi-Collector Inductive Coupled Plasma Mass Spectrometer (*henceforth* MC ICP MS) they required systematic preparation that suited the analytical techniques that were subsequently employed. Thus, the samples will be divided into two groups, one for metallographically analysis (OM and SEM EDS) and the other for isotopic characterization using MC-ICP-MS. The procedures employed from sample preparation and analysis will be explained systematically below.

3.2.3. Sample preparation for Isotopic characterization (MC-ICP-MS)

The initial process of sample preparation commenced with determining the length and weight ideal for the MC-ICP-MS examination. In order, to achieve this goal, the first stage was characterised by cutting a modern copper wire into various lengths ranging from 6mm to 18mm, using handheld mini needle nose pliers. The various lengths had varying weights ranging from 27mg (6mm) to 53.80mg (18mm). The modern copper wire lengths and weight were used as a reference point or a guideline that helped the researcher to choose an ideal length and weight for copper and bronze objects before examination. Based on the results attained from the modern copper wire assessment, the researcher decided to cut the copperbased objects to a length of 9mm. Notably 9mm specimens wound on a vegetable core weighed 39.8mg, whereas those without a vegetable core were 32mg. The extracted 9mm sample for MC-ICP-MS analysis was ideal since it ensured that enough sample size was left behind for further metallographic examination.

The second stage was the cleaning phase which was done to avoid the exterior contamination of samples. The procedure commenced with immersing all samples in 4 millilitres (ml hereafter) 1 % Nitric Acid (HNO_3) solution in a clean Teflon container and placed within the ultra-sonic for about 10 minutes to facilitate the absorbing process. The artefacts were then recleaned using Milli-Q (MQ H_2O) water to remove impurities from handling or HNO_3 used during the preliminary cleaning phase. The MQ H_2O was removed, and the artefacts were strategically placed in an oven at 50°C overnight to dry. The samples were then transferred to the SEM Unit for screening.

3.2.4. SEM EDS analysis of loose copper and copper-based alloy objects

Chemical, microstructural and compositional analysis are the backbone of archaeometallurgical and provenance studies since they enable the researcher to understand the type of metal or alloy that make up their sample. In this case preliminary screening and detailed chemical characterization of the prepared copper and bronze samples was done by SEM EDS to semi-quantitatively determine the various concentrations in the alloys thus, if copper was alloyed with tin (Sn), zinc (Zn), silver (Ag)or lead (Pb) at Great Zimbabwe. SEM is a widely used analytical tool in archaeometallurgical and geological studies across the globe (see Olsen 1983; Miller 2002; Pointing 2004; Caple 2006; Miller and Denbow 2007; Pollard *et al.,* 2007; Thondhlana and Martinon-Torres 2009; Thondhlana 2012; Bandama *et al*., 2013; Oudbash *et al.,* 2013; Molofosky *et al.,* 2014; Moffet 2016; Stephens 2016; Bandama *et al.,* 2018). The widespread use of SEM as an analytical tool is based on the machine's versatility to analyse a variety of specimens, polished blocks and loosely mounted samples, creation of crystal-clear 3D high magnification pictures with good sample depth, specialised section analysis and ability to switch between Black scattered electron imaging mode (BSE henceforth) and the Secondary electronic imaging (SEI) modes (Caple 2006:196-197, Pointing 2004:166-167).

Therefore, due to its versatility, effectiveness, non-invasive nature, ability to screen and comprehensively analyse the major and minor elemental composition of copper-based metals, SEM-EDS was prioritised for the preliminary qualitative analytical phase of samples before lead isotope analysis and was also used for metallographic examination (to be explained later). In this case, SEM analysis was performed using an FEI Nova Nano Sem 230 Scanning Electron Microscopy (SEM) equipped with an Oxford X-Max silicon drift Energy Dispersive Spectrometry (EDS) housed at the Electrone Microscope Unit at UCT. The samples were analysed in two phases. The first phase was the screening of loose cuprous specimens for Sn, Cu, Ag, Pb and Zn. The process was conducted on the first group of samples scheduled for MC-ICP MS and the comprehensive analysis of polished blocks for metallographic purposes (will be explained later under the metallographic examination section).

The loose copper and copper-based alloys specimens were cleaned and prepared for analysis by SEM-EDS. The analytical process was straightforward since it aimed to simply discriminate the elemental composition of the samples understudy. Thus, it was used as a qualitative analytical tool to determine the presence of Cu, Sn, Pb, or Zn in the copper-based objects before lead isotope analysis (LIA *henceforth*) by the MC-ICP-MS. Before SEM analysis the loose cuprous wire samples were labelled, attached to conductive carbon tape and fixed to a SEM sample stub (See Fig 10 Below). The process was very important since it ensured that the samples were identifiable, well earthed, and conductive, to avoid charge built up. However, the samples were not handled with bare hands or even coated since this might have contaminated them before LIA using the MC- ICP-MS. The mounted copper and bronze objects were analysed using the back scatter image (BSE) mode, because its (BSE) signal is proportional to the atomic number of the sample, and it produces images reflecting the composition of the object (Pointing 2004). The instrument was operated at a working distance of 10mm, accelerating voltage of 20 kV, beam current of 1.0 pico-amps, a tilt angle of 0.0 degrees.

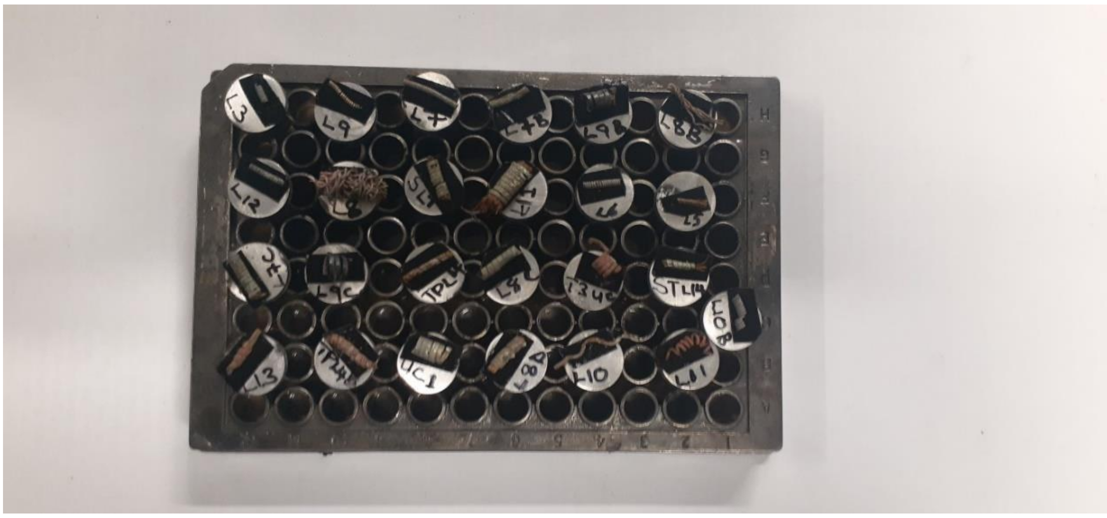

Fig 10: Loose copper and bronze objects on SEM-EDS stub

Analytical results were represented in weight percentages (wt.% *hereafter)* and normalised to 100 percent (% *henceforth*). To ensure compositional comparisons and a clear presentation of the samples, the researcher conducted multiple area scans (≥ four spectrums) per sample, systematically on carbon-free sections (See Fig 11 below). This was reinforced by further analysis of five specimens whereby three scans per sample were done on corroded surface sections of the specimens. The corroded sections were represented by dark angular cracks that penetrate inwards from the edges of metals. The (corroded sections) were analysed to understand the effects of corrosion on the copper and bronze sample's major elements (in this case Cu and Sn) whether they (Cu and Sn) remained constant across the specimen's corroded and uncorroded sections or gradually leaching out. The analysis managed to reveal qualitative data of the concentration percentage of tin and copper in the samples with confidence prior to MC-ICP-MS analysis.

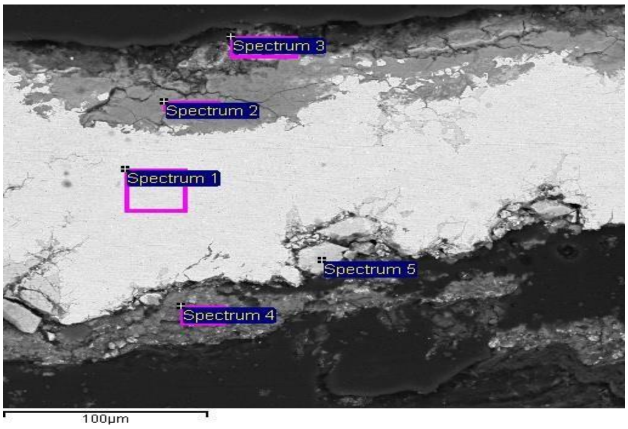

Fig 11: Back Scattered Electron Image showing multiple area scans on carbon-free sections during the screening phase

However, given the nature of the sample understudy and effects of corrosion on most of the samples, a decision was taken to analyse polished blocks, using the same method. Polished blocks are essential since they provide an avenue into the analysis of the metallic matrix after the removal of corrosion by mounting and polishing (Scott 1991, Thondhlana 2007; Moffett 2017).

Protocol and Analysis by MC-ICP-MS

The development and use of the Multi-Collector-Inductive Coupled Plasma-Mass Spectrometer (MC-ICP-MS) revolutionized isotopic analysis and provenance studies (Vanhaecke and Degryse 2012; Hirata 2012). The MC-ICP-MS is a hybrid ICP-MS instrument that is used for measuring isotopic ratios in various fields for example archaeology, geo-cosmochemistry, biogeochemistry, biomedical in clinical studies context and geochronology. The instrument is characterised by an array of ion detectors known as multi collectors (Neff 2011), which enables it to aggregate the potential of superior ionization of the inductively coupled plasma (ICP) source, stability of magnetic mass separation and precision measurement of ion ratios due to simultaneous signal collection. Therefore, due to its plasma source ionization efficiency the MC-ICP-MS instrument studies both traditional (for example Sr, Nd, Pb, Hf) and non-traditional (for example Li, B, Be, Cu, Zn, Cr, Hg, Mo) isotopes (see Vanhaecke and Degryse 2012). Furthermore, data produced by the MC-ICP-MS is more precise as compared to previously utilized lead isotope determination instruments like thermal ionization mass spectrometry

(TIMS) and single collector inductive coupled plasma-massspectrometry (ICP-MS) hence its (MC-ICP-MS) wide acceptance and use in global archaeological provenance studies (see Pointing *et al.,* 2003; Baker *et al.,* 2006; Pollard and Heron 2008; Fen *et al.,* 2009; Stos-Gale and Gale 2009; Neff 2011; Hirata 2012; Barron *et al.,* 2013; Molofosky *et al*., 2014; Stephens 2016; Killick *et al.,* 2020).

Therefore in-order to precisely measure $^{206}Pb/^{204}Pb$, $^{207}Pb/^{204}Pb$ and $^{208}Pb/^{204}Pb$ isotope ratios in the specimens, samples were analysed using one of the two NuPlasma HR instruments at the MC-ICP-MS Facility, Department of Geology Sciences, UCT, equipped with a DSN-1000 desolvating sample introduction system. The MC-ICP-MS instrument at the institution can determine various isotopic systems such as Sr, Nd and Pb by solution and Sr, Pb, Hf, B and Li by laser ablation. In this study, for better precision, the isotopic determination of Pb isotopic system, the samples were analysed as a solution after dissolution and elemental Pb isolation. Cleaned samples were dissolved in ± 4 ml of concentrated, 48M HNO_3 in closed Savillex beakers at 140ºC for 48 hours. Once in solution, the beakers were opened, and samples dried down and redissolved in 2M HNO_3 for elemental separation chemistry. The elemental Pb fraction was isolated using Eichrom Sr.Spec resin and routine, published methods (after Pin *et al*, 2014). The collected Pb fractions from each sample were dried down and redissolved in 2% HNO_3 to a concentration of ±50 ppb Pb for isotope ratio analysis by MC-ICP-MS. All $^{206}Pb/^{204}Pb$, $^{207}Pb/^{204}Pb$ and $^{208}Pb/^{204}Pb$ data presented here are references to accepted normalizing values for the international isotope standard SRM981 for $^{208}Pb/^{204}Pb$, $^{207}Pb/^{204}Pb$, $^{206}Pb/^{204}Pb$ of 36.7219, 15.4963, 16.9405 (Galer and Abouchami, 1998). During analysis, isobaric interference by ^{204}Hg was corrected using on-peak background subtraction. Instrumental mass fraction was corrected using SRM997 Tl standard added to all standards and samples to give ±10:1 Pb:Tl ratio, the exponential law and a $^{205}Tl/^{203}Tl$ value of 2.3889.

The advantages of using this protocol as compared to others employed in provenance studies is that it is cost effective since the resin used can be reused after thorough cleaning, the duration of the whole process is generally short, thus reducing the risk of analyte loss and above all the use of small quantities HCI solution for Pb extraction (Pin *et al*., 2014:1869).

3.2.6. Sample Preparation for Metallographic Examination (SEM -EDS)

The second group (cut offs) of copper and bronze specimens reserved for metallographically examination, were taken to the Thin Section Laboratory in the Department of Geological Sciences at UCT for mounting. During this stage samples were prepared and mounted as polished blocks following standard metallography procedures in the Materials Science Laboratory at UCT, Thin Section Laboratory and guidelines from Scott (1991:63-74). The first procedure was to create an excel spreadsheet with a full list of all 26 specimens which was used for labelling the blocks. The mounting method employed by the researcher was cold mounting. Epoxy resin was used as an embedding material, with 8ml of epoxy being poured first into the Buehler 2,54 cm diameter mold made from silicon rubber. The sample was then carefully laid on the surface of the resin along the edges of the mold and then 7ml of epoxy was added embedding the whole sample. E -poxy was used despite an array of resins being available because it is a two-part system with a catalyst and hardener. The name tags were then added to ensure that the blocks were properly labelled. The embedded samples were cured at room temperature of 23°C under UV light. The curing process was done overnight for 13hours to ensure that the resin sets and attain maximum hardness.

Fig 12: Curing process during its initial stages

After mounting, the resin block was grinded using the Struers Tegra Doser 5 metallography machine housed in the Thin Section Laboratory at UCT. The standardised procedure for sample preparation at this stage was based on Scott (1991:65-66), Thondhlana (2007:27) and guidelines in the Materials Laboratory in the Department of Archaeology. The specimens were subsequently grinded using a wet silicon carbide papers with continuous use of finer grit sizes that ranges from 120, 240,400 and 600. However, given the nature of the cuprous wire samples under preparation, the finest grit that was achieved that did not scratch the specimen was 240.The specimens were further polished with ¼ micron diamond polisher, cautiously cleaned in water, and left to dry to obliterate traces of deformation and abrasiveness that might have been caused by grinding before being examined under the Optical Microscope (OM hereafter).

3.2.7. Sample Examination under Optical Microscopy (OM)

The samples were analysed under the Olympus optical microscope for microscopic examination of the scratch marks or deformations caused by grinding and polishing. The examination under the OM proved essential in adding value to the macroscopic observation of the macrostructures by revealing microstructures of the samples. In this case the OM revealed evidence of minute scratches on most of the blocks that resulted in repolishing using mechanical method. The use of the OM was just a preliminary routine microscopic analysis since the specimens were going to be further examined using SEM-EDS.

3.2.8. Metallographic Examination by SEM -EDS

The current stage involved detailed characterization of the copper-based objects in the form of polished blocks. There is consensus among archaeometallurgists that polished blocks are essential for microscopic analysis of metallic artefacts' microstructure and composition (Scott 1991; Thondhlana 2007,2012; Bandama 2013) since they ensure the scanning of a smoothly cleaned surface area free of accumulated patina. The machine was adjusted to concentrate on major elements such as CU, Sn, Zn, Fe, Au, Ag, As and Pb. The analytical procedures and the working distance employed were similar to those applied when loose cuprous wire specimens were analysed/screened (see under heading 3.2.4). In addition to the above, just like during the analysis of loose copper and bronze objects, multiple area scans (±4 spectrums) were also employed during this process to ensure a comprehensive representation of the sample by SEM-EDS. All analytical results are reported in weight percentages (wt. %) and normalised to 100 %.

3.3. Summary

The chapter gave an overview of the data collection procedures and the analytical protocols employed in this research. It gave an insight into the advantages of the analytical techniques that were employed to understand the nature, microstructure, fabrication techniques and composition of the specimens under investigation. The results are presented in the next chapter.

CHAPTER 4

DATA PRESENTATION, ANALYSIS, AND INTERPRETATION

4.1. Introduction

This chapter presents the results of material analysis obtained from SEM-EDS and MC-ICP-MS analyses of copper and bronze samples examined in this study. SEM-EDS results will be presented first followed by MC-ICP-MS. SEM-EDS results show the various elemental composition, microstructure and working history of the specimens whereas, MC-ICP-MS shows the isotopic composition of the analysed samples. Preliminary archaeometallurgical studies of copper-based material culture from Great Zimbabwe has shown that Cu, Cu-Sn and CuPbZn alloys are pervasive (Stanley 1929; Miller 2002; Bandama *et al.*, 2016:7,2017). Cu-Sn alloys are generally categorised into two standard typologies namely high tin bronze with an Sn content ≥ 14wt %; and low tin bronzes with ≤ 13.9 wt.% tin contents (Scott 1991:25). Miller (2002)'s extensive preliminary research of samples across southern African sites has shown that tin bronzes have a tin percentage that usually ranges between 2.2 to 15.6 wt. %. The range of tin percentage that determines a sample to be classified as a bronze (Cu-Sn alloy) differs from scholars to scholars based on the objective with some scholars setting the standard at 1 wt. % tin content (see Pollard and Bray 2015). However, according to Bandama *et al.,* (2018), the unquestionable archaeological standard of Cu-Sn alloys (tin bronzes) is characterized by Sn weight percentage of ≥ 3. Therefore, this is the standard that will be employed to categorize tin-bronzes in this research, whereas the one used to distinguish between low and high tin-bronzes is based on Scott (1991).

4.2. Results of Material Analysis

Material analysis of the samples revealed that 22 samples were Cu-Sn alloys and the remaining 4 were unalloyed copper. Most of the cross-sections of Cu-Sn alloyed samples showed that they were characterised by a compositional gradient. Based on the quantitative compositional results presented in Table 2, below it is crystal clear that the main metallic elements alloyed at both USTM, and Wall 55 TP 1 were Cu and Sn. Most of the artefacts comprise of traces of Fe, As, Pb, Zn and Ag, but due to the low concentration of these elements as revealed by SEM, the elements can be considered as inherent minor elements of both Cu and Cu-Sn alloy composition. The amount of Cu in

Cu-Sn alloys varies in composition from 90.6 to 96.13wt%, with Sn ranging between 3.15wt. % to 9.6wt%. Whereas, in unalloyed copper samples, Cu reaches up to 99wt%. Based on such compositional inconsistency in Cu and Sn proportions within bronze as revealed by EDS, there is indeed evidence that the alloying process at the southern terrace area of the Hill complex was deliberate and uncontrolled, with the smiths consciously deciding to produce low Cu-Sn alloys and unalloyed Cu for aesthetic, cultural and technological reasons. Such a phenomenon in cuprous metallurgy seems to be common across various contexts at Great Zimbabwe (see published copper artefacts compositional tables compiled from various publications in Bandama *et al.*, 2016:8-11).

Table 2. Normalized SEM-EDS compositional results

Number	Sample Name	Context	Fe	Cu	Zn	As	Ag	Sn	Pb	Total	Metal type
1	Wall 55 TP1 L1	Wall 55 Test Pit	1.96	92.1	bdl[1]	0	bdl	5.94	bdl	100	low tin bronze
2	Wall 55 TP1 L4	Wall 55 Test Pit	0.10	93.90	bdl	0	bdl	6	bdl	100	low tin bronze
3	Wall 55 TP1L5	Wall 55 Test Pit	0.50	97.58	bdl	0.92	bdl	1	bdl	100	unalloyed copper
4	Wall 55 TP UC-T3	Wall 55 Test Pit- Under Collapse	3.22	92.60	bdl	2.19	bdl	1.83	0.16	100	unalloyed copper
5	Wall 55 TP UC1	Wall 55 Test Pit-Under Collapse	0.29	99.01	bdl	0.02	bdl	0.68	bdl	100	unalloyed copper
6	Wall 55 TP L4b	Wall 55 Test Pit	0.55	93.55	bdl	1.19	bdl	3.78	0.78	100	low tin bronze
7	Wall 55 ST:TP1 L14	Wall 55 Test Pit: Southern Terrace Section	0	93.18	bdl	0	bdl	6.82	bdl	100	low tin bronze
8	USTM L1 Step 2	Upper Southern Terrace Midden	0	90.8	bdl	bdl	bdl	9.2	bdl	100	low tin bronze
9	USTM L3	Upper Southern Terrace Midden	1.20	91.89	bdl	0.10	1.80	4	0.80	100	low tin bronze
10	USTM L3 artefact	Upper Southern Terrace Midden	1.02	94.80	bdl	0.08	bdl	4.10	bdl	100	low tin bronze
11	USTM L6	Upper Southern Terrace Midden	0.88	96	bdl	bdl	bdl	3.22	bdl	100	low tin bronze
12	USTM L7	Upper Southern Terrace Midden	0.18	96.81	bdl	bdl	bdl	3.01	bdl	100	low tin bronze
13	USTM L7B	Upper Southern Terrace Midden	2.78	88.8	bdl	1.09	bdl	7.33	bdl	100	low tin bronze
14	USTM L7C	Upper Southern Terrace Midden	0.83	90.17	bdl	bdl	bdl	9	bdl	100	low tin bronze

[1] bdl means below instrument detection limit

15	USTM L8	Upper Southern Terrace Midden	bdl	95.6	bdl	0.04	bdl	4.4	bdl	100	low tin bronze
16	USTM L8(B)	Upper Southern Terrace Midden	2.55	93.57	bdl	bdl	bdl	3.88	bdl	100	low tin bronze
17	USTM L8C	Upper Southern Terrace Midden	0.80	93.49	0	0.03	0	5	bdl	100	low tin bronze
18	USTM L8(D)	Upper Southern Terrace Midden	0.13	93.01	bdl	bdl	bdl	5.91	0.95	100	low tin bonze
19	USTM L9	Upper Southern Terrace Midden	3.10	86.95	bdl	0.12	1	7.02	0.82	100	low tin bronze
20	USTM L9(B)	Upper Southern Terrace Midden	2	92.59	bdl	bdl	bdl	3.13	0.80	100	low tin bronze
21	USTM L9C	Upper Southern Terrace Midden	1.80	92.4	bdl	bdl	bdl	5.80	bdl	100	low tin bronze
22	USTM L10	Upper Southern Terrace Midden	2.25	93.06	0.12	2.09	bdl	2.48	0.33	100	unalloyed copper?
23	USTM L10(B)	Upper Southern Terrace Midden	0.49	95.22	bdl	bdl	bdl	4.29	bdl	100	low tin bronze
24	USTM L11	Upper Southern Terrace Midden	4.89	91.08	bdl	bdl	bdl	4.03	bdl	100	low tin bronze
25	USTM L12	Upper Southern Terrace Midden	0.72	96.13	bdl	bdl	bdl	3.15	bdl	100	low tin bronze
26	USTM L13	Upper Southern Terrace Midden	1.01	93.92	bdl	bdl	bdi	3.75	1.32	100	low tin bronze?

Pb is also detected as a minor element among most Cu-Sn alloys, with most of it being below 1wt% except for samples USTM L13 where it is 1.32 wt. %. One of the most striking observations is that there is a significant amount of visible Pb globules found within Cu matrixes (See Fig 13 below) and very few within Sn metallic phases. Thus, enough proof that Pb is insoluble with Cu (Scott 1991; Oudabeshi and Davin 2014:76) and it might be an element inherent in Cu ores due to its omnipresence in Cu metallic phases. This is based on the fact that the number of visible Pb globules in a metallic matrix represents the concentration of the element in a sample (see Oudbash and Hsanpour 2016), thus confirming that Pb was a major element in Cu rather than Sn. Previous archaeometallurgical studies have shown that Pb globules within copper matrixes or grain boundaries are formed during the solidification process of copper-lead solutions because copper solidifies first resulting in the formation of Cu-Pb eutectic and segregation of Pb (Scott 1991:23). Notably, there is documented evidence of leaded metals from other archaeological contexts at Great Zimbabwe that postdates the Hill Complex southern Terrace area, with the most notable one being a finger ingot pewter (Sn 23 wt % and Pb 77%) from the Valley Ruins (Huffman and Vogel 1991; Miller 2002). In addition, there is documented evidence of elevated levels of Pb in most metals (gun metals) across southern African polities (for instance such as Mapungubwe, Thulamela and even the Swahili Coast) see (Miller 2002; Killick et al 2002) and even the famous leaded Igbo-Ukwu bronzes with varying Pb composition (see Chikwendu *et al.,* 1989; Shaw *et al.,* 1989; Craddock *et al.,* 1997). Thus, ancient metal workers across sub–Saharan Africa intentionally mixed Pb, Cu, Sn to produced leaded tin bronzes and other gun metals. However, evidence from this study shows that the amount of Pb in both unalloyed Cu and Cu-Sn alloys is very low for it to be considered an intentional addition, thus it was a mere impurity associated with metallic Cu ores exploited at the site.

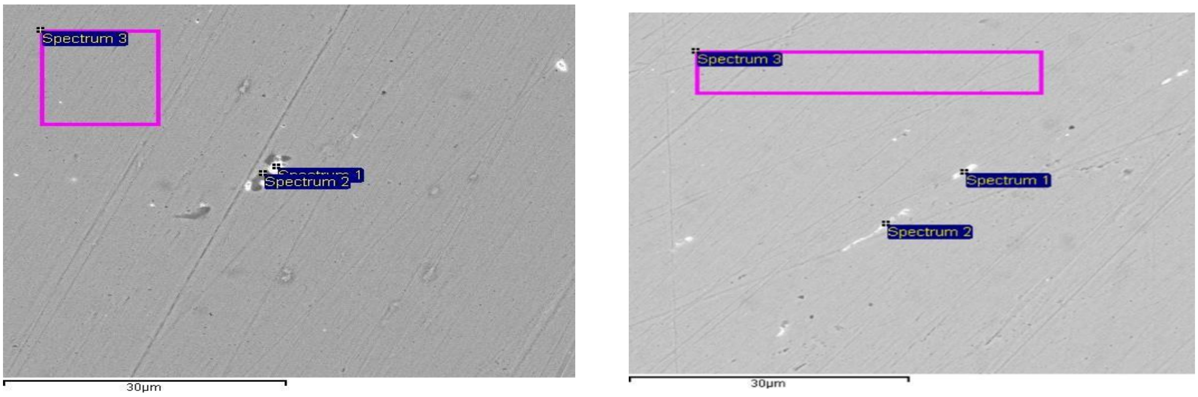

Fig 13: SEM BSE images showing evidence of Pb globules in sample USTM L 9b and elongated Pb inclusion in Sample Wall 55 TP L4b, respectively (from left to right).

In addition, there is evidence of dark/black inclusions of various shapes and sizes. The inclusions appear across most Cu-Sn alloy objects microstructure as spherical minute dots, smears or elongated lines (see Wall 55 TP L4 Fig 14). Micro-compositional analysis of the black dots by EDS shows that the dark inclusions have high Cu concentration, which suggests that there were by-products of the partial transformation process of sulphidic Cu ores into metal due to its low miscibility (see Oudbashi and Davami 2014:76, Silver *et al.*, 2008). The partial transformation process of sulphide copper might have been made possible by the fact that ancient smiths at Great Zimbabwe did not intentionally roast their Cu ores before smelting them. This is backed up by the contemporary lack of tangible evidence of Cu-S ore roasting in the form of copper matte at any Great Zimbabwe or other Iron Age sites in southern Africa (see Miller 2002:1102). Hence there is a higher probability that Cu-S ores sourced from several deposits and mines across south-central Africa (see Stephens 2016 and table 6 further below for deposits and mines with sulfidic ores) were directly smelted at Great Zimbabwe. Aided with the presence of Fe $\leq$ 4.wt % across most Cu and Cu-Sn alloys there is indeed a higher probability that the smiths at Great Zimbabwe Hill Complex southern terrace areas smelted Cu containing ores such as chalcopyrite ($CuFeS_2$), chalcocite (Cu_2S) or even bornite (Cu_5FeS_4).

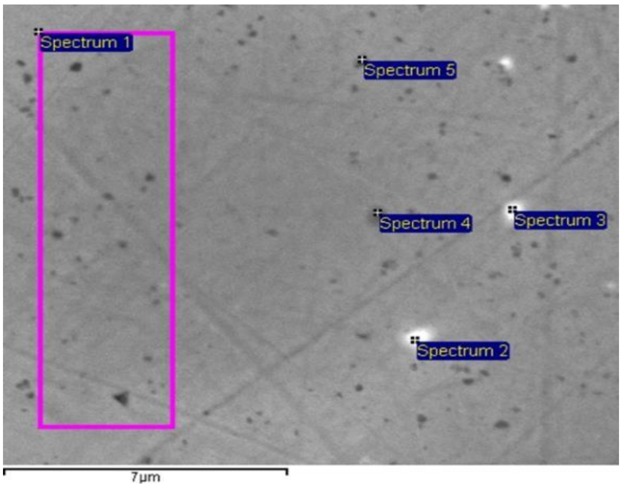

Fig 14: SEM-BSE Images of the central section of sample No:6 Wall 55 TP L4 showing minute dotted black Cu-S inclusions, bright white Pb inclusions and twining lines within a bronze. NB this is a Cu rich phase.

One of the most striking inclusions are Zn and Ag which are very rare and only occur in two separate samples. Zn occurs in a Cu-Sn sample USTM L10, which is also characterised by strain lines, intergranular cracking, and the development of a pseudomorphic corrosion layer on the surface of the sample. The availability of Zn in a Cu phase of sample USTM L10, at very low concentration, confirms previous observation by Foreman Bandama and colleagues of brass metallurgy at Great

Zimbabwe as evidenced by traces of Zn within a smelting crucibles GZ 34 and GZ 49 found in the Hill Complex (see Bandama *et al.*, 2016; 2017). There is consensus among archaeometallurgists that Zn mixed with Cu to manufacture brasses at Great Zimbabwe and other polities was sourced from the Indian Ocean (Miller 2002; Thondhlana and Martinon Torres 2009; Bandama *et al.*, 2016, 2017, 2018; Chirikure *et al.*, 2019). However, in this case, given that the smiths at the site knew how to add adequate amounts of Zn in Cu to manufacture brass, there is a higher probability that the small trace of Zn in this sample was either an impurity in Cu ore from a complex mineralised mine or was accidentally smelted in a crucible used to manufacture brass.

Similarly, traces of Ag occur in very small quantities, in sample number 9 (USTM L3) and 20(USTM L9 b), suggests the use of Cu ores from polymetallic deposits that had gold (Au) and silver or reuse of crucible moulds used to melt gold at the site. The reason being preliminary analyses of crucibles and prills from Great Zimbabwe revealed evidence of Au with very high amounts of Ag (see Bandama *et al.*, 2017). To note, Sample USTM L9b is the only sample characterised by both Ag and Pb impurities homogenous distributed across its Cu metallic phase. See Images below with bright white Ag inclusions within a Cu-Sn matrix.

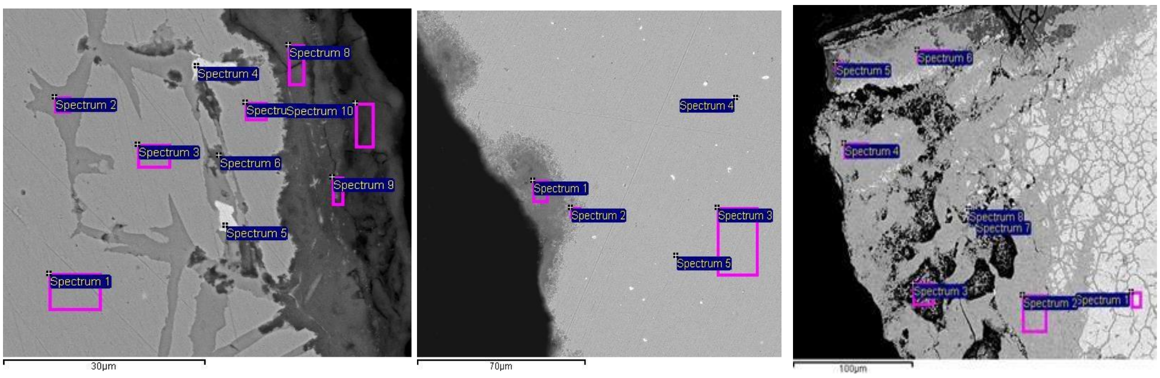

Fig 15: SEM BSE Images showing evidence of Au in Cu matrix in sample USTM L 3 (spectrum 4 and 5) and Sample USTM L9b with traces of Pb and Ag from the core to the edge of sample especially on spectrums (images on the centre to far right)

Most unalloyed Cu samples are composed of varying Cu percentage between 93.18 wt% up to 100wt %. Three samples are made up of a nearly homogenous structure with pseudophomic corrosion developing at the edge of the samples. To note sample USTM L 10 which is classified as an unalloyed Cu fragment is characterised by traces of Fe, As and Sn ≤ 3wt %. Therefore, despite the presence of Cu-Sn-Zn-Fe being observed in this object the elemental amount is not enough for it to be classified as a ternary alloy with Cu-Sn-As-Pb-Fe alloy, rather most of the elements seem to be impurities inherent within the Cu ores that was smelted and fabricated to make the specimen. Sample number 22 (USTM L10) confirms with certainty that traces of Fe, Pb, As and Zn are inherent within Cu hence why they were mainly visible within Cu phases across all samples even Cu-Sn alloys. However, despite traces of Fe within the Cu and Sn matrixes (microstructure), there was no visible evidence of exsolved Fe in sample number 22 (USTM L10) or even other samples analysed in this study.

Microstructurally, most of the samples are characterised by recrystallised grain size with distinctive strain and twinned lines. The twinned lines appear to inform of straight lines and cut across the Cu-Sn matrixes (see Fig 13 below of Fig 14 above), whilst the strained lines appear close to the edge or surface of most of the Cu-Sn samples examined under EDS which is typical of most prehistoric binary Cu alloys objects found across the world see (Scott 1991; Oudebashi and Davin 2014; Oudbashi and Hasanpour 2016:4). Evidence of twin lines and longitudinal striations suggest that both Cu-Sn alloy and Cu objects went through cycles of cold and hot working, before being wire drawn through draw plate (Child 1995; Miller 2002; Thondhlana 2007; Bandama et al., 2016). To note, wire drawing was done concurrently with the annealing process since it ensured that the objects were ductile and remained soft during fabrication (Scott 1991). SEM evidence from Great Zimbabwe's Hill Complex Southern Terrace area presented here, agrees with preliminary metallography analyses of Cu-Sn, Cu, Zn, Au objects from various Iron Age sites namely Jahunda, Mapela, Danamombe (Khami), Mapungubwe, Bosutwe, Thulamela, Rooiberg and even Bosutwe (Miller 2002; Thondhlana 2007; Thondhlana and Martinon Torres 2009; Bandama 2013, *et al.*, 2018). This, therefore, shows that the fabrication techniques used to manufacture non-ferrous coiled and wound wire specimens were homogenous at Great Zimbabwe, across south-central African sites that predate, are contemporary and postdate Great Zimbabwe.

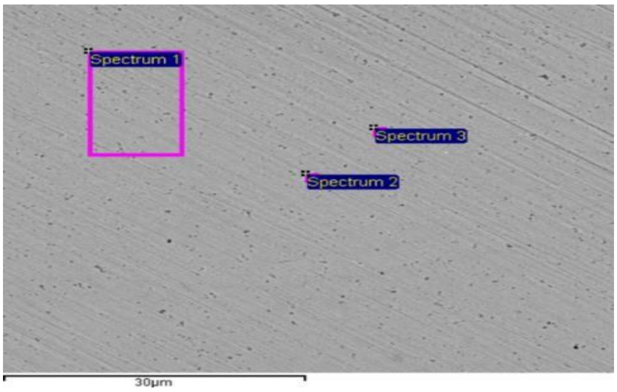

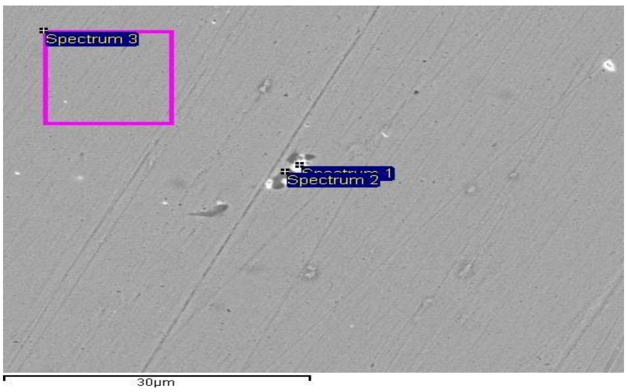

Fig 16: SEM BSE Images of samples USTM L 1 and USTM L9b showing evidence of annealing twins, black and white inclusions respectively.

In addition, most Cu-Sn alloy samples are characterised by clearly distinguished phase segregation and cored dendritics. Based on SEM the microstructure of the samples shows dendritic arms and the existence of binary-phase microstructures which are characterised by two colours namely white and grey. NB SEM does not produce coloured images. The shades of the two main colours, white and grey vary from sample to sample (See Fig 17 below). In this case, phases are loosely defined as the homogenous state of the objects with a clearly defined composition (Scott 1991:5). EDS microanalysis of the distinctively coloured phases revealed that the samples were characterised by compositional gradient, whereby the whitish phase is Cu rich, the greyish/silver grey is Sn enriched and the black edges being oxide dominated due to corrosion. According to (Scott 1991:5) compositional gradient occurs during the cooling and solidification of tin bronze whereby the alloy solidifies by dendritic segregation with copper-rich constituencies solidifying first whilst tin percentage increases in the outer surfaces. The process is also referred to as coring and it is pervasive among tin-bronzes, however, some Cu-Sn alloys and unalloyed Cu samples were characterised by a nearly homogenous phase across the whole sample as seen in sample USTM L10 presented below.

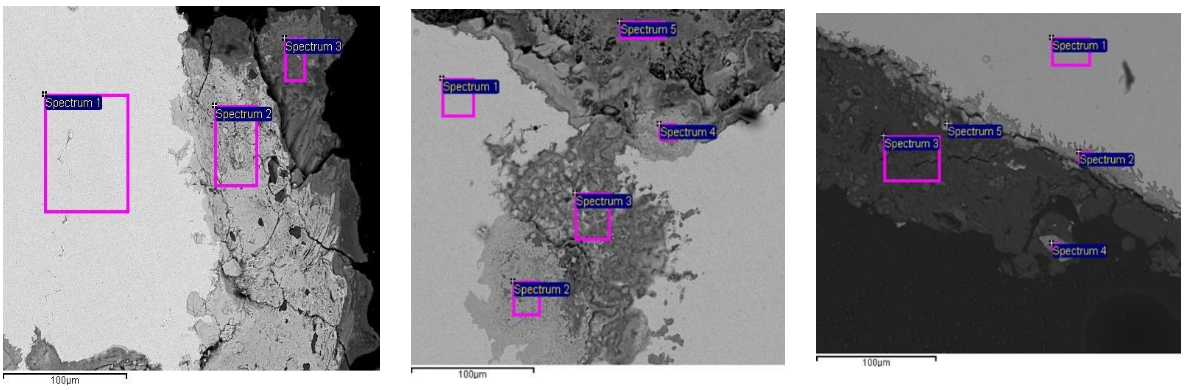

Fig 17: SEM-BSE images showing evidence of phase segregation, development of a dendritic within a Cu matrix and corrosion layer on the edge of sample Wall 55 TP 1

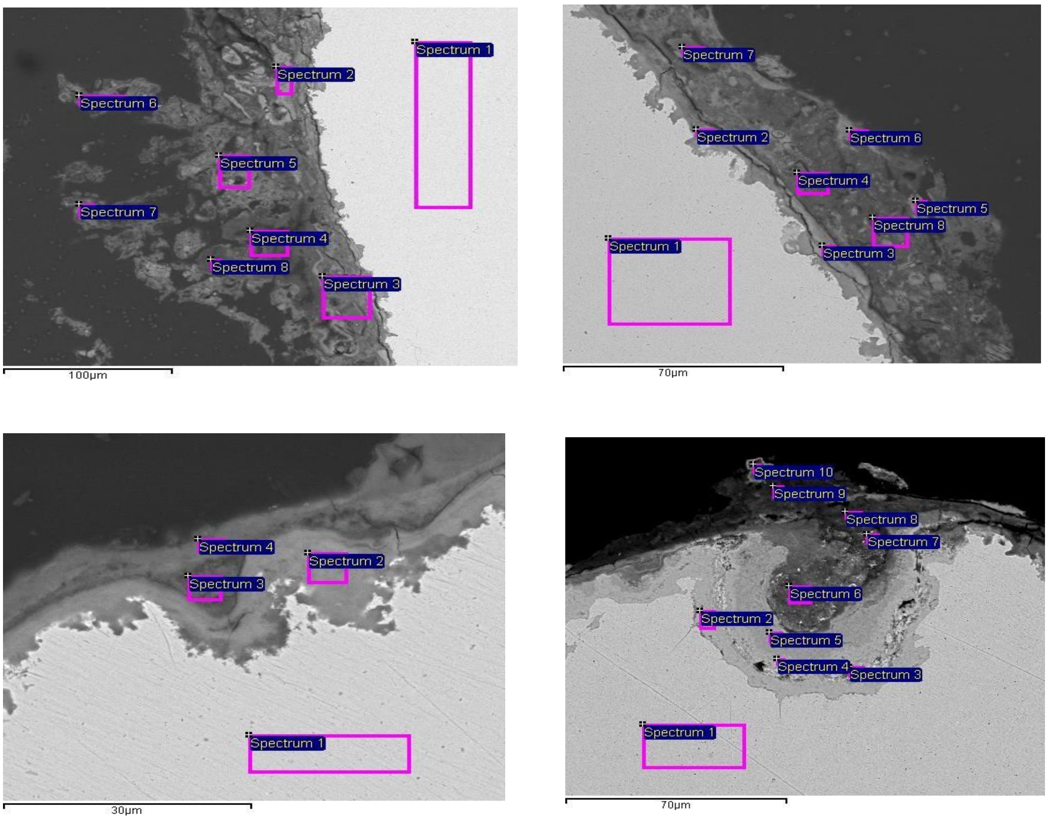

Fig 18: SEM -BSE images showing evidence of a nearly homogenous phase across USTM L10 (sample number 22) which is dominated by a whitish colour rich in Cu.

In addition, some of the samples exhibited the development of corrosion mostly on the surface, with some being attacked and penetrated inside resulting in intergranular corrosion. It seems like the process eventually resulted in the development of a pseudomorphic corrosion layer over the bronze metallic matrix and enhanced localized surface cracking close to the edge of the surface of sample number 26 (USTM L13) presented below in Fig 19. Notably cracking localized on the margin of most samples seems to have been a result of stress-induced on samples during mechanical working processes such as wire drawing and coiling on a vegetable core, before being colonized by corrosion after deposition. The reason is, microanalysis that was done on the edge of some samples showed varying results, that ranged from homogenous composition with the rest of the sample to evidence of decuprification which is typical of corrosion. According to Piccardo *et al.*, (2007:242) decuprification is the selective dissolution of copper which results in Sn enrichment since it acts as a stabilizing agent for patina development.

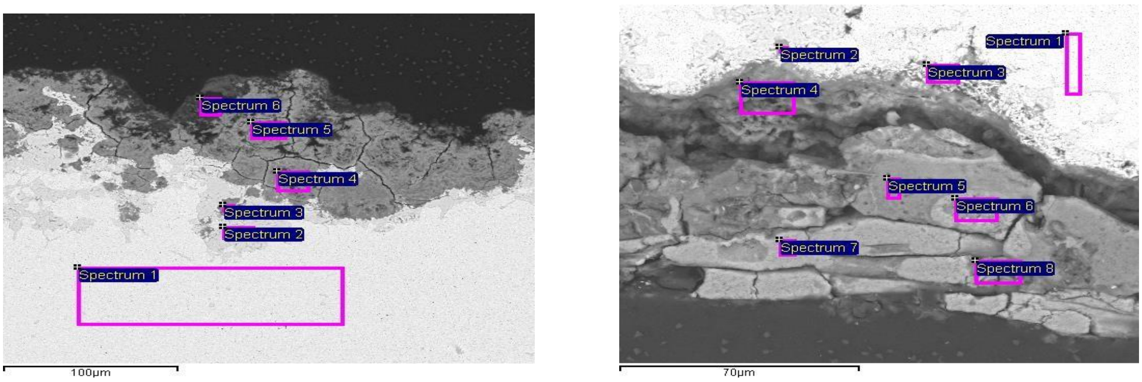

Fig 19: SEM-BSE Images showing evidence of cracking on the edge of the sample number 26 (USTM L13) and development of a corrosion layer dark greyish in colour. Note that the image to the right is a zoomed image of the area to the edge of the sample.

In contrast to the above, there was also evidence of a black phase that cut across the centre of some of the samples analysed in this study. This phenomenon was limited mostly to specimens that were wound Cu- Sn specimens that were wound on a vegetable core, with it being evident on specimens Wall 55 UC T3, USTM L3, USTM L8a, and USTM L12. Micro-EDS analyses were conducted randomly on the black coloured areas revealed that on an unalloyed Cu sample the elemental composition remained homogenous whereas on all Cu-Sn alloys there seem to be enriched As, which might have been a result of a gradual chemical reaction between the fibre and the metallic phase. Tylecotte (1979) showed that different environmental conditions result in different organic effects on copper and tin bronzes, with most organic materials decomposing and forming oxides and protective layer around the copper, however, this is a different case scenario since a vegetable core (organic material) was wrapped inside the tin bronze wire. Therefore, the black phase might have been a protective layer on top of a metallic phase.

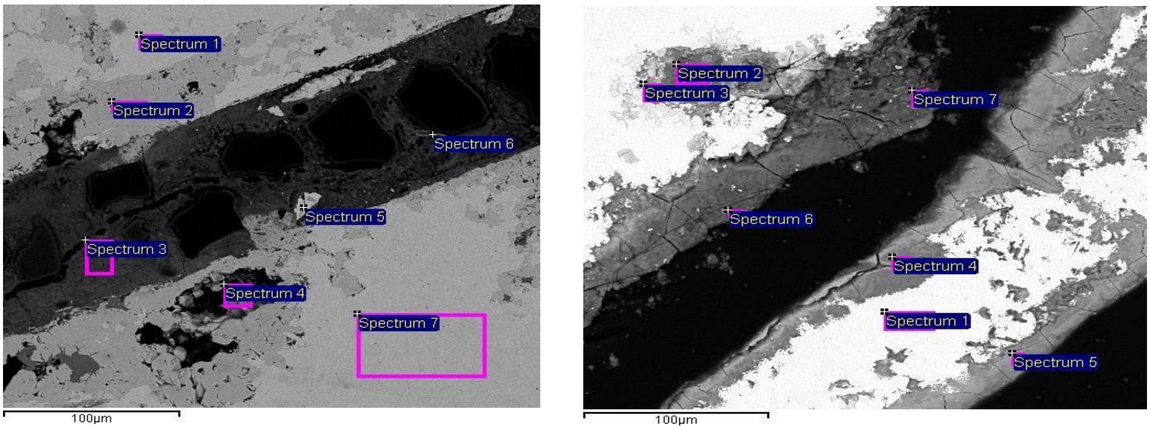

Fig 20: SEM-BSE images showing evidence of a black phase cutting across the core of samples 4 and 15 (Wall 55 UC T3 and USTM L8)

4.3. Results of lead isotope analysis (LIA)

High-precision isotopic measurements were conducted on a total of 26 flexible coiled wire fragments from Great Zimbabwe. Notably the reported isotopic ratios are results of cleaned copper and tin-bronzes wires with no green jacket analysed in this study. The measured isotopic ratios from Great Zimbabwe are presented in Table 3 below. The isotopic data from Great Zimbabwe will be used to assess the effectiveness of LIA as a fingerprinting tool by matching it against various metalliferous ore deposits from across south-central Africa that were exploited in precolonial Africa. The ore data utilised in this study were documented and published by Killick *et al* (2020), as additional material titled ARCM 12573-sup- 001 see link attached in Appendix 3. Notably the database is characterized by Pb isotopic ratios (LIR *henceforth*) from various regions namely southern Africa, Caucasus, Arabia, Tibet, China, Europe, Mediterranean and South America. However, for the purposes of this study Pb ratios from the southern African region were prioritised. The LIR from both the Great Zimbabwe samples and metalliferous southern African database were analysed and interpreted using a standardised traditional biplot system of $^{207}Pb/^{204}Pb$ vs $^{206}Pb/^{204}Pb$ and $^{208}Pb/^{204}Pb$ vs $^{206}Pb/^{204}Pb$ (Baron *et al.,* 2014) and the Mu-Kappa-T system (MATLAB Script) based on Stacey and Kramer (1975) and Albarede *et al.,* (2012). Importantly, isotopic data or ratios in this research were presented in the form of the radiogenic to non-radiogenic isotope.

Table 3. Calculated Pb ratios of analysed copper and tin bronzes

Number	Sample Name	$^{208}Pb/^{204}Pb$	±2s internal	$^{207}Pb/^{204}Pb$	±2s internal	$^{206}Pb/^{204}Pb$	±2s internal	type of metal
1	WALL 55 #1	39.4899	0.0019	16.0337	0.0006	20.3177	0.0008	low tin bronze
2	WALL 55 TPL5	39.2237	0.0030	15.7866	0.0011	18.9094	0.0011	copper
3	W55 TP1L4	41.3386	0.0026	16.9980	0.0009	27.7263	0.0011	low tin bronze
4	WALL55 UC-T3	46.7839	0.0026	16.3352	0.0007	20.1721	0.0008	copper
5	WALL55 UC1	39.2215	0.0022	15.9787	0.0007	20.0293	0.0008	copper
6	WALL 55 TPL4b	37.7086	0.0028	15.6589	0.0009	18.1758	0.0010	low tin bronze
7	WALL 55 ST:TP1 L14	39.1256	0.0037	15.9005	0.0012	19.4173	0.0017	low tin bronze
8	USTM L1 Step 2	38.6601	0.0028	15.7053	0.0010	18.4254	0.0010	low tin bronze
9	USTM L3 a	37.9375	0.0033	15.6580	0.0010	18.1590	0.0010	low tin bronze
10	USTM L3 b	37.9112	0.0027	15.6536	0.0009	18.1310	0.0008	low tin bronze
11	USTM L6	37.7351	0.0021	15.6417	0.0007	18.0914	0.0007	low tin bronze
12	USTM L7	38.3881	0.0028	15.7584	0.0009	18.7104	0.0008	low tin bronze
13	USTM L7B	37.9198	0.0030	15.6543	0.0011	18.1399	0.0010	low tin bronze
14	USTM L7C	39.0247	0.0029	15.9816	0.0010	19.9431	0.0010	low tin bronze
15	USTM L8 artefact	38.7783	0.0033	15.6782	0.0010	18.6105	0.0010	low tin bronze
16	USTM L8(B)	48.5534	0.0047	17.3662	0.0012	31.7271	0.0045	low tin bronze

17	USTM L8C	37.9798	0.0022	15.6581	0.0008	18.1981	0.0007	low tin bronze
18	USTM L8(D)	39.0585	0.0034	15.7424	0.0012	18.5778	0.0011	low tin bronze
19	USTM L9	37.9936	0.0031	15.6579	0.0010	18.2166	0.0010	low tin bronze
20	USTM L9(B)	37.6950	0.0027	15.6430	0.0009	18.1088	0.0008	low tin bronze
21	USTM L9C	37.6824	0.0026	15.6400	0.0009	18.0967	0.0009	low tin bronze
22	USTM L10	44.5798	0.0038	16.4261	0.0013	20.5199	0.0013	copper
23	USTM L10(B)	38.8041	0.0029	15.7255	0.0010	18.5415	0.0009	low tin bronze
24	USTM L11	35.2543	0.0020	15.3830	0.0008	15.7318	0.0007	low tin bronze
25	USTM L12	38.8934	0.0025	15.7019	0.0009	18.6209	0.0010	low tin bronze
26	USTM L13	45.0377	0.0040	20.6785	0.0016	88.8247	0.0068	low tin bronze

The lead isotopic ratios from the Great Zimbabwe Southern Terrace area and various mineralogical deposits across south-central Africa were tabulated in Microsoft Excel before plotting using CoPlot, IsoPlot R and MATLAB. During the tabulation phase, data from southern African metalliferous deposits was classified and given unique codes (Numbers 1-36) based on the location of the mine (country, tectonic and provincial deposit) and the number of samples from a certain mine or provincial deposit in the absence of mines. These variables played an essential role since mines that were characterized with 5 isotopic data ratios were classified into a single class (characterized by a unique number), whereas those that contributed less than 5 isotopic data ratios were searched on Google Earth to cross-check their proximity in relation to other mines, with the closest ones regarding geographical distance, provincial and tectonic deposits being grouped together to form a single class. (Notably except for Rooiberg mine and Mazowe deposits). In addition to the above, the data was further grouped into 16 groups based on the classes developed earlier (assigned with unique codes). The groups were influenced by the total number of LIR from each class with unique codes (see Table 4 further down with simplified classes and groups). Such an approach was done to ensure easy data management during plotting, avoid clustering and enhance visualization of the data on the scatter plots, since most of the characterized ore deposit isotopic ratios available (+480) from most of central and southern Africa tend to overlap and closely cluster together.

Furthermore, a decision was taken to present and plot isotopic data ratios in the simplified form of radiogenic to non-radiogenic ratios $^{206}Pb/^{204}Pb$ versus $^{207}Pb/^{204}Pb$ since the technique is better at recognising or discriminating samples or ores sources, easily calculatable and offers a window into understanding the unevenness of isotopic signatures of all three isotopic ratios ($^{208}Pb/^{204}Pb$, $^{207}Pb/^{204}Pb$ and $^{206}Pb/^{204}Pb$) based on their typical decay chain (Doe and Stacey 1974:758; Baron *et al.,* 2014:677) compared to the conventional way of $^{207}Pb/^{206}Pb$ and $^{208}Pb/^{206}Pb$ (see Doe and Stacey 1974:758; Barron *et al.,* 2014:677; Longman *et al*., 2018; Killick *et al.,* 2020).

4.3.1. Great Zimbabwe Copper and Bronze Lead Isotopic Composition

The Great Zimbabwe Southern Terrace area yielded a wide range of LIR as indicated on the uranogenic Pb isotopes ^{206}Pb and ^{207}Pb. These can be classified into two main types namely highly radiogenic (also known as abnormal or anomalous lead) and radiogenic isotopic ratios (see Table 3 above). Generally, these two main groups (highly radiogenic and radiogenic lead isotopic ratios) are indicated by the composition of $^{206}Pb/^{204}Pb$, with high radiogenic Pb isotopic values ≥ 19.5 (Molofsky *et al.,* 2014; Rademakers *et al.,* 2019; Liu *et al.,* 2018:22). Based on the Stacey and Kramer model radiogenic Pb isotopes values are slightly above common Pb ratios in the earth's crust (see Stacey and Kramer 1975 two stage model). In this study, only 8 samples can be classified as containing highly anomalous lead isotopic ratios. Based on their chemical composition three of the samples are unalloyed Cu whilst the rest are tin bronzes (low tin bronzes). In addition to the above, samples with high radiogenic lead isotopic ratios (LIR hereafter) are evenly distributed between the main archaeological contexts within this study (USTM and Wall 55 TP 1 area), with each context having four samples with highly radiogenic ratios. Thus, showing that there is no distinctive correlation between metallic typologies, LIR and the archaeological context in this study.

Generally, the highly radiogenic Pb isotopes ratios from Great Zimbabwe exhibit a range of $^{206}Pb/^{204}Pb$ = 19.95-88.82, $^{207}Pb/^{204}Pb$ = 15.98-20.68 and $^{208}Pb/^{204}Pb$ = 39.02-48.55. In particular, the most distinctive ratios across the two uranogenic Pb plots (derived from radiogenic decay of uranium in this case ^{238}U and ^{235}U respectively) are 88.82 for $^{206}Pb/^{204}Pb$ and $^{207}Pb/^{204}Pb$ =

20.68. These ratios are all displayed by a single low tin bronze sample USTM L13. Furthermore, most of the remaining samples are characterised by radiogenic Pb isotopic ratios which have values slightly below highly radiogenic Pb values, with $^{206}Pb/^{204}Pb$ = 18.10-19.4 and $^{207}Pb/^{204}Pb$ between 37.68-39.22. Samples with radiogenic isotopic ratios derived from the radioactive decay of thorium in this case ^{232}Th (thorogenic) have values that are less variable as compared to samples with highly radiogenic Pb ratios, since their ratios are ≤ 40 ($^{208}Pb/^{204}Pb$ = 35.2443-39.2237). Notably the most distinctive sample in this class (Sample with radiogenic Pb values) is USTM L11. It (USTM L11) is a low tin bronze with very low radiogenic Pb ratios across the two uranogenic values with $^{206}Pb/^{204}Pb$ = 15.73 and $^{207}Pb/^{204}Pb$ = 15.3829.

4.3.2. Matching Great Zimbabwe LIR versus Southern African Deposit LIR using Conventional Biplots

The initial stage before exploring Pb isotopic ratios in detail was to formulate general biplots ($^{207}Pb/^{204}Pb$ vs $^{206}Pb/^{204}Pb$ plots and $^{208}Pb/^{204}Pb$ vs $^{206}Pb/^{204}Pb$), to assess the pattern of LIR produced by MC-ICP-MS in relation to the available database ratios. Thus, the procedure was done to check if coiled wire samples Pb ratios were compactible or had any consistency with the characterized Pb ratios in the southern African database. The plots showed that most of the samples analysed in this study do match and deviate with various metalliferous ore samples from various deposits across southern Africa. However, due to the overlapping nature of southern African database isotopic ratios and the total number of variances or series that was plotted it was difficult to develop good distinctive conventional Pb plots as presented in Fig. 21 below.

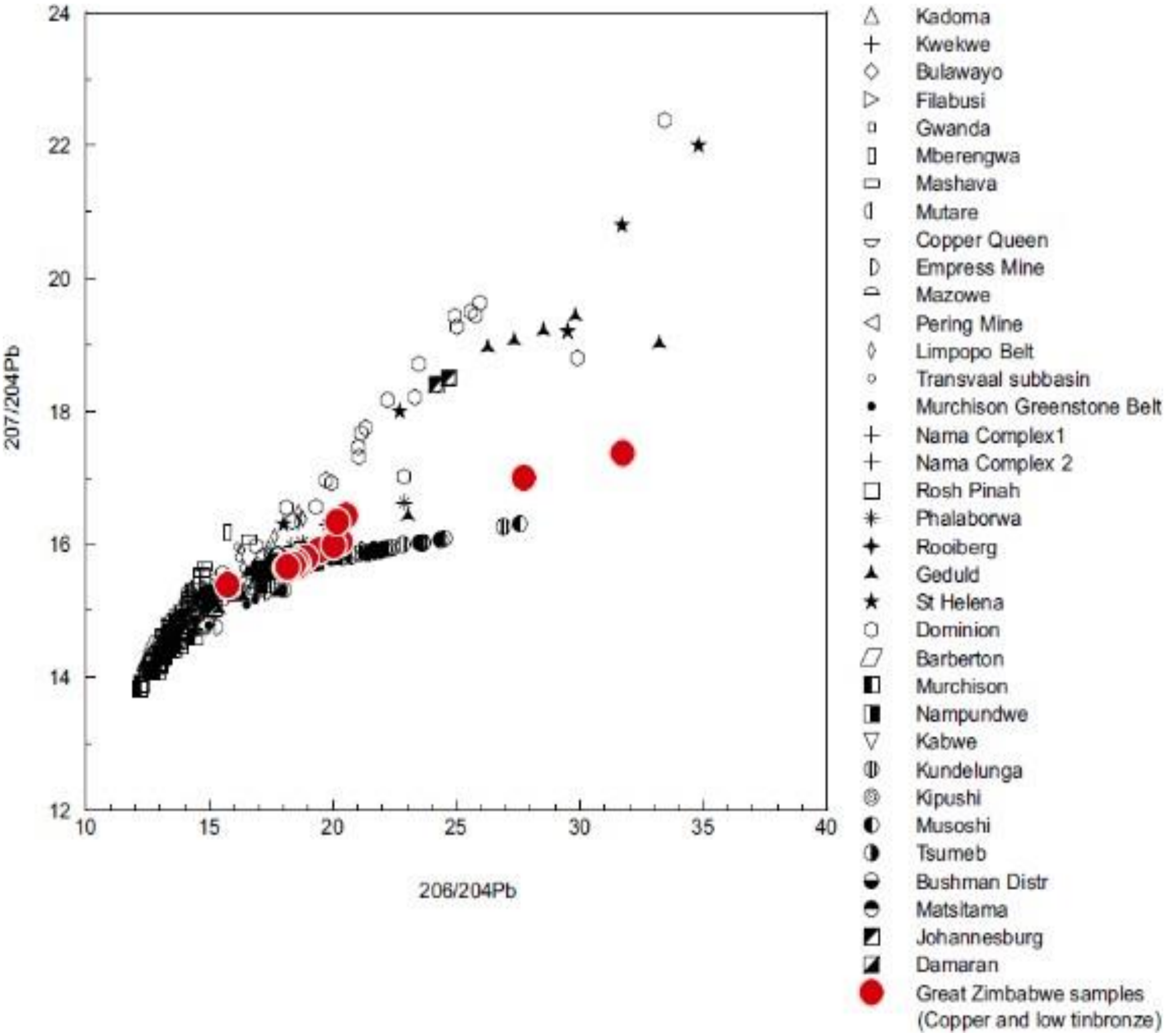

24
22
20
18
16
14
12
10
15
20
25
30
35
40
207/204Pb
206/204Pb
Kadoma
Kwekwe
Bulawayo
Filabusi
Gwanda
Mberengwa
Mashava
Mutare
Copper Queen
Empress Mine
Mazowe
Pering Mine
Limpopo Belt
Transvaal subbasin
Murchison Greenstone Belt
Nama Complex1
Nama Complex 2
Rosh Pinah
Phalaborwa
Rooiberg
Geduld
St Helena
Dominion
Barberton
Murchison
Nampundwe
Kabwe
Kundelunga
Kipushi
Musoshi
Tsumeb
Bushman Distr
Matsitama
Johannesburg
Damaran
Great Zimbabwe samples
(Copper and low tinbronze)

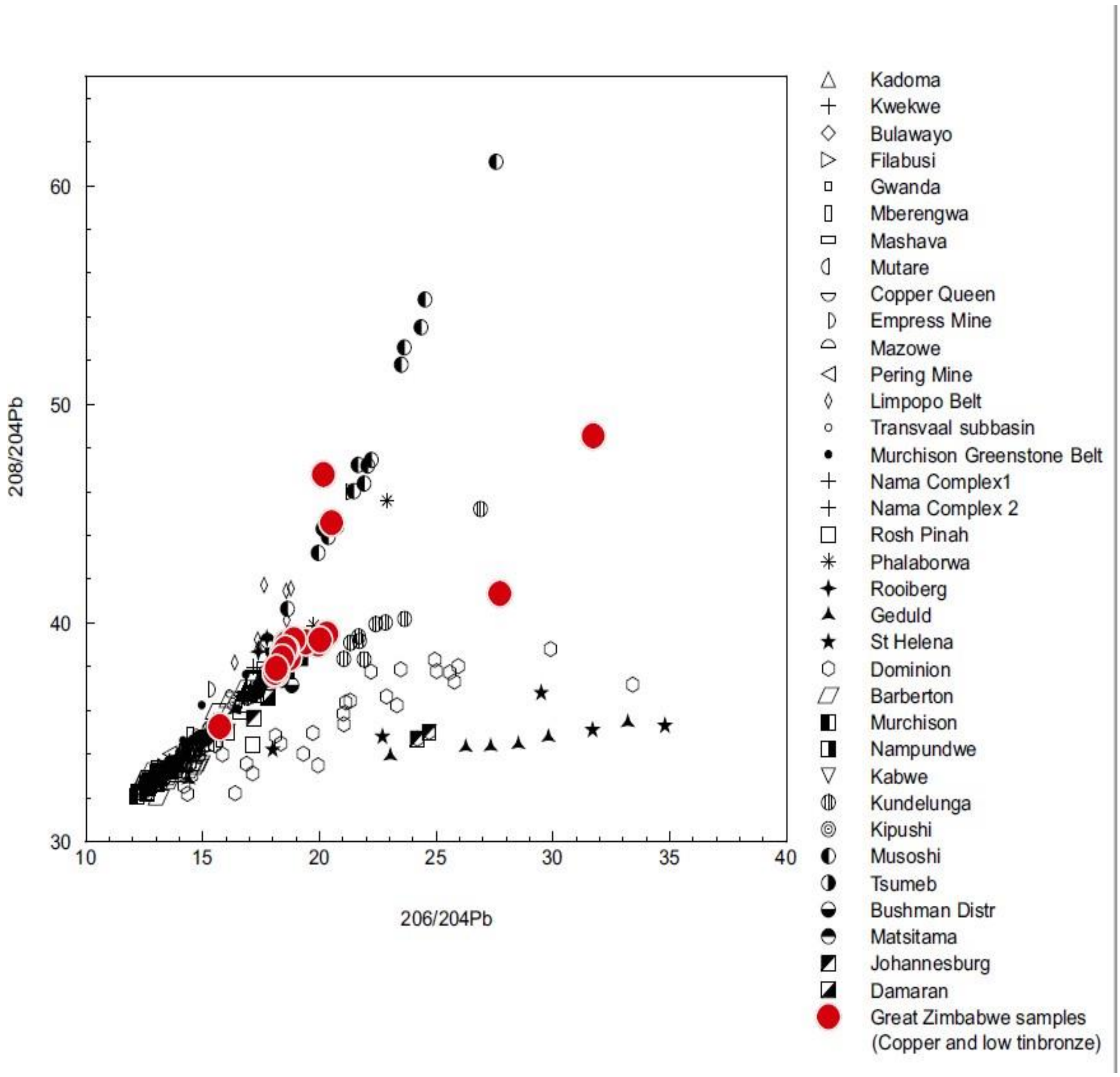

Fig 21: Initial biplots comparing Great Zimbabwe wire samples LIR against Southern African Database LIR on a $^{207}Pb/^{204}Pb$ vs $^{206}Pb/^{204}Pb$ plots and $^{208}Pb/^{204}Pb$ vs ^{206}Pb vs ^{204}Pb.

Therefore, a decision was taken to plot Great Zimbabwe coiled wire sample LIR versus grouped LIR of ore data presented in Table 4 below on a $^{207}Pb/^{204}Pb$ vs $^{206}Pb/^{204}Pb$ and $^{208}Pb/^{204}Pb$ vs $^{206}Pb/^{204}Pb$ biplots. This helped to fix the tight clustering problem and minuscule resolution which obscured easy identification of isotopic relationship (sample to sample correlation), on the initial plots presented in Fig.21. Noteworthy (Fig.21 above and Fig 22 below were plotted using Coplot). Replotting proved essential since most of the plotted data especially Cu-Sn alloys from the site matched with ore sample data from groups 2, and 10 which is made up of isotopic data ratios from mining areas such Copper Queen, Empress Mine, Mazowe Jumbo and Dikulushi mine, Luembe, Mwatapile and Kikonkula mines respectively. It is important to note that within the afore mentioned groups the low tin bronzes from Great Zimbabwe correspond strongly with Pb ratios from Dikulushi Mine (Kundelungu Plateau) and Empress Mine (Bulawayo Greenstone Belt) (See Fig. 22 biplots below).

In addition, the same isotopic ratios were plotted on $^{208}Pb/^{204}Pb$ vs $^{206}Pb/^{204}Pb$ and most low tin bronzes showed a strong correspondence with group 10 samples especially those from Dikulushi Mine, with a few others being consistent with group 2 sample isotopic ratios (Empress Mine), thus agreeing with results from $^{207}Pb/^{204}Pb$ vs $^{206}Pb/^{204}Pb$ plots. The use of both the normalized uranogenic and thorogenic Pb plots ensured easy discrimination of the isotopic ratios of Great Zimbabwe samples from other deposits and helped fingerprint the samples to certain classified district deposits with confidence. Therefore, in this case, most of the samples were isotopically consistent with ore sample ratios from the Damaran Lufian Fold Belt deposit in the Democratic Republic of Congo (DRC *henceforth*) and the Midlands Greenstone Belt's Empress mafic complex (Empress Mine). Thus, biplots show that the Damaran Lufian Belt (Katanga Copper belt) was not the only source of copper for the inhabitants of Great Zimbabwe southern terrace areas.

Fig 22: Biplots that shows the relationship between Cu and Cu-Sn alloys from Great Zimbabwe and available Pb ore ratios from the southern African metalliferous deposits.

Plot a $^{207}Pb/^{204}Pb$ vs $^{206}Pb/^{204}Pb$ grouped and reduced ratios

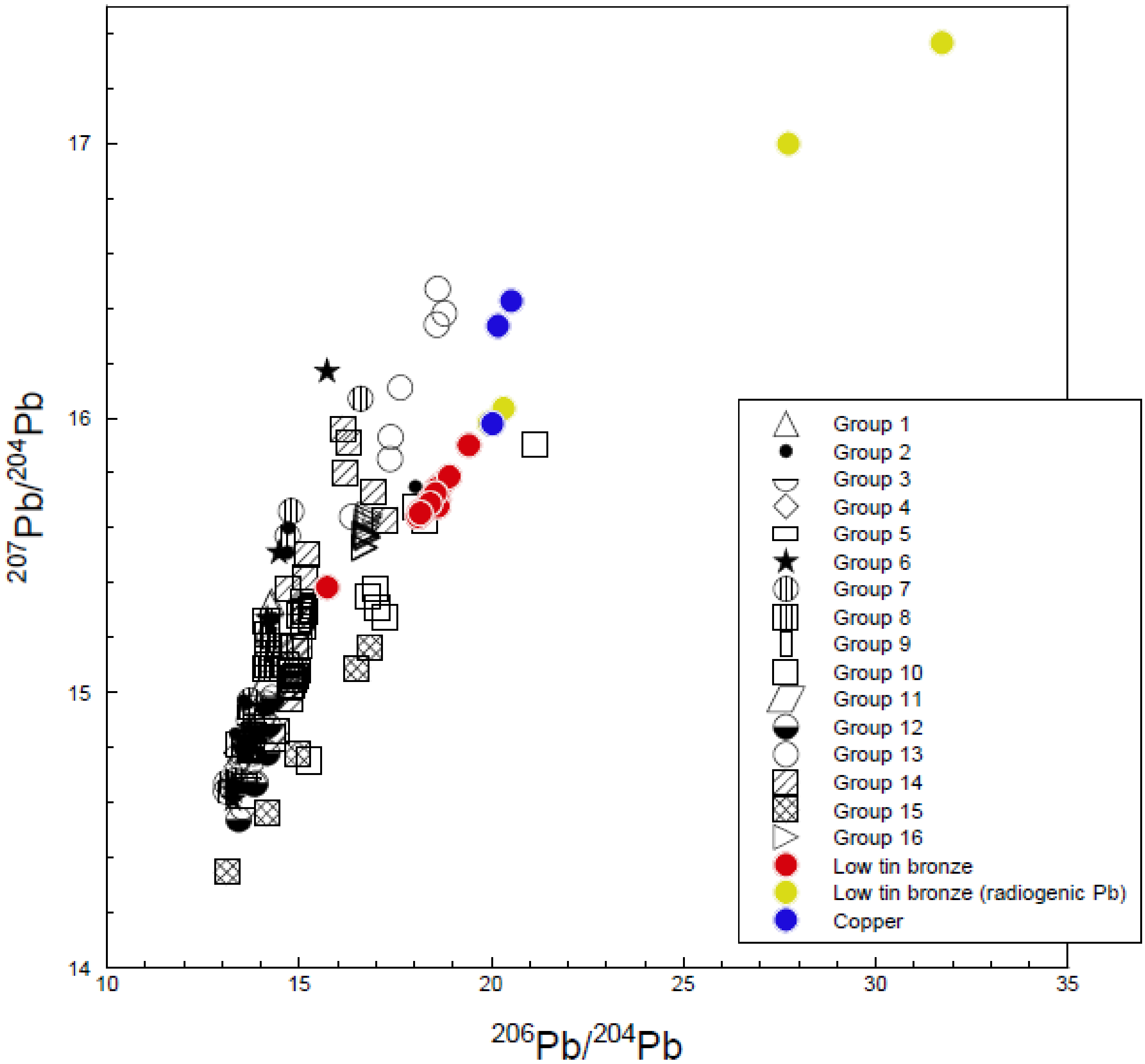

Plot b $^{208}Pb/^{204}Pb$ vs $^{206}Pb/^{204}Pb$ grouped and reduced ratios

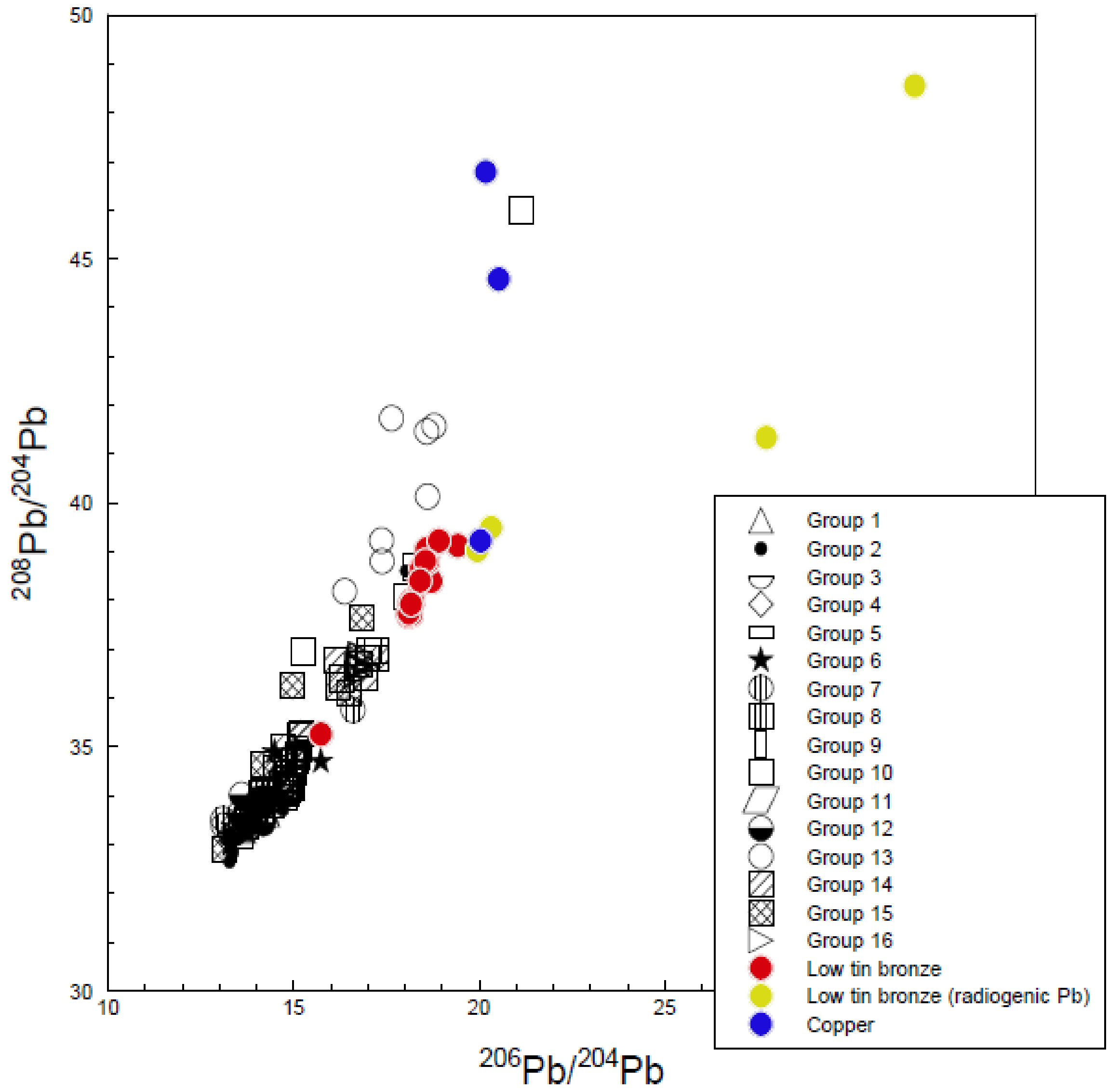

Table 4. The grouped data and codes assigned to exhibited groups in Figures 22

Group	Tectonic Deposit	Deposit	Code	Sample Source (Provincial or District Deposit and Mine)	Sample Total	N^0 of mines	District/ Places	Country
1	Zim Craton		1-5	Kadoma, Kwekwe, Bulawayo, Filabusi, Gwanda,	35	0	5	Zim
2	Zim Craton		6-11	Mberengwa Mashava, Mutare, Copper Queen, Empress, Mazowe Jumbo	41	3	3	Zim
3	Limpopo Sedimentary Basin	Griqualand West Sub-basin Limpopo Belt Transvaal Sub-basin	12-14	Pering Mine, Bush Park, Banghoek, Geelbek Dam, Kalkfontein, Balloch, Lugrug, Pafuri Nickel Mine, Campbell Mine, Messina, Bushfoelk, Kafferskraal, Witkop Stryfontein, Bokkraal, Prospect, Dornrandje	46	3		Zim
4	Kaapvaal Craton Namaqualand	Murchison Belt Namaqualand Complex	15-17	Malati Pump Mine, Prieska, Aggenys, Gamsberg, Rozynebosch, O'Okiep, Haib Copper Prospect	39	2	5	SA
5	Gariep Belt	Gariep Belt Phalaborwa and Rooiberg Complexes	18-20	Rosh Pinah Mine, Phalaborwa, Rooiberg Blaauwbank, Rooiberg Vellefontein	19	3	1	SA
6	Kaapvaal Craton	Witwatersrand Sequence	21-23	Durban Roodepoort Deep Central Rand, Free State Geduld Mines, St. Helena Gold Mine, Afrikander Lesses Mine, Vaal Reef, West Driefontein Gold Mine, Dominion Reefs Gold Mine, Stilfontein Gold Mine, South Roodepoort, Sub-Nigel Gold Mine, East Geduld Gold Mine, Vaal Reef, East Champ D'Or Gold Mine, South Roodepoort, Van Dyk Consoolidated	51	12	3	SA

				Mine, Government Gold MineHelena Gold Mine, Afrikander Lesses Mine, Vaal Reef, West Driefontein Gold Mine, Dominion Reefs Gold Mine, Stilfontein Gold Mine, South Roodepoort, Sub-Nigel Gold Mine, East Geduld Gold Mine, Vaal Reef, East Champ D'Or Gold Mine, South Roodepoort, Van Dyk Consolidated Mine, Government Gold Mine				
7	Kaapvaal Craton	Barberton Greenstone Belt	24	Rosetta, Gypsy Queen, Eagles Nest, Sheba Queen, Sheba Queen, Ivanhoe, Daisy, Comstock, Contractors, Middle Marker, Consort Bar, Agnes, Rochfort, Unity, Rosetta, Daylight, Consort Bar, French Bobs, Alfstrom, Mica, Swaziland, Fairview, Rosseta,	41	3	22	SA
8	Kaapvaal Craton	Murchison Greenstone Belt	25	Old-star, Monarch East, Letaba, Romotshidi, Maranda J, Mon Desir, Solomons, LCZ	33	8		SA
9	Damaran Lufian Fold Belt	Zambezi Belt, Damaran Lufian Belt	26-27	Nampubwe and Kabwe	16		2	Zambia
10	Damaran Lufian Fold Belt	Kundelungu Plateau	28	Kikonkula, Kibila, Luemba, Mwatipile, Dikulushi	31	1	4	DRC
11	Damaran Lufian Fold Belt	Damaran Lufian Fold Belt	29	Kipushi	39	1		DRC
12	Damaran Lufian Fold Belt	Zambian Copper Belt	30	Musoshi Ore Deposit	15			DRC
13	Damaran Lufian Fold Belt	Damaran Lufian Belt	31	Tsumebi	10			Namibia

14	Damaran Lufian Fold Belt	Bushaman District	32-33	Mapanipani North, Bushman, Dihudi, Thakadu, Magogophate, Torome	22	Botswana
15	Limpopo Belt	Sabie, Sudwala Area	34	Johannesburg, Olifants geraamte, Rietvallei, Sudwalaskraal	5	SA-Zim
16	Damaran Lufian Fold Belt	Damaran Lufian Fold Belt	35	Kolwezi, Lombe, Kengere, Kinsenda	11	DRC

4.3.4. The *mu-kappa-T system* (MATLAB Script) technique

Furthermore, in a bid to assess the matches revealed by biplots above, the Pb isotopic ratios of Great Zimbabwe samples were run in the MATLAB Script developed by Dr Vincent Hare (UCT Department of Archaeology) based on Alberade *et al.,* (2012). The technique employed is called the mu-kappa-T system and has been used with great success by researchers to develop model ages for both artefacts and ore samples, discriminate and suggest possible sources for non-radiogenic, radiogenic, and highly radiogenic bronze and copper artefacts from Potosi Mexico, Southern Spain, China and Botswana respectively (see Albarede *et al.,* 2012; Pollard *et al.,* 2018; Liu et al., 2021; Stephens et al., 2020 in that order). It was also used to calculate model age for various ores samples in the database shared by Killick *et al.,* (2020). The mu-kappa-T approach is therefore an extension of the Stacey-Krammers two stage model of Pb evolution (Stacey and Krammer 1975). For this reason, it takes into account the effects of ore formation and consequently accounts for more of geological "history" of a parent deposit than Pb biplots. Generally, the effectiveness of the mu-kappa-T system is embedded in its ability to calculate the complex and gradual decay history and relationship of uranium (U), thorium (Th) and Pb. The system calculates the separation of U and Pb by calculating the starting ratio of $^{238}U/^{204}Pb$ (μ) and the concentration and variation of Th based on the evolution of 232Th/238U (κ), and back calculate model ages (*T*) associated with tectonic or provincial deposit and even artefact (Alberede *et al.*, 2012; Stephens et al., 2020; Pollard et al., 2018; Liu *et al.,* 2021). Thus, the technique offers a window into understanding the geochemical and geological characteristics associated with the parent deposit that can be used to discriminate possible sources of artefacts or ores based on variation in κ and μ and the modelled age (*T*) of a deposit's mineralization (Albarede *et al.,* 2012; Pollard et al., 2018; Liu *et al.,* 2021), hence making it an important technique for testing results produced by the convectional Pb biplot system. Therefore, in this study the technique was used to develop model ages for the samples and compare them with readily available ages compiled by Stephens (2016) which informed the database used in this study and additional model ages in the southern African metalliferous database. It was also employed to explore the relationship between κ and μ, however, their variation and concentration were deemed beyond the scope of this study. In addition to the above, the model ages were treated with caution since they are not accurate geochronometric dates.

Table 5. The ratios of μ, κ and model age (T) for Great Zimbabwe artefacts

Number	Sample	$^{208}Pb/^{204}Pb$	±2s internal	$^{207}Pb/^{204}Pb$	±2s internal	$^{206}Pb/^{204}Pb$	±2s internal	type of metal	$^{238}U/^{204}Pb$ (μ)	$^{232}Th/^{238}U$ (κ)	T (Ma)	± T (Ma)
1	Wall 55 TP L 1	39.4899	0.0019	16.0337	0.0006	20.3177	0.0008	low tin bronze	10.94769	3.4676	-3221	2.54
2	Wall 55 TP1L4	41.3386	0.0026	16.9980	0.0009	27.7263	0.0011	low tin bronze	13.94352	2.0760	-326.2	15.2
3	Wall 55 TPL5	39.2237	0.0030	15.7866	0.0011	18.9094	0.0011	low tin bronze	10.238113	4.0498	108.3	1.03
4	WALL55 UC-T3	46.7839	0.0026	16.3352	0.0007	20.1721	0.0008	copper	12.1342	6.7509	293.3	36.2
5	Wall 55 UC-1	39.2215	0.0022	15.9787	0.0007	20.0293	0.0008	copper	10.78151	3.4791	-230.5	21.8
6	Wall 55 TPL 4b	37.7086	0.0028	15.6589	0.0009	18.1758	0.0010	copper	9.903607	3.6874	482.6	4.09
7	Wall 55 ST:TP1 L14	39.1256	0.0037	15.9005	0.0012	19.4173	0.0017	low tin bronze	10.58280	3.7350	447.7	1.67
8	USTM L1 Step 2	38.6601	0.0028	15.7053	0.0010	18.4254	0.0010	low tin bronze	10.02621	4.0535	386.0	6.28
9	USTM L3	37.9112	0.0027	15.6536	0.0009	18.1310	0.0008	low tin bronze	9.8944884	3.8273	505.6	3.92

10	USTM L3 artefact	37.9375	0.0033	15.6580	0.0010	18.1590	0.0010	low tin bronze	9.904645	3.8258	493.2	4.10
11	USTM L6	37.7351	0.0021	15.6417	0.0007	18.0914	0.0007	low tin bronze	9.856708	3.7514	513.1	3.29
12	USTM L7	38.3881	0.0028	15.7584	0.0009	18.7104	0.0008	low tin bronze	10.17055	3.9969	278.9	8.95
13	USTM L7B	37.9198	0.0030	15.6543	0.0011	18.1399	0.0010	low tin bronze	9.894323	3.8264	500.4	3.93
14	USTM L7C	39.0247	0.0029	15.9816	0.0010	19.9431	0.0010	low tin bronze	10.080501	3.4384	-1653	2.17
15	USTM L8 artefact	38.7783	0.0033	15.6782	0.0010	18.6105	0.0010	low tin bronze	9.874682	3.9882	200.5	3.97
16	USTM L8(B)	48.5534	0.0047	17.3662	0.0012	31.7271	0.0045	low tin bronze	15.14294	2.6248	-5384	2.88
17	USTM L8C	37.9798	0.0022	15.6581	0.0008	18.1981	0.0007	low tin bronze	9.894108	3.8224	464.9	3.97
18	USTM L8(D)	39.0585	0.0034	15.7424	0.0012	18.5778	0.0011	low tin bronze	10.13792	4.1715	344.2	8.22
19	USTM L9	37.9936	0.0031	15.6579	0.0010	18.2166	0.0010	low tin bronze	9.888215	3.8176	451.1	3.88
20	USTM L9(B)	37.6950	0.0027	15.6430	0.0009	18.1088	0.0008	low tin bronze	9.857068	3.7180	503.7	3.31
21	USTM L9C	37.6824	0.0026	15.6400	0.0009	18.0967	0.0009	low tin bronze	9.848149	3.7179	506.1	3.16
22	USTM L10	44.5798	0.0038	16.4261	0.0013	20.5199	0.0013	copper	12.41713	5.5767	226.6	40.3
23	USTM L10(B)	38.8041	0.0029	15.7255	0.0010	18.5415	0.0009	low tin bronze	10.07879	4.0577	393.4	7.2
24	USTM L11	35.2543	0.0020	15.3830	0.0008	15.7318	0.0007	low tin bronze	10.11689	3.7749	186.1	4.66
25	USTM L12	38.8934	0.0025	15.7019	0.0009	18.6209	0.0010	low tin bronze	9.966120	4.0425	280.6	5.54
26	USTM L13	45.0377	0.0040	20.6785	0.0016	88.8247	0.0068	low tin bronze	43.1671	0.2689	-1492	7.33

Based on results produced by the *mu-kappa-T* system as shown in Table 5 above, the model ages (*T*) developed from Great Zimbabwe samples ranges between 108- 580 Ma. These model ages are associated with anomalous Pb ratios whereas most of the highly radiogenic Pb isotopes exhibited negative model ages that were thousands of years into the future, except for Cu samples (USTM L 10 and Wall 55 UC T3) which produced model ages of 226 Ma and 293 Ma respectively. The model ages exhibited by highly radiogenic Pb isotopes seem to match with some model ages associated with low tin bronzes. In general, the ages associated with most of the samples are reasonable and seem to reinforce the matches shown by biplots created above. The reason is that most of the samples from Great Zimbabwe, despite exhibiting a wide date range, are concentrated between 280-506 Ma which fits within the Palaeozoic geological age in Africa. The Palaeozoic age is a bit younger as compared to the dominant Precambrian (Archaean) geological age where most of the greenstone belts that were worked in antiquity across south-central Africa (in countries such as Zimbabwe, South Africa, Botswana, Zambia, Namibia, DRC etc) are located (Killick *et al.,* 2020). However, it is important to note that despite most southern African countries tectonic deposits being associated with Precambrian ages there is also evidence of very young model ages especially within mobile belts and areas that were formed during the Cenozoic, Mesozoic, Palaeozoic, Proterozoic ages, and others that underwent post-cratonization during the later stages of mineralization. This, therefore, proves Killick *et al.,* (2020) observation that southern African metalliferous deposits were formed over a broad range of geological time span (3300-400 Ma). However, based on evidence from Great Zimbabwe samples there is a higher probability that deposits that postdate the age bracket of 3300-400 Ma were exploited by precolonial inhabitants of Great Zimbabwe from areas around the site. Therefore, to evaluate if samples from Great Zimbabwe matched with available dates of characterized deposits and the accuracy of model ages provided in the Killick *et al.*, (2020) database, the isotopic ratios of the whole database was recalculated, using the *mu-kappa-T* system (MATLAB Script).

The recalculated model ages from the southern African database in this study, show little variation from the ones developed by Stephens (2016) and Killick *et al.,* (2020). For the purposes of this study, the database compiled and developed by Stephens (2016) was employed since it is comprehensive and seem to inform the southern African Pb isotopes database in ARCM 12573-sup- 001. To note the table is also characterized by isochron ages which are quite important but deemed out of the scope of this study.

Table 6 below shows a glimpse of the available model ages and MSWD isochron ages developed by Stephens (2016) which informed the current database. The table is an important summary of the characterized tectonic deposits across southern Africa and the types of ores that were analysed. However, as visible from Table 6, most of the model ages and isochron ages are based on tectonic deposits which overshadow the variability of small or zonal (district) deposits which might have been influenced by localised geological events hence affecting the uniformity of deposits over large geographical area. Therefore, in this study a table with recalculated model ages of the whole database was formulated, with the aim of capturing mining sites or zonal areas model ages. The model ages data will be categorized for further analysis. See Table 7, presented further below with model ages developed from characterized isotopic ratios within the database.

Table 6. Model ages and isochrone ages for deposits within the southern African metalliferous database developed by Stephens (2016)

Province	Location	Age	Type of deposits	Ores	Evidence of prehistoric exploitation	Pb isotopic range	Recalculated model age range
Barberton Greenstone Belt	South Africa	Archean	Igneous	porphyry vein, vein, and stratiform type nickel, iron, copper, and lead sulfides	Yes	$^{206}Pb/^{204}Pb$ = 12.51 - 17.01 $^{207}Pb/^{204}Pb$ = 14.12 - 15.45 $^{208}Pb/^{204}Pb$ = 32.01 - 37.01	Common lead model ages: 2820 - 3800 Ma Isochron ages: 3166±280 Ma MSWD = 24, 2964±440 Ma MSWD = 16, 4000 Ma
Murchison Greenstone belt	South Africa	Archean	Igneous	sphalerite, galena, pyrite, pyrrhotite, and chalcopyrite, and trace deposits of magnetite, cassiterite, stannite, tennantite, bornite, chalcocite, and native copper	Yes	$^{206}Pb/^{204}Pb$ = 12.20 - 36.80 $^{207}Pb/^{204}Pb$ = 13.81 - 20.27 $^{208}Pb/^{204}Pb$ = 32.05 - 49.75	Common lead model ages: 2600 - 3000 Ma, Isochron ages: 3198±31 Ma MSWD = 35
Transvaal Sequence	South Africa	Archean - Proterozoic	Sedimentary	galena, sphalerite, pyrite, chalcopyrite, silver, and gold.	Yes	$^{206}Pb/^{204}Pb$ = 13.43 - 24.70 $^{207}Pb/^{204}Pb$ = 14.54 - 18.50 $^{208}Pb/^{204}Pb$ = 33.24 - 36.79	Common lead model ages: 654 - 2800 Ma

Limpopo Belt	South Africa, Zimbabwe, Botswana	Archean – Proterozoic	Metamorphic	lead, copper, and iron sulfides	Yes	$^{206}Pb/^{204}Pb$ = 17.36 - 18.78 $^{207}Pb/^{204}Pb$ = 15.74 - 16.47 $^{208}Pb/^{204}Pb$ = 38.80 - 41.73	Common lead model ages: 900 - 1400 Ma
Phalaborwa Complex	South Africa	Proterozoic	Igneous	copper sulfides, iron oxides, apatite, nickel, gold, silver, thorium, uranium, zirconium, REE and PGE metals	Yes	$^{206}Pb/^{204}Pb$ = 18.34 - 172.1 $^{207}Pb/^{204}Pb$ = 15.96 - 32.31 $^{208}Pb/^{204}Pb$ = 38.24 - 224.6	Isochron ages: 2446±44 Ma MSWD = 2.6
Namaqualand Metamorphic Complex	South Africa	Proterozoic	Metasedimentary	copper, zinc, iron, and lead sulfides	Yes	$^{206}Pb/^{204}Pb$ = 16.70 - 17.20 $^{207}Pb/^{204}Pb$ = 15.52 - 15.60 $^{208}Pb/^{204}Pb$ = 36.46 - 37.98	Common lead model ages: 1100 - 1450 Ma
Gariep Belt	South Africa	Proterozoic	Metasedimentary	lead and zinc sulfides	No	$^{206}Pb/^{204}Pb$ = 17.13 - 17.21 $^{207}Pb/^{204}Pb$ = 15.59 - 15.62 $^{208}Pb/^{204}Pb$ = 37.37 - 37.50	Common lead model ages: 1097 - 1137 Ma
Bulawayan Greenstone belt	Zimbabwe	Archean	Igneous	lead and copper sulfides	Yes	$^{206}Pb/^{204}Pb$ = 13.26 - 18.26 $^{207}Pb/^{204}Pb$ = 14.61 - 15.63 $^{208}Pb/^{204}Pb$ = 32.99 - 38.68	Common lead model ages: 2695 - 3193 Ma Empress Mine samples – No Date
Sebakwian Greenstone Belt	Zimbabwe	Archean	Igneous	lead and copper sulfides	Yes	$^{206}Pb/^{204}Pb$ = 13.09 - 15.73 $^{207}Pb/^{204}Pb$ = 14.64 - 16.17 $^{208}Pb/^{204}Pb$ = 32.65 - 34.89	Common lead model ages: 2731 - 3388 Ma
Shamva Greenstone belt	Zimbabwe	Archean	Igneous	lead and copper sulfides	No	$^{206}Pb/^{204}Pb$ = 14.15 - 14.20 $^{207}Pb/^{204}Pb$ = 15.01 - 15.03 $^{208}Pb/^{204}Pb$ = 33.86 - 33.91	Common lead model ages: 2694 - 2709 Ma

Harare-Shamva Greenstone belt	Zimbabwe	Proterozoic	Igneous	pyrrhotite, arsenopyrite, and chalcopyrite	No	$^{206}Pb/^{204}Pb$ = 35.92 - 118.1 $^{207}Pb/^{204}Pb$ = 19.05 - 28.84 $^{208}Pb/^{204}Pb$ = 36.21 - 37.83	Isochron age: 1921±67 Ma MSWD of 4.9
Kgalagadi Province - typo error the belt is called Magondi	Zimbabwe	Proterozoic	Metamorphic	copper, zinc, lead sulfides	Yes	$^{206}Pb/^{204}Pb$ = 15.14 - 15.25 $^{207}Pb/^{204}Pb$ = 15.26 - 15.31 $^{208}Pb/^{204}Pb$ = 34.70 - 34.87	Common lead model ages: 2154 - 2206 Ma
Bushman Group	Botswana	Proterozoic	Metasedimentary	pyrite, chalcopyrite, galena, and sphalerite with secondary minerals of chalcocite, bornite, malachite, azurite, chrysocolla, brochantite, cuprite, and native copper	Yes	$^{206}Pb/^{204}Pb$ = 17.36 - 17.81 $^{207}Pb/^{204}Pb$ = 15.67 - 15.84 $^{208}Pb/^{204}Pb$ = 36.86 - 37.75	Common lead model ages: 100 - 1000 Ma
Matsitama Schist belt	Botswana	Proterozoic	Sedimentary	pyrite and chalcopyrite, with minor amounts of chalcocite, bornite, galena, and sphalerite	Yes	$^{206}Pb/^{204}Pb$ = 14.77 - 14.98 $^{207}Pb/^{204}Pb$ = 15.15 - 15.26 $^{208}Pb/^{204}Pb$ = 34.43 - 34.75	Common lead model ages: 2300 - 2400 Ma
Damaran-Lufilian Fold belt	Zambia, the DRC, Namibia	Proterozoic - Cambrian	Metasedimentary	Arsenopyrite, galena, tennantite, sphalerite, chalcocite, bornite, and enargite with minor chalcopyrite, germanium, gallium, vanadium,	Yes	$^{206}Pb/^{204}Pb$ = 17.64 - 18.22 $^{207}Pb/^{204}Pb$ = 15.49 - 15.73 $^{208}Pb/^{204}Pb$ = 37.25 - 38.46	Common lead model ages: 380 - 721 Ma

Kundulungu Plateau	The DRC	Proterozoic - Cambrian	Metasedimentary	chalcopyrite, bornite, chalcocite, pyrite, arsenopyrite, sphalerite, and galena, Ag-rich chalcocite and diginite, and barite	No	$^{206}Pb/^{204}Pb$ = 18.07 - 23.65 $^{207}Pb/^{204}Pb$ = 15.68 - 16.02 $^{208}Pb/^{204}Pb$ = 38.33 - 40.17	Common lead model ages: 340 - 604 Ma Isochron age: 656±110 Ma MSWD of 5.8
Central African Copperbelt	Zambia and the DRC	Proterozoic - Cambrian	Metasedimentary	Carrollite, chalcopyrite, bornite, and pyrite	Yes	$^{206}Pb/^{204}Pb$ = 18.63 - 97.64 $^{207}Pb/^{204}Pb$ = 15.72 - 20.44 $^{208}Pb/^{204}Pb$ = 40.64 - 140.6	Isochron age: 608±26 Ma MSWD of 7.9
Zambezi Belt	Zambia	Proterozoic – Cambrian	Metasedimentary	pyrrhotite, magnetite, chalcopyrite, sphalerite, pyrite, and galena	No	$^{206}Pb/^{204}Pb$ = 17.89 - 19.34 $^{207}Pb/^{204}Pb$ = 15.69 - 15.74 $^{208}Pb/^{204}Pb$ = 37.62 - 38.97	Reported age: 908 Ma, date could not be confirmed

Table 7. Recalculated model ages for southern African database

Country	Tectonic Deposit	District Area/ Greenstone Belt	Area/ Mine	Group	Code	T (Ma)	$^{238}U/^{204}Pb$ (μ)	$^{232}Th/^{238}U$ (κ)	Samples total N^0
Zim	Zim Craton		Kadoma	1	1	2730-3065	11.19-15.31	3.53-3.95	7
			Kwekwe	1	1	747-3320	10.33-18.24	3.20-4.41	8
		Bulawayo Greenstone Belt	Bulawayo	1		2719-2804	9.88-10.88	3.63-3.93	7
		Bulawayo Greenstone Belt	Filabusi	1	1	2791-3206	10.90-14.99	3.81-4.58	6
		Bulawayo Greenstone Belt	Gwanda			2814-3014	10.33-12.80	3.35-4.20	8
		Mberengwa Greenstone Belt	Mberengwa	2	6	2734-3182	11.12-17.24	3.82-4.96	10
		Mashava-Ultramafic Zone (Masvingo Greenstone Belt)	Mashava	2	7	2869-3349	12.96-18.49	3.60-5.39	10
		Mutare Greenstone Belt	Mutare	2	8	2820-3210	12.42-15.33	3.72-4.38	6
		Magondi Greenstone Belt	Copper Queen	2	9	2157- 2209	10.27-10.45	3.80-3.91	5
		Midlands Greenstone Belt (Mafic Zone)	Empress Mine	2	10	364-1195	7.08-857	3.79-5.71	6
		Mazowe	Jumbo Mine	2	11	2688-2702	11.17-11.21	3.89-4.02	2
SA	Kaapvaal Craton	Griqualand West Subbasin	Pering Mine	3		2725-2868	9.16-10.74	3.95-4.54	3
			Bushy park	3		2471-2538	8.80-10.17	3.69-4.09	3
			Banghoek Mine			2332	8.68	3.26	1
						3002	12.37	5.14	1
		Limpopo Belt	Campell Mine	3	13	1224-1437	11.54-12.77	5.05-5.64	2

Limpopo Belt	Messina	3	13	1159-1505	11.14-13.41	4.94-6.71	4
Transvaal subbasin	Buffelshoek	3	14	2072-2207	8.91-9.59	3.31-3.54	4
Transvaal subbasin	Rhenosterhoek	3	14	2093-2116	8.821-9.20	3.35-3.76	3
Transvaal subbasin	Western Deep Levels	3	14	2140-2243	9.34-10.06	3.39-3.69	2
	Elandsfontein	3	14	2062-2124	9.17-931	3.32-3.35	2
	Leeuwbosch	3	14	2169-2208	10.18-1052	3.93-4.06	2
Murchison Greenstone Belt	Malati Pump Mine	4	15	555-2840	7.05-8.50	3.67-3.91	5
Namaqualand Complex	Prieska	4	16	1340-1346	9.97-9.99	3.94-3.98	3
Namaqualand Complex	Aggenys	4	16	1312-1438	9.96-10.48	3.95-4.18	18
Namaqualand Complex	Gamsberg	4	17	1315-1392	10.01-10.41	3.95-4.11	7
Namaqualand Complex	Rozynenbosch	4	17	1170-1232	9.85-10.15	3.80-3.94	3
Namaqualand Complex	O'Okiep	4	17	1107-1117	10.07-1011	4.57	2
Gariep Belt	Rosh Pinah	5	18	1097-1171	9.99-10.12	2.25-9.11	9
Phalaborwa Complex	Phalaborwa	5	19	466-865	11.14-12.83	3.73-4.56	4
	Rooiberg Blauwbank	5	20	714-1969	9.80-10.03	4.24-4.89	3
Witwatersrand sequence	Free State Geldud	6	21	276-2386	3.13-27.28	1.88-9.89	13
Witwatersrand sequence	St.Helena Gold Mine	6	22	276-1509	3.13-27.28	1.18-7.71	5
Witwatersrand sequence	Dominion Reef Gold Mine	6	23	1033-2244	11.73-26.92	1.90-3.20	12
Witwatersrand sequence	Stilfontein Gold Mine	6	23	943-1309	15.10-19.04	1.70-1.85	3
Witwatersrand sequence	East Champ D'Or Gold Mine	6	23	2015-1343	7.70-8.96	1.45-2.41	3
Witwatersrand sequence	Van-Dyk Consolidated Mine	6	23	2081-2241	9.56-10.21	3.49-4.05	2

		Witwatersrand sequence	Government Gold Mine	6	23	672-769	19.52-19.77	11.5	2
		Barberton Greenstone Belt	Rosetta	7	24	3319-3338	12.28-13.91	4.19-3.32	2
		Barberton Greenstone Belt	Sheba Queen	7	24	838-2822	7.52-9.05	2.66-4.07	5
		Barberton Greenstone Belt	Daisy	7	24	1165-2446	9.00-9.55	3.79-4.36	4
		Barberton Greenstone Belt	Middle Marker	7	24	1722-2935	9.19-11.42	4.14-4.52	2
		Barberton Greenstone Belt	Swaziland	7	24	2938-2942	11.38-13.46	3.77-4.22	2
		Murchison Greenstone Belt	Old Star	8	25	3318-3420	9.27-12.04	3.84-4.59	4
		Murchison Greenstone Belt	Monarch East	8	25	609-2345	7.02-9.00	3.39-3.89	5
			Romotshidi	8	25	2680-3074	7.14-8.49	3.62-4.42	4
			Letaba	8	25	2991-3078	7.88-8.81	3.78-413	4
			Maranda J	8	25	2642-2970	6.37-9.28	3.43-4.49	5
			Mon Desir	8	25	2788-2895	7.58-8.77	3.96-4.49	3
			Solomons	8	25	2783-2996	7.86-10.44	3.80-4.31	4
			LCZ	8	25	2750-3168	7.62-9.56	3.29-3.95	4
Zambia	Lufilian Arc	Zambezi Belt	Nampundwe	9	26	510-737	9.87-10.80	3.60-3.96	5
Zambia	Lufilian Arc		Kabwe	9	27	675-719	10.01-10.24	4.18-424	11
DRC	Damaran Lufian Fold Belt	Kundelungu Plateau	Kikonkula	10	28	513-516	10.13-1017	4.23-4.25	2
		Kundelungu Plateau	Dikulushi Mine	10	28	119-579	9.62-10.73	2.72- 4.18	25
		Kundelungu Plateau	Kibila	10	28	Negative Ages	10.24-10.36	2.38-3.60	2
		Kundelungu Plateau	Luemba	10	28	Negative Ages	10.36	2.38	1
			Mwitapile	10	28	Negatives Ages	13.62	3.04	1

		Damaran-Lufilian Fold Belt	Kipushi	11	29	379-682	8.56-10.17	1.24-3.90	39
		Zambia Copperbelt	Musoshi ore deposit	12	30	272 + negatives	10.05-10.92	4.94-5.82	15
Namibia	DamaranFold Belt	Damaran Orogeny	Tsumebi	13	31	501-596	9.93-10.13	4.03-4.10	10
Botswana	Limpopo Sedimentary basins	Bushman District	Mapanipani North	14	32	397-1096	10.10-10.80	3.05-4.07	10
		Bushman District	Bushman	14	32	605-1029	10.23-10.82	3.18-4.01	2
		Matsitama Belt	Dihudu	14	32	2332-2375	10.28-10.81	3.90-4.08	4
		Matsitama Belt	Thakadu	14	32	2300-2434	10.62-11.12	4.01-4.15	4
			Johannesburg area	15	34	654-751	19.44-19.69	1.11-1.15	2
		Sudwala Area	Sudwala Area	15	34	728-1416	9.05-9.12	9.05-9.12	2
DRC	Damaran-Lufilian Fold Bel	Damaran-Lufilian Fold Belt	Kolwezi	16	35	263-511	9.77-10.14	3.46-3.74	3
		Damaran-Lufilian Fold Belt	Lombe	16	35	448-720	9.64-9.74	3.44-3.75	3
		Damaran-Lufilian Fold Belt	Kengere	16	35	449-528	9.66-9.78	3.63-3.77	2
		Damaran-Lufilian Fold Belt	Kinsenda	16	35	140-858	8.71-10.06	3.18-4.13	3

The table above shows the recalculated models ages of ore samples that make up the southern African database. Notably despite all the isotopic data in the southern African database being analysed in this study, some of the mines represented by a single ores isotopic ratio were not presented in the table above. Based on the evidence presented, there are very few mines and district deposits with young model ages that correspond to the ones associated with Great Zimbabwe samples (see Table 5). However, based on the model ages presented in Table 7, young model ages that correspond with those from Great Zimbabwe samples are confined to mines in groups 2, 10 and 11 with the most probable candidates in those classes being Empress Mine, Dikulushi Mine and Kipushi Mine respectively. Additional mines such as Free State Geduld Mine (276-2386 Ma), St. Helena Gold Mine (276-1509 Ma), Phalaborwa (466-865 Ma), Tsumeb (501-596 Ma) and Kinsenda (140-858 Ma) have model ages that slightly overlap with those from Cu and Cu-Sn alloy samples from Great Zimbabwe there are therefore other possible candidates. Therefore, the creation of model age *T* data illuminated the nature and variation of the model ages associated with the characterized ore deposits across southern Africa from a micro-zonal level. Hence, I ruled out other district areas and mines based on negative ages and older model ages, at the same time zooming in on potential mines that had young model ages similar to the samples understudy. It is important to note that model ages on their own cannot be used to discriminate and confirm the source of archaeological artefacts with certainty since they are not geo-chronologically accurate. Such evidence inspired the researcher to further analyse LIR from Great Zimbabwe and metalliferous ores deposits from across southern Africa by testing ratios of model age (*T*) versus μ, and model age (*T*) versus κ, of mines with young model ages based on the data above and biplot results.

This procedure aimed to further discriminate and discredit deposits that were not exploited by the inhabitants of Great Zimbabwe from those that were exploited, based on the starting composition of U and Th values and its consistency with model age *T*. Such an approach proved essential since it enabled the researcher to make sense of deposits or districts that had similar model ages to Great Zimbabwe but did not exhibit any isotopic correspondence on the $^{207}Pb/^{204}Pb$ vs $^{206}Pb/^{204}Pb$ biplots. However, before plotting biplots of $^{238}U/^{204}Pb$ (μ) vs model age *T* and $^{232}Th/^{238}U$ (κ) vs model age *T* ratios, the researcher compared the μ and κ ratios of all zonal districts and mines versus the mean and range of μ and κ ratios from Great Zimbabwe wound copper and bronze samples (objects). Such analysis enabled the researcher to rule out deposits with young model ages that were characterized by either high or low μ and κ ratios as compared to the calculated ratios associated with Great Zimbabwe copper and bronze samples. Great Zimbabwe samples were characterised by mean values of 11.04 for μ and 3.75 for κ (Noteworthy the mean values are inclusive of highly radiogenic ratios). Therefore, mines such as the Free State Geduld Mine and St Helena within the Witwatersrand sequence are characterised by high μ ratios ≥ 14.54, Tsumebi has high level κ with a mean of 4.05 whilst Kinsenda has a mean μ 9.59 and Phalaborwa a mean μ of 11.82 as compared to Great Zimbabwe, hence they were dismissed as possible sources. Notably despite including Kinsenda and Phalaborwa mining areas they were both characterised by 3 model ages each with only a single Pb ratio (ore sample) corresponding with Great Zimbabwe samples, thus the sample size was not representative enough statistically. Finally, the observed high starting ratios of U and Th in the μ and κ ratios of the Free State Geduld Mine, St Helena, Tsumebi, Kinsenda and Phalaborwa is generally associated with older geological deposits such as the Precambrian ages, since older ages are associated with high levels of μ and κ (see Albarede *et al.*, 2012's observation of Cordellian associated deposits in Peru). This is very valid since most of the above-mentioned mines are characterised by model ages within the Proterozoic-Precambrian age. Thereby, leaving Empress Mafic zone, the Dikulushi and Kipushi mines as the strongest candidates that could have been sourced for copper by the inhabitants of Great Zimbabwe based on their T-μ-κ consistency with Great Zimbabwe Cu and Cu-Sn sample ratios as shown on the biplots below.

Fig 23a: Model age T vs $^{238}U/^{204}Pb$ (μ) of Great Zimbabwe's Cu and Cu-Sn alloy objects, Dikilushi, Empress and Kipushi mines.

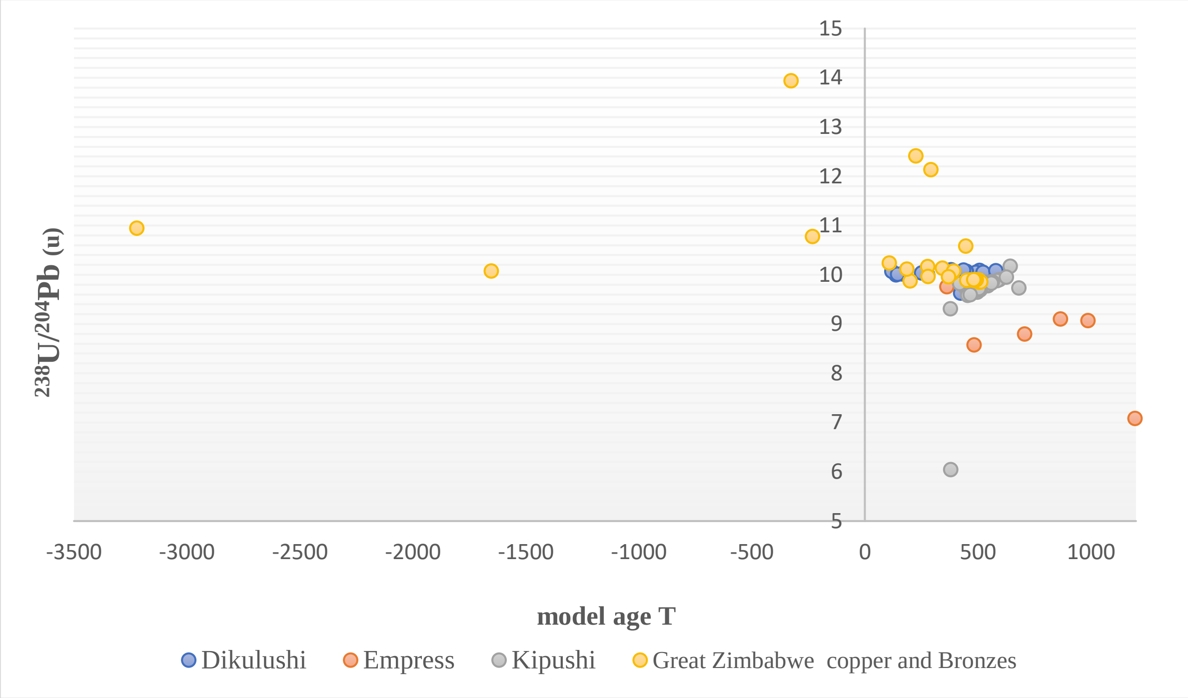

Fig 23b: Model age T vs 232Th/238U (κ) of Great Zimbabwe Cu and Cu-Sn wires, Dikilushi, Empress and Kipushi mines presented below

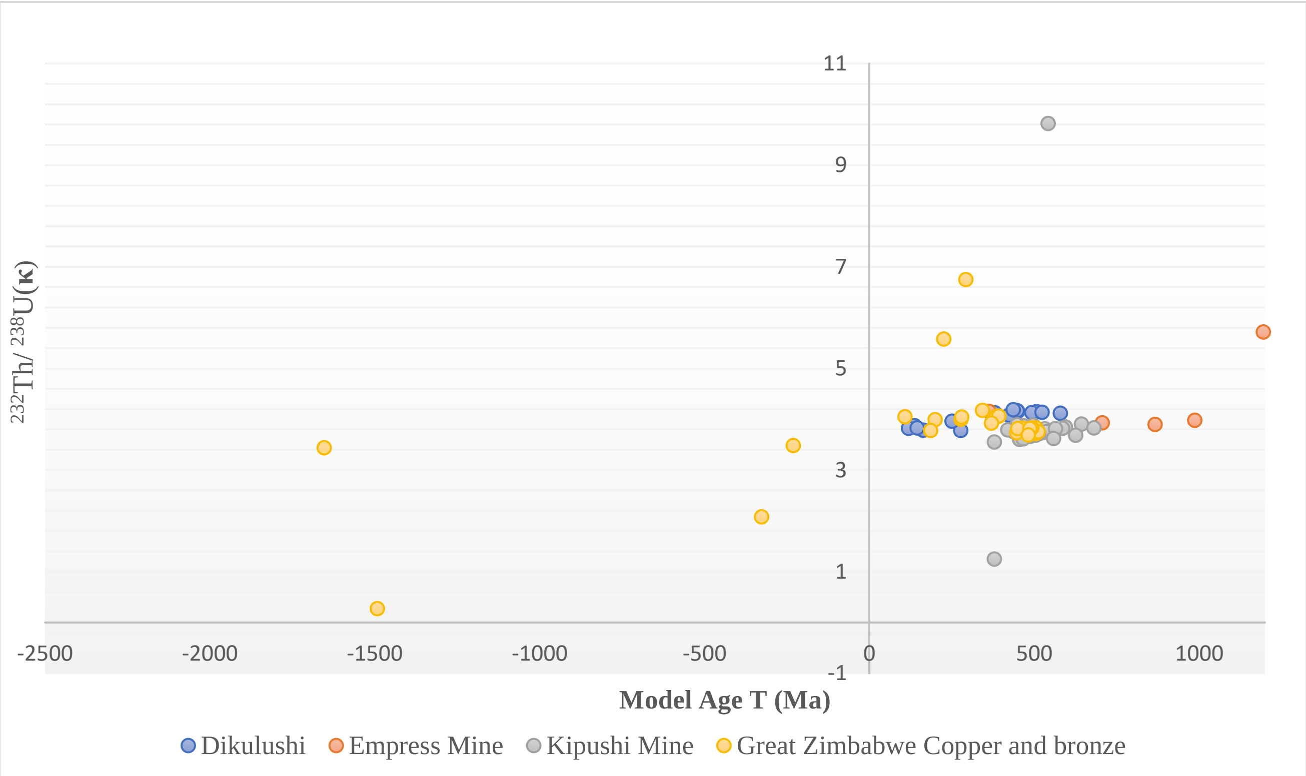

Fig. 23 (a and b) presented above shows the excellent substantial correspondence between μ and κ ratios across Empress mine, Dikulushi, Kipushi and Great Zimbabwe copper and bronze wire objects. The matching of ratios and model ages indeed reveal that copper used as the principal metal in cuprous metallurgy at Great Zimbabwe was most likely sourced from the Damarian Lufian Orogeny belt (Dikulushi and Kipushi Mines) and, possibly also nearby greenstone belts deposits such as the Empress Mafic zone. Noteworthy the consistency between unalloyed Cu and Cu-Sn alloys with copper deposits suggest that the dominant Pb within the objects was coming from Cu ores rather than Sn ores. The reason being most Sn ores are generally composed of very low Pb amounts ≤ 50ppm (Killick *et al.*, 2020) and Cu-Sn alloys are composed of more Cu as compared to Sn (Stos-Gale and Gale 2009; Pernicka 2011:254). There is also a possibility that they were other sources of copper that were exploited by ancient miners and metallurgists at Great Zimbabwe that are not characterized in this study. This is exhibited by the inconsistency of some of the Great Zimbabwe Cu and Cu-Sn objects isotopic ratios with the available ore ratios on both the conventional biplot data (Fig. 22) and Fig. 23 based on both age *T* vs $^{238}U/^{204}Pb$ (μ) and $^{232}Th/^{238}U$ (κ) respectively.

4.4 Summary

The SEM-EDS and MC-ICP-MS (chemical and isotopic composition) results presented in this chapter gave insight into the nature of cuprous metallurgy at Great Zimbabwe's Southern Terrace area. The microstructural and compositional data revealed that the fabrication techniques employed in the manufacturing of both copper and bronze were similar and that bronze was probably the most preferred alloy as compared to other cuprous alloys such as brass or gun metal at the Southern Terrace area. Isotopic data analysed and presented in this section revealed that copper used to manufacture coiled wire bangles at Great Zimbabwe was sourced from various deposits across south-central Africa. These deposits are located within the vicinity of Great Zimbabwe whereas others are situated in distant localities well known for copper production such as the Katanga region. The following chapter will discuss in detail the isotopic and compositional results presented in this chapter in line with the research questions and aims of the study.

CHAPTER 5

DISCUSSION, CONCLUSION AND RECOMMENDATIONS FOR FUTURE STUDIES

5.1. Introduction

The chapter discusses the thesis results in relation to the research questions and objectives of the study. Thus, it gives within limitations, some insight into the nature of copper metallurgy and circulation across southern Africa. In addition, it will try to evaluate the nature and trajectory of contemporary LIA in southern African archaeology and its implications on future studies.

5.2. Nature of copper-based metallurgy in Great Zimbabwe

Optical microscopic and compositional analyses revealed that the metallurgists of Great Zimbabwe manipulated copper and tin. The pervasiveness of standardized low tin bronzes with varying composition of ≤ 10wt % Sn and more Cu in terms of magnitude at USTM and Wall 55 TP 1 points toward uncontrolled intentional alloying of low tin bronzes. The objects were hammered through cycles of hot and cold working, while wire was drawn through gauges of different sizes and coiled around a vegetable core (see Miller 2002). Various fabrication techniques observed in this study are reinforced by evidence of technical ceramics and prills from Wall 55 TP 1 and USTM, wire drawing plates, hammers, tongs, crucibles, casting moulds and skimmers retrieved from Great Enclosure, Northern Rock Shelter (Hill Complex) and much recently at Mtuzu mountain that was used for hammering, casting and wire drawing (Caton-Thompson 1931; Garlake 1973; Bandama *et al.*,2016, 2017; Mukwende 2021 per coms). The similarity in fabrication techniques across the Southern Terrace area (Wall 55 TP1 and USTM) and technical material culture used for Cu and bronze fabrication across the site, suggest uniformity, resilience, circulation and the passing on of fabrication techniques and knowledge from household-to-household overtime. This trajectory seems to transcend over a wider region across hinterland south-central Africa as evidenced from Ngoma, Divuyu, Mapungubwe Thulamela, Jahunda, Mapela, Khami, Ingombe llede, Chomnungwa, northern Zimbabwean sites with evidence of uniformity in light of fabrication techniques employed to manufacture non-ferrous materials (Miller 2001,2002; Bisson 2000; Thondhlana 2007, Thondhlana and Martinon-Torres 2009; Chirikure *et al.,* 2013, 2017; Bandama *et al*., 2016, 2017, 2018; Nyamushosho 2020). Despite the omnipresence of archaeological evidence indicating wire drawing in southern, eastern and east-central Africa region, it has been suggested that the technique was not practiced in the southern parts of the Copperbelt region (Herbert 1984;

Bisson 2000).

In addition, excavated evidence of primary copper and bronze smelting and casting debris, and finished cuprous metal artefacts (Cu, Cu-Sn alloy) from USTM and Wall 55 TP 1 shows that the southern terrace area inhabitants produced copper at a small scale, just like the rest of the site's walled and unwalled areas (see Bandama *et al.*, 2016). The reason being during excavations the terrace area did not yield massive archaeometallurgy production debris and based on available evidence Cu and bronze fabrication was done within walled and domestic spaces.

Furthermore, the characterization of the metals shows no evidence of pure tin, which reasserts previous observation by Foreman Bandama and colleagues that tin was rarely used on its own across most southern African communities, but it was cast with copper to produce bronze (Bandama *et al.,* 2016, 2018). Thus, the ancient metalworkers at the southern terrace area consciously took a techno-cultural decision to manufacture unalloyed copper or mix different proportions of Cu and Sn to produce differently colored Cu-Sn alloys that were aesthetical, culturally and economically sustainable. Therefore, the omnipresence of wound Cu and bronze across the materials analysed in this study and across Great Zimbabwe in general (Bandama *et al* 2016), was not simply rooted in a simplified technological and political economy choice, rather it had an intrinsic value that cascaded from a societal ideology that revered Cu and its alloys (Herbert 1973, 1984; Childs and Killick 1993; Bisson 2000).

Due to its ritualistic significance and healing properties copper effortlessly fitted within traditional ethnopharmacology or medicinal anthropology. It was the metal of choice for various traditional therapeutic healing techniques, rituals and surgeries conducted by the traditional healers (n'anga/sangoma). In addition, wound cuprous wire on a vegetable (herb) core related amulets, anklets, bangles, waist, rings and necklaces were used for the acceptance and embellishment of the presence and protection of the ancestral spirit against evil spirits (*mamhepo),* wondering spirits (*mashavi),* bad luck, witchcraft, accidents, healing the sick, sexual enticement and boosting fertility (Shoko 2007; Herbert 1973; Herbert 1984; Pistorius 1998; Bvocho 2005; Bandama 2018). In addition, cuprous metals were also used to manufacture minute implements such as needles and razor blades which were found in the archaeological record across south-central Africa (see evidence in Bisson 2000; Mukwende 2016), that were used for traditional incisions *(nyora),* lacerations and scarring for the application of medicinal herbs for preventive and sanative measure against illnesses, headaches, backbones problems (see Shoko 2007) and general beauty purposes (see Joyce and Thomas 1908; Ellert 1984; Walker 2015) (see Figs 24 below).

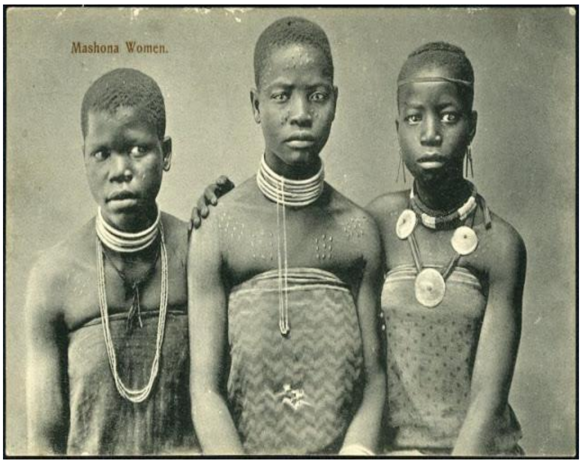

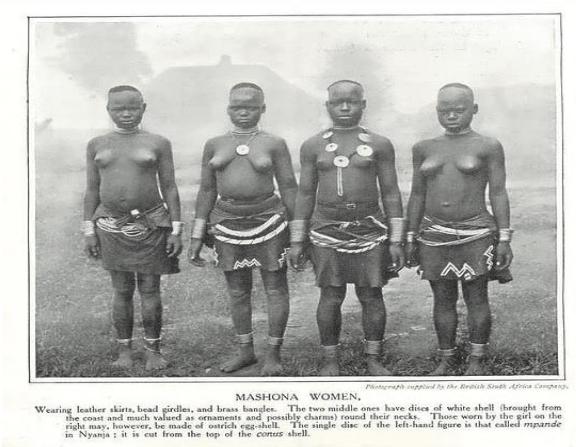

Fig 24: Woman with lacerations and wearing cuprous metallic jewellery. Images from left to right: adopted from the Rhodesian study circle and the one to the far right of Njanja women was taken from women of all nations; Joyce and Thomas eds (1908: 306).

Furthermore, copper played an important role in physical and spiritual ornamentation, with an array of copper, bronze and brass jewellery (beads, bangles, rings) being selectively crafted for personal adornment regardless of gender, age or status, whilst in other contexts, they were used as a symbol of power, status, grandness and elite hood or kingship within socio-economic, ritualistic and ceremonial spaces (see Ellert 1984; Herbert 1973,1984, 1993;Dewey 1994; Bisson 2000; Bvocho 2005; Huffman 2007; Thondhlana and Martinon Torres 2009; Thondhlana 2012; Walker 2015; Moffet 2017; Bandama *et al.*, 2018; Moffet and Hall 2020). Copper was also fused with other valuables ornaments such as iron, cowries, soapstone, glass beads, bone and other easily degradable material to enhance value to its aesthetic appearance or even spiritual adornment (Reynolds 1977; Dewey 1996; Bvocho 2005; Chirikure 2015) hence it became indispensable heirlooms ever-present in ancestral worshiping and ubiquitous as funerary goods across southern African burial contexts at sites such as Mapungubwe, Ingonde llede, Castle Kopje, Tsindi Ruins, Musimbira, Danamombe, Mapungubwe, Ingombe Illede (Munroe and Spies 1975; Huffman 2007; Walker 2015; Chirikure 2015).

There is also a consensus amongst scholars that copper and its associated alloys were repositories of wealth (Herbert 1984; Bisson 1975,1982, 2000; Thondhlana 2007, 2012; Swan 2007; Rademakers et al., 2019; Stephens et al., 2020) thus it was used as a form of currency used to pay taxes, bride price (roora/lobola), tribute, and acquire young stock, cultivated grain (sorghum and millet mainly), exotic traded goods such as glass beads, cowries, ceramics, cloth. Various copper ingots/croisettes such as the lerale, Musuku, X-shaped HIH, HXR, HH, HX were all used as mediums of exchange or currency across sub-Saharan African communities especially in areas of archaeological significance within central Congo, Zambia, coastal Mozambique, Zimbabwe and northern South Africa (Hannisch 1974; Bisson 1975, 1982; Miller *et al.,* 2001; Miller 2002; Thondhlana 2012; Swan 2007,2008; Moffett 2017; Nikis 2017; Rademakers *et al.,* 2019). There is a higher probability that given the amount of Cu in these ingots they had more value economically as compared to unprocessed ores or finished articles across south-central Africa. However, both cuprous metals ingots and finished specimens were an essential component of a multi-complex circulation system that sustained households, villages, capitals, state territories political economies across hinterland south-central Africa.

5.3. The nature of copper deposits and circulation system

The lead isotopic ratios (LIR) of the studied objects (both Cu and Cu-Sn alloys) fall into the radiogenic and highly radiogenic Pb categories. However, it must be understood that southern and central Africa is a vast region with many deposits having their Pb Isotope ratios unknown. This affects most of the deposits around Great Zimbabwe where it is not clear if they have different mineralisations with different lead isotope profiles. Furthermore, some of the copper and tin was coming from the Indian Ocean (Bandama *et al.*, 2016). In addition, we do not have trace elements for some of our samples and the ore geology in the wider region. Regardless of these constraining factors, and the mitigating availability of some limited published data, it is possible to make cautionary but signalling statements regarding the circulation of copper in southern Africa. In thinking about sources of copper and tin used in Great Zimbabwe and beyond, another pertinent point relates to the source of the lead in the Cu-Sn samples. Previous studies have argued that most Sn ores (e.g cassiterite) are generally characterized by very low Pb amounts (≤ 50ppm) (Killick *et al.,* 2020). Also, in most Cu-Sn alloys there is more Cu as compared to Sn such that the Pb was contributed by Cu ores (see Pernicka 2011:254, Stos-Gale and Gale 2009, Stephen *et al.,* 2020, and references therein).

The availability of highly radiogenic lead in copper objects suggests that the inhabitants of Great Zimbabwe sourced their copper from highly radiogenic Cu deposits or mines and mixed it with Sn to produce highly radiogenic tin bronzes. Such an observation is supported by the strong correspondence between Pb isotopic rations of both unalloyed copper and low tin bronzes samples with LIR from copper deposits (see Fig 22 and 23). Based on the conventional biplot and mu-kappa-T system results presented in the previous chapter, it can be suggested that the metallurgists of Great Zimbabwe sourced their copper from nearby (Midlands Greenstone belt's Empress Mafic Zone) and distant distinctive copper mining deposits within the Damara Orogeny namely Dikulushi and Kipushu mines. The main caveat is that we do not have trace element analyses for our samples and LIA alone cannot determine provenance (Pernicka 2014). Although insightful, this raises questions about the missing mines where there are no values for Pb isotope ratios, or the total number of LIR is not representative enough (see Fig 8 and table 25 below). Of course, modern political boundaries did not exist pointing to the presence of micro and macro networks in which copper was circulated. Historical evidence and the presence of iron gongs and copper crosses point to linkages between southern and central Africa in different directions. However, in the absence of trace element analysis and Pb isotope ratios of other mines caution is required before linking Great Zimbabwe objects with Cu-Ag and Cu-Fe-Pb-Zn mining zones within the Damaran Orogeny. The mineralisation ages of most of the 'missing mines' are not known, and the generalisation that the Pb values in most Pre-Cambrian copper deposits is old does not always hold, because some mines have older and younger mineralisation.

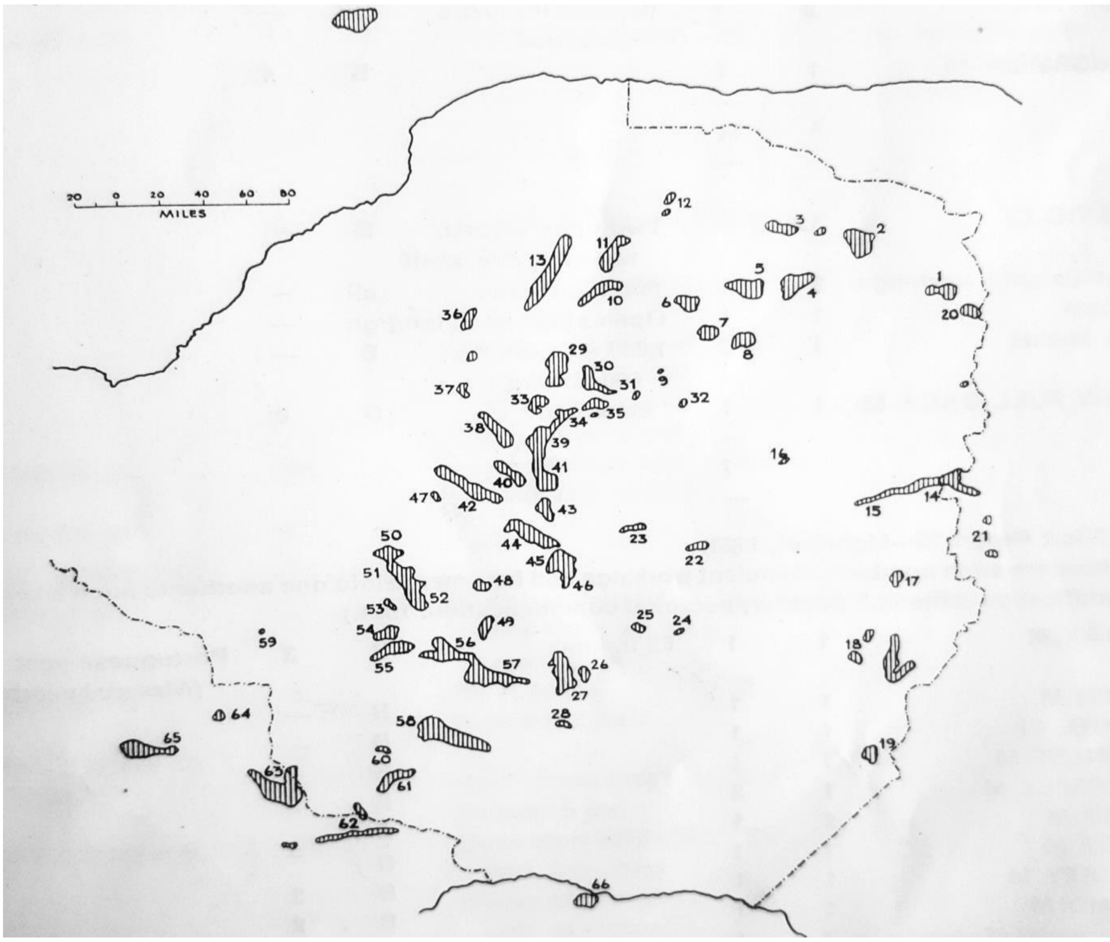

Fig 25: Map with documented evidence of ancient mines associated with Au, Sn and Cu mining across Zimbabwe, northern South Africa, and north-western Botswana (adopted from Summers 1969:37). NB see detailed Table 8 below with the list of Cu, Sn mines most of which are missing in the current Pb isotopic database.

Table 8: Mines with documented evidence of ancient exploitation from Summers (1969; 35-103) that missing in the current Pb isotopic database

Arch-Survey Number	Country	Documented name	Mordern name of deposit	Geological detail	District/ Area	Mine name	Ancient working type	ancient mines	Technical details	Cultural Evidence	Output in ounces	Metal mined
1	Zim.	Makaha	Makati Makaha	gneiss	Makaha	Gairesi v Matisi river	Open stopes	2	Very small			Cu
10		Hurungwe Area	Mangondi Belt		Mhangura area	Alaska Mine			Big - (1700 x 150 x 70 ft deep)			Cu, Ag
10			Mangondi Belt	Lomangundi		United Kingdom CI	Open stopes	1	1000 x 200 x 35 ft		100 000-300 000	Cu, Ag
11		Ayshire	Mangondi Belt	Pirirwiri Series		Silverside M	Open stopes	7	$1^1/_2$ miles along with few gaps			Cu
13		Piriwiri	Mangondi Belt	Piriwiri Series	Piwiriri	Angwa R	Open stopes		alluvium	Iron, spearhead hinese sherds, Portuguese Damba nearby		Cu
13		Piriwiri-Dewera	Mangondi Belt	Pirirwiri Series		Anzac Mine	Open stopes	1	Very small			Cu
13			Mangondi Belt	Piriwiri Series		Condie Mine	Open stopes	2	Slope, 2000 ft long: hole 300			Cu

								x 100 x 36 ft deep		
13		Mangondi Belt	Piriwiri Series		Crescent Mine	Open stopes	5	Typical: 900 x 60 x 60 ft		Cu
13		Mangondi Belt	Piriwiri Series		Gondia Mine	Open stopes	1			Cu
13		Mangondi Belt	Piriwiri Series		Norman Mine	Open stopes	1	1200 ft long		Cu
13		Mangondi Belt	Piriwiri Series		Northern Star Mine	Open stopes	2	800 ft long: 200 ft long x 40 - 50 ft deep		Cu
13		Mangondi Belt	Piriwiri Series		Victory Ci Mine	Open stopes	1			Cu
13		Mangondi Belt	Piriwiri Series		Wealth M	Open stopes	1			Cu
14	UmtaliArea	Mutare-Odzi-Rusape Greenstone belt	Bulawayan System	Mutare	Nyamakwarara R	Open stopes	1			Cu
17	Upper Sabi	Odzie-Mutare - Manica Greenstone Belt	Bulawayan System	Upper Save area	Odzi R	Open stopes	1		3	Cu
14		Odzie-Mutare -	Bulawayan System	Penhalonga Area	Penhalonga V	Open stopes	1	small opening		Cu

		Manica Greenstone Belt								
15	Odzi	Odzie-Mutare - Manica Greenstone Belt	Bulawayan System	Odzie Area		Shafts and open stopes	2	60 ft long x 65 ft deep shafts, 2 ft 6in, rubble	Coin of antoninus + Cu @ 70ft found by Bent	Cu
18	Umkondo	Umkondo Basin	Umkondo System	Umkondo	CHI-IMP-CI	Open stopes	1	small opening		Cu
18		Umkondo Basin	Umkondo System		Copius A and B CI	Open stopes	1	300ft long		Cu
18		Umkondo Basin	Umkondo System		Elephant Mine	Shafts and open stopes	1	100 ft long x120 ft		Cu
18		Umkondo Basin	Umkondo System		Hot Springs CI	Open stopes	1		Ziwa Sherds	Cu
18		Umkondo Basin	Umkondo System		Mofouni Ci	Open stopes	1			Cu
18		Umkondo Basin	Umkondo System		Marie Louise and Clara Ci	Open stopes	2			Cu
18		Umkondo Basin	Umkondo System		Mossurise r	Open stopes	3			Cu
18		Umkondo Basin	Umkondo System		Nyamasaka Ci	Open stopes	1			Cu

18	Masvingo/ Chipinge	Umkondo Basin	Umkondo System		Umkondo Mine	Open stopes	4	Largest 1500 x 180 x 80, Shafts 2 ftx 6, tunnels with timber	Skeletal remains	Cu
18		Umkondo Basin	Umkondo System		Vesuvius, ETC Cis	Open stopes	4	Shallow pits (2sq miles)		Cu
19	Chiredzi (Hippo Area)	Masvingo Greenstone Belt/ Limpopo Belt	Post Karoo system	HippoVall ey	Gombi Ci	Open stopes	1			
17	Hippo	Masvingo Greenstone Belt/ Limpopo Belt	Post Karoo	Hippo Valley	Hippo M	Open stopes	1		Stone hammers, iron gads	
17	Victoria	Masvingo Greenstone Belt/ Limpopo Belt	Post Karoo		Hippo Ci	Open stopes	1			
24-25		Masvingo Greenstone Belt/ Limpopo	Post Karoo		P & O M	Open stopes	1		Stone hammers	

		Belt								
25	Masvingo (Victoria)	Masvingo Greenstone Belt	Bulawayan System		Zimbabwe Copper	Shafts and open stopes	1	Potholes and open stope		Cu
		Masvingo Greenstone Belt	Bulawayan System			Open stopes				
	Golden Valley		Bulawayan System		Copper Duke Mine	Open stopes	1	100 x 38 ft	very small 100-500 oz	Cu
36	Lower Umniati (Munyati)	Magondi Belt	Piriwiri Series	Munyati	Copper King Mine	Open stopes	1			
36			Piriwiri Series		Copper Queen	Open stopes	1			
36					Copper Royal	Open stopes	1			
38	Mafungabusi		Buluwayan System		Copper Empress Mine	Open stopes	1	Scratchings	very small 100-500 oz	
39	Battlefields	Kadoma Greenstone Belt	Shamvamvian	Between modern day Kadoma and Kwekwe	Umniati Railway Bridge	Open stopes	1	12 ft deep		Cu & Sn

40	Sinanombi		Buluwayan System		Skipper Mine	Open stopes	1	450 x 200 ft			
41	Que Que		Sebakwian Ssytem	Kwekwe	24 Miles South of Gaika	Open stopes	6				Cu
42	Lower Gwelo		Buluwayan System	Lower Gweru	Copper Emperor	Open stopes	1	300 ft long x 100 ft deep			Cu
43	Gweru	Midlands Greenstone Belt	Buluwayan System	Hunters Road	Redfields Farm	Open stopes	1				
45	Gweru	Midlands Greenstone Belt	Buluwayan System	Guinea Fowl	Lorne CI	Open stopes	1	800 ft overall shallow			
45	Gweru	Midlands Greenstone Belt	Buluwayan System	Guinea Fowl	Mount Morgan Ci	Open stopes	1	600 x 60 +ft deep			
46		Midlands Greenstone Belt	Buluwayan System		Rocket Mine	Open stopes	1				Cu
48		Mazowe Greenstone Belt (Upper Bulawayan Group)	Sebakwian Ssytem	Shangani	Shangani r	Open stopes	1				Cu
54	Bulawayo	Bulawayo Greenstone	Buluwayan System	Bulawayo **	Main Reef	Open stopes	1	+ 27 ft deep	Fe and Cu bangles	moderate 5000-10000	

		Belt							oz	
62	Shashi		Undifferentiated		Manjande	Open stopes	1			Cu
62			Undifferentiated		Bamangwato Dst	Open stopes	2			Cu
62			Associated with Precambrian Deposit		Bamangwato Dst	Open stopes	1			Cu
62			Associated with Precambrian Deposit		Bamangwato Dst	Open stopes	1			Cu
62			Associated with Precambrian Deposit		Shashi Copper Ci	Open stopes	1			Cu
*Isolated Zim mines (Page 79)	Masvingo	Masvingo Greenstone Belt	Gneiss	Chiredzi Mining District	Dambalagwe Ci	Open stopes	1			Cu
	Mvuma	Mvuma Greenstone Belt	Associated with Older Granites		Mercury Mine	Open stopes	1			Cu
	Mvuma	Mvuma Greenstone Belt	Bulawayan System		Falcon Mine	Shafts with undergr.	+ 13	Small several shafts +30 ft deep	considerable 10000 - 50000 oz	Cu, Ag

							Stopes				
63.	Bots.	Tati Concession		Bulawayan System	Tati Area + 200	Penhalonga Mine	Open stopes	200			Cu
63				Bulawayan System		Selkirk Mine	Open stopes	1			Cu
63				Bulawayan System		Farm 416	Open stopes	1			Cu
65	Bots	Matsitama	Mtsitama Belt	Undifferentiated		Matsitama r (Main Site: 20 sq. miles around)	Open stopes	45	Largest stope- 600 x 100 x 15 - 20 ft deep	Undecorated potsheads, beads associated with Khami ruins	
65			Mtsitama Belt			Bushman M	Open stopes	1			
66	SA	Musina	Limpopo Belt	Messina System		Messina	Shafts- with undergr. stopes	1	Shafts with steps 80 ft-deep,		Cu
66			Limpopo Belt	Messina System		Harper M		1			Cu
66			Limpopo Belt	Messina System		Campell M	Shafts with undergr. stopes	1	Collapsed stope at foot of ±80 ft shaft	Skeletal remains	Cu

66	Limpopo Belt	Messina System	Artonvilla	Open stopes	1	small		Cu
66	Limpopo Belt	Messina System	site near Atinvilla	Open stopes	1	small	Stone hammers and slag	Cu

The issues to do with sampling and representativity also raise other interesting directions of debate. Previous lead isotope studies of tin ingots, prills and low tin bronze objects showed, based on samples from the Curio Shop area of Great Zimbabwe that the tin came from Rooiberg in South Africa (see Molofosky 2009; Molofosky *et al.*, 2014). Results in this study shows that, the inhabitants of the Hill Complex's southern Terrace area made use of Sn with very low Pb ratios as compared to Cu. Rooiberg was evidently not the sole source of tin for most southern African sites especially Great Zimbabwe (Grant 1995; 1999, Miller 2002) and strengthens the possibility of the exploitation of other cassiterite deposits from around Great Zimbabwe such as Bikita, Concurpia and Kamativi which were not analysed in this study but do have evidence of ancient exploitation. In any case, it makes sense that a place as large and as long lived as Great Zimbabwe would have different sources of metal, through time. Some of the southern terrace samples are from chronological contexts that are earlier than the ingots studied by Mike Grant, Lisa Molofsky and others.

These preliminary conclusions based on Pb isotope ratios seems to confirm typological, historical, and ethnographical data that have always linked Great Zimbabwe, Upemba and Katanga polities due to similarities in material culture such as x- shaped croisettes, casting moulds and double-flanged bells which were manufactured in the northern Zambezi and central African region (Garlake 1973; Bisson 1979, 1982, 2000; Killick 2017; Swan 2007, 2008; Chirikure 2015; 2019). Isotopically the croisettes (x-shaped ingots) are characterized by a wide range of Pb ratios that are compatible with the Copper Belt's Damaran fold belt and the Kundelungu Plateau deposits (Rademakers *et al.*, 2019). However, Swan (2007) suggests that HIH copper ingots at Great Zimbabwe were acquired through a relay. Communities in the current day Hurungwe area in northern Zimbabwe acted as intermediaries connecting areas to the north and south of Zimbabwe during the Ingombe IIede period. It must also be borne in mind that there are copper mines in Hurungwe and adjacent areas making it possible that the ingots at Great Zimbabwe were northern Zimbabwe imitations of those from the Copper Belt (Chirikure 2017). Again, this motivates studies of more samples, especially from the surrounding mines. The effect of mixing metal from different sources must be quantified. This makes sense because Great Zimbabwe yielded significant evidence in the form of wire draw plates, tongs, pincers, crucibles and other materials associated with gold and copper metallurgy (Bandama *et al.,* 2016; Mukwende 2021 per comms).

That modern political boundaries are artificial is reinforced by the different circulation networks that connected communities to the north and south of the Zambezi and those to the north and south of the Limpopo. The mechanics of circulation were very complex, often following where people were and where production took place. This attests to the presence of groups that specialised in production and distribution in southern and central Africa (see Hanisch 1974, Bisson 2000, Miller *et al.,* 2001, Thondhlana 2007, Swan 2007, 2014 Chirikure 2015, 2017, 2019, Moffett 2020). According to Bandama (2013), the Tsonga people were one of the most itinerant traders in regions to the south of the Limpopo while vashambadzi (Mudenge 1974, 1988) were itinerant traders between the Limpopo and Zambezi rivers. Then there are groups such as the Mbara who crossed the Zambezi linking north Zambezi with south Zambezi. While copper and metal were one commodity, the system also included other resources such as cattle, grain, ores, salt, ivory and skin and many others (Garlake 1982). This dynamic intra southern African circulation is not always given the prominence that it deserves.

In summary, the main objectives of this study were achieved especially the characterisation of manufacturing technology. The manifold methodological, technical, and geological constraints especially the lack of comparative geological samples from key mineral provinces meant of the regions with data, our LIA ratios corresponded with the Empress Ultramafic Complex (Cu-Ni mineralization) and the Katanga Region especially at Dikilushi and Kipushi (Cu-Ag and Cu-Pb-Ze-Fe mineralization). However, while there is potential for LIA and trace element studies, in addressing questions related to copper circulation, good databases of geological, chemical, historical, and sociological information is vital.

5.4. Limitations and suggestions for future studies

The use of LIA in this study proved not to be immune to various methodological, geological, and technical constraints that have hampered the technique’s use in archaeology worldwide. As mentioned earlier, cost limitations mandated that we could not perform trace elemental analysis of the studied materials Great Zimbabwe. This will be rectified in subsequent studies. The application of lead isotopes in African archaeology is still exploratory. This means that most of the issues that have been resolved or partly resolved for other regions are still major limitations. The impact of mixing ores and metals from different sources has not yet been determined. The lack of detailed knowledge on local and regional geological deposits affects metal provenance studies in archaeology because regional deposits are characterized by geochemical and model ages that tend to overlap thus heavily obscuring statistical discrimination of lead isotopic signatures between artefacts and deposits with certainty (Balliana 2013;2974, Tomcyzk 2021). The available small sample sizes do not help much. There is need for improved regional databases with adequate gitological information (Baron *et al.*, 2014, Tomczyk *et al.*, 2021).

Furthermore, some of the samples must be collected from ancient mines and smaller deposits that were worked in the past but are not commercially viable for the present. According to Stos-Gale and Gale (2009) '*for a mine to be completely characterized there is need for at least 30-50 isotopic measurements to be done*.' The available southern African datasets come nowhere nearer to this number (see Killick *et al.*, 2020). Therefore, the current southern African database, despite being an essential starting point in provenance studies within the region it needs to be updated and modified. This could also involve incorporating more archival information and grey literature in the repositories of different institutions. Finally, there is need for comprehensive sampling and characterisation of copper, tin bronzes, brass, tin artefacts (ingots, bracelets, bangles, wires, spears, arrowheads) from various archaeological contexts at Great Zimbabwe to have a complete sequence or well characterised cuprous metallurgical industry of Great Zimbabwe. This will shed more light on the nature of copper-based metallurgy at various households at Great Zimbabwe and might point to changing sources through time. While the potential is huge, more work is required in future to unlock this potential.

REFERENCES

Ackermann, K.J., Branscombe, K.C., Hawkes, J.R., and Tidy, A.J.L. 1968. The geology of some beryl pegmatites in Southern Rhodesia. (Verhandelinge van die Geologiese Vereniging van Suid Afrika) *Transactions of the Geological Society of South Africa*. 69(1), pp 1-38.

Albarède, F., Desaulty, A.M. and Blichert-Toft, J. 2012. A geological perspective on the use of Pb isotopes in archaeometry. *Archaeometry*, 54(5), pp 853-867.

Aliya D and Lampman S. Physical metallurgy concepts in interpretation of microstructures, Metallography and Microstructures in *ASM Metal Handbook.* 9, (1), pp 44–70.

Anderson, M.S. 2009. Marothodi: The Historical Archaeology of an African Capital. Woodford: Atikkam Media.

Artioli, G., Canovaro, C., Nimis, P. and Angelini, I., 2020. LIA of prehistoric metals in the central Mediterranean area: A review. *Archaeometry*, 62, (5) pp. 53-85.

Baker, J., Stos, S., and Waight, T., 2006. Lead isotope analysis of archaeological metals by multiple collector inductively coupled plasma mass spectrometry. *Archaeometry*, 48(1), pp 45–56.

Bandama, F. 2013. *The Archaeology and Technology of Metal Production in the Late Iron Age of the Southern Waterberg, Limpopo Province, South Africa*. Unpublished Ph.D. thesis, Department of Archaeology, University of Cape Town, Cape Town.

Bandama, F., Chirikure, S. and Hall, S., 2013. Ores sources, smelters and archaeometallurgy: exploring Iron Age metal production in the Southern Waterberg, South Africa. *Journal of African Archaeology*, *11*(2), pp.243-267.

Bandama, F., Hall, S, and Chirikure, S. 2015. Eiland crucibles and the earliest relative dating for tin and bronzeworking in southern Africa. *Journal of Archaeological Science* 62, pp 82-91.

Bandama, F., Manyanga, M., and Chirikure, S., 2018. Copper wire objects from Jahunda and Little Mapela: technology, value systems and networks in Iron Age southern Africa. *Azania: Archaeological Research in Africa*, *53*(4), pp.528-545.

Bandama, F., Moffett, A. J., Thondhlana, T. P., and Chirikure, S. 2016. The production, distribution and consumption of metals and alloys at Great Zimbabwe. *Archaeometry* 58, pp 164-181.Bandama, F., Moffett, A., J., and Chirikure, S. 2017. Typological and technological attribute of metallurgical crucibles from Great Zimbabwe (1000-1700 CE) Legacy collections: *Journal of Archaeological Science Reports* 12. pp 646-657.

Baron, S., Tămaş, C. G. and Le Carlier, C., 2014. How Mineralogy and Geochemistry Can Improve the Significance of P b Isotopes in Metal Provenance Studies. *Archaeometry*, *56*(4), pp.665-680.

Baxter, M. J., Beardah, C. C. and Westwood, S., 2000. Sample size and related issues in the analysis of lead isotope data. *Journal of Archaeological Science*, *27*(10), pp.973-980.

Beach, D. 1998. Cognitive archaeology and imaginary history at Great Zimbabwe 1. *Current Anthropology* 39, (1), pp 47-72.

Beach, D. N. 1976. Second thoughts on the Shona Economy: Suggestions for Further Research. *The Journal of The Central Africa Historical Association*, 7, (1), pp 1-13.

Beach, D. N. 1980. *The Shona and Zimbabwe 900–1850. An Outline of Shona History*. London: Heinemann.

Beach, D. N. 1984. *Zimbabwe before 1900*. Gweru: Mambo Press.

Beach. D. N. 1998. From Heroism to History: Mapondera and the Northern Zimbabwean Plateau. 1840-1904. *History in Africa,*15, pp 85-161.

Bent, J. T. 1896. *The Ruined Cities of Mashonaland.* Bulawayo, Books of Rhodesia.

Bhila, K. H. H. 1968. Manyika Relations with Monomotapa,Changamire and the Portuguese from the sixteenth Century to the End of the Nineteenth Century . Unpublished *paper Commonwealth Institute of London.*

Bisson, M. S., 1975. Copper currency in central Africa: the archaeological evidence. *World Archaeology*, *6*, pp.276-292.

Bisson, M. S. 1982. Trade and Tribute. Archaeological Evidence for the Origin of States in South Central Africa. Cahiers *d'études africaines, systèmes étatiques africains*. 22 (87), pp 343-361.Bisson, M. S., 2000. Precolonial copper metallurgy: socio-political context. *Ancient African metallurgy: the sociocultural context*, pp.83-146.

Bisson. M. S. 2000. Precolonial copper metallurgy: socio-political context.? In Ancient African Metallurgy: The Sociocultural Context, edited by J.O. Vogel, 83:146. Walnut Creek: AltaMira Press.Blenkinskop, T. G. 1991. Controls on Archaean gold mineralization in the Mashava area, Zimbabwe. Institution of Mining and Metallurgy, *African Mining*,91 pp 323-367.

Blenkinsop, T. G., Martin, A., Jelsma, H. A., Vinyu, M. L., 1997. The Zimbabwe Craton. In: de Wit, M. J., Ashwal, L. D. (eds.), *Greenstone Belts*. Oxford University Press, Oxford, pp 567-580.

Brandl, G., Cloete, M., Anhaeusser, C.R., Johnson, M.R. and Thomas, R.J., 2006. Archaean greenstone belts. *Geological Society of South Africa/Council for Geoscience Johannesburg/Pretoria.* pp. 9-56.

Bray, P. J., Pollard, A. M. 2012. A new interpretative approach to the chemistry of copper-alloy objects: source, recycling and technology. *Antiquity* 86, (333), pp 853–867.

Bray, P.J, Cuenod, A., Gosden, I. C., Hommel, P., Liu, R and Pollard, A. M. 2015. Form and Flow: the 'Karmic Cycle' of copper. *Journal of Archaeological Science* 56, pp 202-209.

Brill, R. H., and Wampler, J. M., 1967, Isotope studies of ancient lead. *American Journal of Archaeology*, 71, (1), pp 63–77.

Buchholz., P., Herzig., P., Friedrich, G and. Frei, R. 1998. Granite-hosted gold mineralization in the Midlands greenstone belt: a new type of low-grade gold deposit in Zimbabwe. *Mineralium Deposita*, 33, (5), pp 437-460.

Budd, P., Haggerty, R., Pollard, A. M., Scaife, B., and Thomas, R. G., 1995, New heavy isotope studies in archaeology,*Israel Journal of Chemistry*, 35, (2), pp 125–30.

Bullock, C. 1927. *The Mashona: The Indigenous Natives of Southern Rhodesia*. Cape Town: Juta Cambridge.

Bvocho, G., 2005. Ornaments as social and chronological icons: A case study of southeastern Zimbabwe. *Journal of Social Archaeology*, 5, (3), pp.409-424.

Chanaiwa, D. 1972. Politics and Long-Distance Trade in the Mwene Mutapa State During the Sixteenth Century: *The International Journal of African Historical Studies*, 5, (3), pp424-435.

Chikumbirike, J., Bamford, M. K., and Esterhuysen, A. B. 2016. A Study of Charcoal from Great Zimbabwe *South African Archaeological Bulletin* ,71, (204), pp 107-118.

Child, T. S. and Killick, D. 1993. Indigenous African Metallurgy: Nature and Culture. *Annual Review of Anthropology*, 22, pp 317-337.

Chimhanda, F. 2014. African Theology of the Land. A Shona Perspective. *Journal of Theology for Southern Africa.* 148, pp 33-47.

Chimhundu, H. 1992. Early Missionaries and the Ethnolinguistic Factor During the ‘Invention of Tribalism’ in Zimbabwe. *The Journal of African History* 33, (1), pp 87-109.

Chipunza, K. T., 1994. A Diachronic Analysis of the Architecture of the Hill Complex at Great Zimbabwe (Studies in African Archaeology 8). *Societa Archaeologica Upsaliensis, Uppsala*.

Chirikure, S. 2006. New light on Njanja iron working: Towards a systematic encounter between ethnohistory and archaeometallurgy. *South African Archaeological Bulletin*, 61, (184), pp 142-151.

Chirikure, S. 2007. Metals in society: Iron production and its position in Iron Age communities of southern Africa. *Journal of Social Archaeology*, 7, (1), pp 72-100.

Chirikure, S. 2013. The Archaeology of African Metalworking. In The Oxford Handbook of African Archaeology. *Edited by P. Mitchell and P.J. Lane*. *The Oxford handbook of African archaeology*. OUP Oxford.

Chirikure, S. 2014. Geochemistry of Ancient Metallurgy: Examples from Africa and Elsewhere. In Cerling, T. and Turerekian, K, (eds*) Treatise on Geochemistry Archaeology and Anthropology. Elsevier*, 14. pp 169-189.

Chirikure, S. 2014. Land and Sea Links: 1500 Years of Connectivity Between Southern Africa and the Indian Ocean Rim Regions, AD 700 to 1700. *African Archaeological Review*, 31, (4), pp 705-724.

Chirikure, S. 2015. *Metals in Past Societies: A Global Perspective on Indigenous African Metallurgy*, Springer, Cham, Switzerland.

Chirikure, S. 2020. *Great Zimbabwe: Reclaiming a 'confiscated'past*. Milton Park Avenue; Oxon: Routledge.

Chirikure, S., 2020. New perspectives on the political economy of Great Zimbabwe. *Journal of Archaeological Research*, *28*, (2), pp.139-186.

Chirikure, S., and Pikirayi, I. 2008. Inside and outside the dry-stone walls: Revisiting the material culture of Great Zimbabwe. *Antiquity*, 82, (318), pp 976-993.

Chirikure, S., Bandama, F., Chipunza, K., Mahachi, G., Matenga, E., Mupira, P., and Ndoro, W. 2017. Seen but not told: Re-mapping Great Zimbabwe using archival data, satellite imagery and geographical information systems. *Journal of Archaeological Method and Theory*, 24, (2), pp 489-513.

Chirikure, S., Hall, S. and Miller, D. 2007. One hundred years on: what do we know about tin and bronze production in southern Africa? In La Niece, S., Hook, D. & Craddock, P. eds *Metals and mines: studies in archaeometallurgy*:112-119. London: Archetype Publications.

Chirikure, S., Heimann, R.B. and Killick, D. 2010. The technology of tin smelting in the Rooiberg Valley, Limpopo Province, South Africa, ca. 1650–1850 CE. *Journal of Archaeological Science*, 37, (7), pp 1656-1669.

Chirikure, S., Pollard, A. M., Manyanga, M., and Bandama, F. 2013. A Bayesian chronology for Great Zimbabwe: Re-threading the sequence of a vandalised monument. *Antiquity*, 87, (337), pp 854-872.

Chirikure, S., Thondhlana, T. P., and Bandama, F. 2013. Pre-colonial mining and metal working in Southern Africa: An overview with specific reference to Great Zimbabwe. In Munyaradzi Manyanga and Seke Katsamudanga (eds) *Zimbabwean Archaeology in the Post-Independence Era*. Mount Pleasant Harare. Sage publishers. pp143-153.

Chirikure, S., Manyanga, M., Pollard, A. M., Bandama, F., Mahachi, G. and Pikirayi, I., 2014. Zimbabwe Culture before Mapungubwe: new evidence from Mapela Hill, south-western Zimbabwe. *PloS one*, *9*, (10), pp 111-224.

Chirikure, S., Thondhlana, T. P., Martinon-Torres,M. and Rehren T. 2017. The Mutapa and The Portuguese: Archaeometallurgy and Regional Interaction In Southern Africa In: M. Manyanga & S. Chirikure (Eds) 2017, *Archives, Objects, Places And Landscapes –Multidisciplinary Approaches To Decolonised Zimbabwean Pasts*. Langaa Publishing, Cameroon.

Chirikure., S., Heimann., R. B., and Killick., D. 2010. The technology of tin smelting in the Rooiberg

Valley, Limpopo Province, South Africa, ca. 1650–1850 CE. *Journal of Archaeological Science* 37, (7), pp1656–1669.

Collett, D.P., 1993. Metaphors and Representations of Precolonial Iron-Smelting in Eastern and Southern Africa. In A. Shaw, T; Sinclair; Andey, B. Okpoko, eds. *The Archaeology of Africa. Food MN´Metals and Towns,* pp 499-511. London and New York: Routledge.

Collett, D., Vines, A., and Hughes, G. 1992. Dating and chronologies of the Valley Enclosures: Implications for the interpretation of Great Zimbabwe. *African Archaeological Review*, 10, (1), pp 139-161.

Craddock, P. T., Ambers, J., Hook, D.R., Farquhar, R. M., Chikwendu, V. E., Umeji, A.C and Shaw, T. 1997. Metal sources and the bronzes from Igbo-Ukwu, Nigeria. *Journal of Field Archaeology* 24, (4), pp405–29.

Crocker, I.T., Eales, H.V. and Ehlers, D.L. 2001. The Fluorite, Cassiterite and Sulphide Deposits Associated with the Acid Rocks of the Bushveld Complex. *Memoir of the Council for Geoscience, South Africa*, 90, pp 151, Pretoria.

Decrée, S., Deloule, É., De Putter, T., Dewaele, S., Mees, F., Yans, J. and Marignac, C., 2011. SIMS U–Pb dating of uranium mineralization in the Katanga Copperbelt: Constraints for the geodynamic context. *Ore Geology Reviews*, 40, (1), pp.81-89.

Dickin, A.P., 1995. *Radiogenic isotope geology*. Cambridge, Cambridge University Press.

Dickson, R.W. 1975. The Archaeology of the Sofala Coast. *The South African Archaeological Bulletin*, 30, (119/120), pp 84-104.

Dittrich, T., Seifert, T., Schulz, B., Hagemann, S., Gerdes, A. and Pfänder, J., 2019. *Archean rare-metal pegmatites in Zimbabwe and Western Australia: Geology and metallogeny of pollucite mineralisations*, 134, Springer International Publishing.

Doe, B.R. and Stacey, J.S., 1974. The application of lead isotopes to the problems of ore genesis and ore prospect evaluation: a review. *Economic Geology*, *69*, (6), pp.757-77

Eales, H.V., 1964. Mineralogy and petrology of the Empress nickel-copper deposit, Southern Rhodesia. *South African Journal of Geology*, *67*(01), 173-201.

Ehret, C. 2002. The Civilizations of Africa: A history to 1800. Charlottesville: University Press of Virginia.

Eshel, T., Erel, Y., Yahalom-Mack, N., Tirosh, O. and Gilboa, A., 2019. Lead isotopes in silver reveal earliest Phoenician quest for metals in the west Mediterranean. *Proceedings of the National Academy of Sciences*, *116*(13), pp.6007-6012.

Evers, T. M. & van den Berg, R. P. 1974. Ancient mining in southern Africa with reference to a copper mine in the Harmony Block, north-eastern Transvaal. *Journal of the Southern African Institute of Mining and Metallurgy, 74*(6), pp.217-226.

Fagan, B. 1969. Trade and Raw Materials in South Central Africa. *Journal of African History*. 10, (1), pp 1-13.

Faure, G., and Mensing, T. M., 2005, *Isotopes: Principles and applications*, John Wiley & Sons, Hoboken.

Fenn, T.R. 2011. *Applications of Heavy Isotope Research to Archaeological Problems of Provenance and Trade in Cases from Africa and the New World*. *PhD.* Dissertation, Department of Anthropology, University of Arizona.

Fontein, J. 2003 *The Silence of Great Zimbabwe: Contested Landscapes and The Power of Heritage.* Unpublished Doctoral Thesis University of Edinburgh.

Forster, H., Koenemann, F.H. and Knittel, U., 1996. Regional framework for gold deposits of the Odzi-Mutare-Manica greenstone belt, Zimbabwe-Mozambique. *Transactions of the Institution of Mining and Metallurgy-Section B-Applied Earth Science*, 105, pp60-73.

Forsyth, M.B., 1987. Base metal resources of South Africa. *South African journal of science*, 83, (5), pp281-284.

Galer SJG, and Abouchami W.1998. Practical application of lead triple spiking for correction of instrumental mass discrimination. *Min. Mag.* 62A, (1), pp491–492.

Garlake, P., S. 1982.Prehistory and Ideology in Zimbabwe. *Journal of the International African Institute*,Past and Present in Zimbabwe, 52, (3), pp1-19.

Glynn, S.M., Master, S., Frei, D. and Wiedenbeck, M., 2020. U-Pb zircon geochronology of the Dete-Kamativi Inlier, NW Zimbabwe, with implications for the western margin of the Archaean Zimbabwe Craton. *Precambrian Research, 346,* pp.105-824.

Goscombe, B., Armstrong, R. and Barton, J.M., 2000. Geology of the Chewore Inliers, Zimbabwe: constraining the Mesoproterozoic to Palaeozoic evolution of the Zambezi Belt. *Journal of African Earth Sciences*, 30, (3), pp.589-627.

Grant, M.R., 1999. The Sourcing of Southern African Tin Artefacts. *Journal Of Archaeological Science*, 26, (8), pp 1111-1117.

Grant, M. R., Huffman, T. N., and Watterson, J. I. 1994. The role of copper smelting in precolonial exploitation of the Rooiberg tin field. *South African Journal of Science,* 90, (2), pp 85-90.

Gwavava, O. and Ranganai., R., T. 2009. The Geology and Structure of The Masvingo Greenstone Belt and Adjacent Granite Plutons from Geophysical Data, Zimbabwe Craton. *South African Journal of Geology* 112. (3-4), pp. 277-290.

Haest, M. and Muchez, P., 2011. Stratiform and vein-type deposits in the Pan-African Orogen in Central and Southern Africa: evidence for multiphase mineralisation. *Geologica Belgica*. 14, pp23-44.

Hall, M. 1984. Archaeology the Burden of Tribalism: The Social Context of Southern African Iron Age Studies. *American Antiquity*. 49, (3), pp 455-467.

Hall., R., N., 1912. Journeys into the Mo-Karanga (Southern Rhodesia). *The Geographical Journals,*39, (2), pp 137-139.

Hall, S., Miller, D., Anderson, M. & Boeyens, J., 2006. An exploratory study of copper and iron production at Marathodi, an early 19th century Tswana Town, Rustenburg District, South Africa. Journal of African Archaeology 4, (1), pp 3-35

Hall, W., S. 2013 Geology and Paragenesis of The Boseto Copper Deposits, Kalahari Copperbelt, Northwest Botswana. Colorado School of Mines. Masters Dessertation in Geology. ProQuest LLC Publishers.

Hammel., A., White., C., Pfeiffer., C. and Miller, D. 2000. Pre-colonial mining in southern Africa. The *Journal of The South African Institute of Mining and Metallurgy*. 100, (1), pp 49-56

Hanisch, E., O., M 1974. Copper Working in The Messina District. *Journal Of the South African Institute of Mining and Metallurgy.* 74, (6), pp 250-254.

Hauptmann, A., 2007*, The Archaeometallurgy of copper: Evidence from Fenan, Jordan*, Springer, New York.

Hechter-Schulz, K., 1963. Wire bangles, a record of a Bantu craft: A note on the making of brass wire bangles by a Shangaan on the Gold Mines near Springs. *South African Journal of Science*, 59, (2), pp.51-53.

Herbert, E. 1984. Red Gold of Africa: copper in pre-colonial history and culture. Madison: University of Wisconsin Press.

Herbert, E.W. 1973. Aspects of the use of the use of Copper in Pre-Colonial West Africa. *Journal of African History*. XVI (2). pp 179-194.

Herbert, E.W. 1993 Iron, Gender, and Power: Rituals of Transformation in African Societies African Systems of Though. Bloomington and Indianapolis. Indiana University Press.

Herbert, E. W. 1996. Metals and Power at Great Zimbabwe. In Pwiti, G and Soper, R. C (eds) *Aspects of African Archaeology: Papers from the 10th Congress of Pan-African Association for Prehistory and Related Studies*, pp 641-647. Harare: University of Zimbabwe.

Herbert, E.W. 2002. Mining as a Microcosm in Pre-Colonial sub-Sharan Africa. In A, Bernad., Knapp., Vincent., P. Piggot and Eugenia, W. Herbert (eds*). Social Approaches to an Industrial Past: The Archaeology and Anthropology of Mining*. New York and London Routledge.

Hirata T 1996 Lead isotopic analyses of NIST standard reference materials using multiple collector inductively coupled plasma mass spectrometry coupled with a modified external correction method for mass discrimination effect. *The Analyst.* 121, (10), pp1407– 1411.

Huffman, T.N. 1974. Ancient mining and Zimbabwe. *Journal of the South African Institute of Mining and Metallurgy*, 74, (6), pp 238–242.

Huffman, T.N. 1972. The rise and fall of Zimbabwe. *Journal of African History* 13, (3), pp 353–366.

Huffman, T.N. 1996. *Snakes and Crocodiles: Power and Symbolism in Ancient Zimbabwe*, Witwatersrand. University Press, Johannesburg.

Huffman, T.N. 2007. *Handbook to the Iron Age,* University of KwaZulu-Natal Press, Scottsville.

Huffman, T.N., and Vogel, J.C. 1991. The chronology of Great Zimbabwe. *South African Archaeological Bulletin,* 46, pp 61–70.

Huffman, T.N., Van der Merwe, H.D., Grant, M.R., & Kruger, G.S. 1995. Early copper mining at Thakadu, Botswana. *Journal of The South African Institute of Mining and Metallurgy*, 95, (2), pp53–62.

Hunt, J.P. 2005. Geological characteristics of Iron Oxide Copper Gold (IOCG) type mineralisation in the Western Bushveld Complex. Unpublished M.Sc. Thesis. University of the Witwatersrand.

Hunt, J.P., Mutele, L. and Billay, A., 2017. Prospectivity analysis of granite-related polymetallic mineralization in the Bushveld Complex, using knowledge-and data-driven methods. *Proceedings of Exploration*, 17, pp857-861.

Hunter, D.R., and Lenthal, D., H. 1971. Preliminary Review of Tin Mineralization with Particular Reference to The Bushveld Igneous Complex Economic Geology Research Unit: Information Circular Number 1. Johannesburg University of Witwatersrand.

Ixer, R.A., 1999. Role of Ore Geology and Ores in the Archaeological Provenancing of Metals. *BAR International Series*, *792*, pp.43-52.

Jackson, J.B.E., 1965. Observations on mineral deposits of the Lomagundi and Urungwe Districts, southern Rhodesia. *South African Journal of Geology*, *68*, (1), pp.237-256.

Jaguin, J., Poujol, M., Boulvais, P., Robb, L.J. and Paquette, J.L., 2012. Metallogeny of precious and base metal mineralization in the Murchison Greenstone Belt, South Africa: indications from U–Pb and Pb–Pb geochronology. *Mineralium Deposita*, *47*, (7), pp.739-747.

Jelsma, H.A. and Dirks, P.H., 2002. Neoarchaean tectonic evolution of the Zimbabwe Craton. *Geological Society, London, Special Publications*, *199*, (1), pp.183-211.

Jourdan, P. 1990. Minerals Industry of Zimbabwe. *Report 107*. Institute of Mining Research University of Zimbabwe. Harare, Zimbabwe.

Kalbskoff, S and Nutt,T. 2003. Lithological Contrasts and Constraints on Gold Mineralization in Granitoids In The Zimbabwe Craton: Structural Control and Implication for Exploration. *Economic Geology Institute Information Circular Number* 370 University of Witwatersrand.

Killick., D. 2017. Tracing Ingombe Illede Trade connections. *Antiquity*. 91, (358), pp 1087-1088

Killick, D.J., Stephens, J.A. and Fenn, T.R., 2020. Geological constraints on the use of lead isotopes for provenance in archaeometallurgy. *Archaeometry, 62*, pp.86-105.

Killick., D. and Miller., D. 2014. Smelting of magnetite and magnetite-eilmenite iron ores in the northern Lowveld, South Africa, ca. 1000 CE to ca. 1880 CE. *Journal of Archaeological* Science 43, pp 239-255.

Killick., D., Miller., D., Thodhlana., T.P., and Martinon-Torres., M. 2016. Copper mining and smelting technology in the northern Lowveld, South Africa, ca. 1000 CE to ca. 1880 CE. *Journal of Archaeological Science* 75, pp10-26.

Kinnaird, J.A., Nex, P.A. and Milani, L., 2016. Tin in Africa. *Episodes*, *39*, (2), pp.361-380.

Kritzinger, A., 2012. Location of Zimbabwe‟ s sixteenth-century mines identified from a Portuguese document–with particular reference to Manyika in the Eastern Highlands. *Zimbabwea*, *10*, pp.60-84.

Kusimba, C., M., Kim, N., C and Kusimba, S., B. 2017. Trade and State Formation in Ancient East African Coast and Southern Zambezia.In Richard., J. Chacon and Rubén., G. Mendoza eds. *Feast, Famine or Fighting. Multiple Pathways to Social Complexity: Studies in Humana Ecology* .8 pp 61 – 90, Springer, Cham.

Kusky, T. M., & Kidd, W. S. F. 1992. Remnants of an Archean oceanic plateau, Belingwe Greenstone Belt Zimbabwe. *Geology,* 20, (1), pp 40-46.

Kusky, T.M., 1998. Tectonic setting and terrane accretion of the Archean Zimbabwe craton. *Geology*, 26, (2), pp.163-166.

Lenthall, D.H. and Hunter, D.R., 1977. The geochemistry of the Bushveld granites in the Potgietersrus tin-field. *Precambrian Research*, 5, (4), pp.359-400.

Liu, R., Hsu, Y.K., Pollard, A.M. and Chen, G., 2021. A new perspective towards the debate on highly radiogenic lead in Chinese archaeometallurgy. *Archaeological and Anthropological Sciences*, 13, (2), pp 1-7.

Liu, R., Rawson, J. and Pollard, A.M., 2018. Beyond ritual bronzes: identifying multiple sources of highly radiogenic lead across Chinese history. *Scientific Reports*, 8, (1), pp.1-7.

Longman, J., Veres, D., Ersek, V., Phillips, D.L., Chauvel, C. and Tamas, C.G., 2018. Quantitative assessment of Pb sources in isotopic mixtures using a Bayesian mixing model. *Scientific reports*, 8, (1), pp.1-16.

Mackintosh, V., Kohn, B., Gleadow, A., and Tian, Y. 2017. Phanerozoic morphotectonic evolution of the Zimbabwe Craton: Unexpected outcomes from a multiple low temperature thermochronology study. *Tectonics*, 36, (10), pp 2044–2067.

Mahohoma, T. 2020. Experiencing the Sacred. *Studia Historiae Ecclesiasticae*, *46*, (1), pp 1-17.

Maska, D. and Makahamadze, T. 2013. The Proverb of Shona Traditional Religion and Ethical Code. *Journal of Pan African Studies.* 6, (5), pp 132-143.

Master, S., 1991. Stratigraphy, tectonic setting, and mineralisation of the early Proterozoic Magondi Supergroup, Zimbabwe: A review. In: *Information Circular Economic Geology Research Unit,* University of the Witwatersrand, Johannesburg, 238, (1) pp. 1- 75.

Master, S., 1996. The Palaeoproterozoic Magondi Mobile Belt, NW Zimbabwe. In: Master, S. (eds.), Excursion Guidebook, Palaeoproterozoic of Zambia and Zimbabwe. *Econ. Geol. Res. Unit Inform*. Circular: No. 302, EGRU, University of Witwatersrand, Johannesburg, pp27–65.

Master, S., Bekker, A., Hofmann, A., 2010. A review of the stratigraphy and geological setting of the Palaeoproterozoic Magondi Supergroup, Zimbabwe – type locality for the Lomagundi carbon isotope excursion. Precambrian. *Research*. 182, (4), pp254–273.

Matenga, E. 2011. *The Soapstone Birds of Great Zimbabwe: Archaeological Heritage, Religion and Politics in Postcolonial Zimbabwe and the Return of Cultural Property*, Ph.D. dissertation, Department of Archaeology and Ancient History, Uppsala University, Uppsala

Maund., E. 1891.On Matebele and Mashona Land. *Proceedings of the Royal Geographical Society*. 13, (1), pp 1-28.

Melcher, F., Graupner, T., Gäbler, H. E., Sitnikova, M., Henjes-Kunst, F., Oberthür, T., Gerdes,
A. and Dewaele, S. (2015): Tantalum–(niobium–tin) mineralisation in African pegmatites and rare metal granites: Constraints from Ta–Nb oxide mineralogy, geochemistry and U–Pb geochronology. *Ore Geology Reviews* 64, pp 667-719.

Miller, D. 2002. Smelter and Smith: Iron Age Metal Fabrication Technology in Southern Africa. *Journal of Archaeological Science* 29, (10), pp 1083–1131.

Miller, D. 2010 Indigenous Metal Melting and Casting in Southern Africa. *South African Archaeological Bulletin*. 65, (191), pp 45-57.

Miller, D. and Hall, S., 2008. Rooiberg revisited–the analysis of tin and copper smelting debris. *Historical Metallurgy*, 42, (1), pp.23-38.

Miller, D., Killick., D. and van der Merwe., J., I. 2001. Metal Working in the Northern Lowveld, South Africa, A.D. 1000-1890*: Journal of Field Archaeology*, 28, (3-4), pp. 401-417.

Miller, D.E., Young, S.M.M., Green, W.A., Van der Merwe, N.J. and Sandelowsky, B., 2005. Sourcing the ore from the Drierivier copper smelting site in central Namibia, using lead isotope fingerprinting: research in action. *South African Journal of Science*, *101*, (7), pp.344-346.

Moffet., A., J., Hall., S. and Chirikure., S. 2020. Crafting power: new perspectives on the political economy of southern Africa, AD 900–1300. *Journal of Anthropological Archaeology* 59. pp 101-180.

Moffett, A., J. 2017.*'Phalaborwa Where the Hammer is Heard': Crafting Together the Political Economy of Iron Age Communities in Southern Africa, AD 900–1900*. Unpublished Ph.D. thesis, Department of Archaeology, University of Cape Town, Cape Town.

Moffett, A. J., and Chirikure, S. 2016. Exotica in context: Reconfiguring prestige, power, and wealth in the southern African Iron Age. *Journal of World Prehistory* 29, (4), pp337–382.

Molofsky, L. J., Killick, D., Ducea, M. N., Macovei, M., Chesley, J. T., Ruiz, J., Thibodeau, A., and Popescu, G. C. 2014. A novel approach to lead isotope provenance studies of tin and bronze: Applications to South African, Botswanan, and Romanian artifacts. *Journal of Archaeological Science* 50, pp 440–450.

Moore, J.M. 2010. Comparative study of the Onganja copper mine, Namibia: a link between Neoproterozoic mesothermal Cu(-Au) mineralization in Namibia and Zambia. South African Journal of Geology, 113, (4), pp 443–458.

Mtetwa, E. 2011. *An Archaeological Perspective of Iron Production in South-central Zimbabwe*. Unpublished Masters Dissertation, University of Dar es Salaam.

Mtetwa, E. 2017. *Technology, Ideology and Environment: The Social Dynamics of Iron Metallurgy in Great Zimbabwe, AD 900 to the Present*, PhD dissertation, Department of Archaeology and Ancient History, Uppsala University, Uppsala.

Mudenge, S.I., 1988. *A political history of Munhumutapa, c1400-1902*. Harare, James Currey.

Mudenge., S.I. 1974. The Role of Trade in the Rozvi Empire. A Reappraisal. *Journal Of Southern African History.* 15, (3), pp 373-391.

Ndoro, W. 2001. *Your Monument Our Shrine: The Preservation of Great Zimbabwe*, Ph.D. dissertation, Department of Archaeology and Ancient History, Uppsala University, Uppsala.

Ndoro, W., 1994. Natural draught furnaces south of the Zambezi River. *Zimbabwean Prehistory*, 21, (2), pp.29–32.

Nikis, N and Smith, L. 2017 Copper, Trade and Polities: Exchange Networks in Southern Central Africa in the 2nd Millennium CE. 2017. Copper, Trade and Polities: Exchange Networks in Southern Central Africa in the 2nd Millennium CE. *Journal of Southern African Studies*, 43, (5), pp 895-911.

Nyamushosho, R., T. 2020. *States, agency and power on the 'peripheries': exploring the archaeology*

of Later Iron Age societies in precolonial Mberengwa, CE 1300-1600s. Unpublished Ph.D thesis, Department of Archaeology, University of Cape town.
Oudbashi, O. and Davami, P., 2014. Metallography and microstructure interpretation of some archaeological tin bronze vessels from Iran. *Materials characterization*, *97*, pp.74-82.
Oudbashi, O. and Hasanpour, A., 2016. Microscopic study on some Iron Age bronze objects from Western Iran. *Heritage Science*, *4*, (1), pp.1-8.
Pernicka, E. 1992. Evaluating lead isotope data: comments on Sayre et al. 'Statistical evaluation of the presently accumulated lead isotope data from Anatolia and surrounding regions' Comments III. *Archaeometry*, 34, pp 322–326.
Pernicka, E. 2014. Provenance Determination of Archaeological Objects. In Roberts, Benjamin W., Thornton, Christopher (Eds*). Archaeometallurgy in Global Perspective: Methods and Synthesis*. pp 239-268, New York Springer, New York.
Phillipson, D., W. 2005. African Archaeology. Cambridge University Press.
Phimister, I. A. 1974. Alluvial Gold Mining and Trade in Nineteenth-Century South Central Africa. *The Journal of African History,* 15, (3), pp 445-456.
Phimister, I.A, 1974b. Ancient' Mining Near Great Zimbabwe *Journal of The South African Institute of Mining And Metallurgy*, 74, (6). pp 233-237.
Pikirayi, I. 1993. *The Archaeological Identity of the Mutapa State,* Studies in African Archaeology No.6, Department of Archaeology, Uppsala University, Uppsala.
Pikirayi, I. 2001. *The Zimbabwe Culture: Origins and Decline of Southern Zambezian States*, AltaMira, Oxford.
Pikirayi, I. 2009.Palaces, Feiras and Prazos: An Historical Archaeological Perspective of African–Portuguese Contact in Northern Zimbabwe. *African Archaeological Review,* 26, (3), pp 163-185.
Pikirayi, I. 2013. Great Zimbabwe in Historical Archaeology: Reconceptualizing Decline, Abandonment, and Reoccupation of an Ancient Polity, A.D. 1450–1900 *Historical Archaeology,* 47, (1), pp26–37.
Pikirayi, I. 2017. Trade, Globalisation and the Archaic State in Southern Africa. *Journal of Southern African Studies,* 43, (5), 879–893.
Pikirayi, I., 2006. The kingdom, the power and forevermore: Zimbabwe culture in contemporary art and architecture. *Journal of Southern African Studies*, 32, (4), pp.755-770.
Pin, C., Gannoun, A. and Dupont, A., 2014. Rapid, simultaneous separation of Sr, Pb, and Nd by extraction chromatography prior to isotope ratios determination by TIMS and MC-ICP-MS. *Journal of Analytical Atomic Spectrometry*, 29(10), pp.1858-1870.

Pistorius, C.C. 1998.African Metalworking, Metaphors and Medicines. *Southern African Journal of Ethnology*. 21, (4), pp 198-202.

Pollard A.M. and Heron C .2008. Archaeological chemistry, 2nd edition. Royal Society of Chemistry, Cambridge.

Pollard, A. M., 2011, Isotopes and impact: A cautionary tale, *Antiquity*, 85, (328), pp 631–8.

Pollard, A. M., 2018, Beyond provenance: New approaches to interpreting the chemistry of archaeological copper alloys, Leuven University Press, Leuven.

Pollard, A. M., and Bray, P. J., 2015, A new method for combining lead isotope and lead abundance data to characterize archaeological copper alloys, *Archaeometry*, 57, pp 996–1008.

Pollard, A. M., and Heron, C., 2008, *Archaeological chemistry*, Second edition, Cambridge (UK). Royal Society of Chemistry.

Pollard, A. M., Bray, P., Hommel, P., Hsu, Y.-K., Liu, R., and Rawson, J., 2017, Bronze age metal circulation in China, *Antiquity*, 91, (357), pp674–87.

Pollard, A., M. and Bray P.J. 2014. Chemical and Isotopic Studies of Ancient Metals. In Roberts, Benjamin W., Thornton, Christopher (Eds). *Archaeometallurgy in Global Perspective: Methods and Synthesis*, pp217-238, Springer, New York

Pollard, A.M. and Bray, P.J. 2015 A New Method for Combining Lead Isotope and Lead Abundance Data to Characterize Archaeological Copper Alloys. *Archaeometry* 57, (6), pp 996–1008.

Pollard, A.M., 2009. What a long, strange Trip it's been: Lead isotopes and archaeology In: Shortland AJ, Freestone I, Rehren T, Tite MS, editors. *From mine to microscope: Advances in the study of ancient technology*, pp181-189. Oxbow Books.

Pollard, A.M., Bray, P., Gosden, C., Wilson, A and Hamerow, H. 2015. Characterising copperbased metals in Britain in the first millennium AD: a preliminary quantification of metal flow and recycling. *Antiquity* 89, (345), pp 697–713.

Pollard, A.M., Bray, P.J. and Godsen, C. 2014. Is there something missing in scientific provenance studies of prehistoric artefacts. *Antiquity*, 88 (340), pp 625-631.

Prendergast, M., D. and Wingate, M.T., 2007. Zircon geochronology and partial structural re-interpretation of the late Archaean Mashaba Igneous Complex, south-central Zimbabwe. *South African Journal of Geology*, 110, (4), pp585-596.

Pwiti, G. 1991. Trade and economies in southern Africa: The archaeological evidence. *Zambezia* 18, (2), pp119–129.

Pwiti, G. 1996. *Continuity and Change: An Archaeological Study of Farming Communities in Northern Zimbabwe AD 500–1700*, Studies in African Archaeology No. 13, Uppsala University, Uppsala.

Pwiti, G. 2005. Southern Africa and the east African coast. In Stahl, A. B. (ed.), *African Archaeology: A Critical Introduction*, pp 378-391, Blackwell, Oxford

Rademakers, F. W., Nikis, N., de Putter, T., and Degryse, P., 2019, Provenancing Central African copper croisettes: A first chemical and lead isotope characterization of currencies in central and southern Africa, *Journal of Archaeological Science*, 111, (105110), pp105-110.

Rademakers, F.W., Nikis, N., De Putter, T. and Degryse, P. 2018. Copper Production and Trade in the Niari Basin (Republic of Congo) During the 13th to 19th Centuries CE: Chemical and Lead Isotope Characterization. *Archaeometry* 60, pp1251–1270.

Radivojevic, M., Rehren, T., Pernicka, E., Šljivar, D., Brauns, M., and Boric, D., 2010, On the origins of extractive metallurgy:New evidence from Europe, *Journal of Archaeological Science*, 37, (11), pp2775–2787.

Rehren, Th. and Pernika, E. 2008. Coins, Artefacts and Isotopes – Archaeometallurgy and archaeology. *Archaeometry* 50, pp (2), 232–248.

Robinson, K. 1961. Excavations on the Acropolis Hill. *Occasional Papers of the National Museums of Rhodesia*, 3(23A), pp 159–192.

Sayre, E. V., Yener, K. A., Joel, E. C., and Barnes, I. L., 1992, Statistical evaluation of the presently accumulated lead isotope data from Anatolia and surrounding regions, *Archaeometry*, 34, (1), pp73–105.

Scott, David A. 1991. *Metallography and Microstructure of Ancient and Historic Metals*. Marina del Rey, CA: Getty Conservation Institute in association with Archetype Books.

Shaw, R.A., Goodenough, K.M., Deady, E.A. and Nex, P., 2019. The Kamativi pegmatite: an opportunity for economic development in Zimbabwe? *The Canadian Mineralogist*, 57, (5), pp.791-793.

Silva, R.J.C., Figueiredo, E., Araújo, M.F., Pereira, F. and Braz Fernandes, F.M., 2008. Microstructure interpretation of copper and bronze archaeological artefacts from Portugal. In *Materials Science Forum*. 587, pp. 365-369. Trans Tech Publication Limited.

Sinclair., P., Ekblom, K and Wood., M. 2012. Trade and Society on The South-East African Coast in The Later First Millennium AD: The Case of Chibuene. *Antiquity* 86, (333), pp.723–737.

Stacey, J. S., and Kramers, J. D., 1975, Approximation of terrestrial lead isotope evolution by a two-stage model, *Earth and Planetary Science Letters*, 26, (2), pp 207–221.

Stephens, J. A. 2016. Assessing the suitability of southern Africa for archaeological provenance studies with Lead isotopes.MA thesis, School of Anthropology, University of Arizona.

Stephens, J., Killick, D., Wilmsen, E., Denbow, J. and Miller, D., 2020. Lead isotopes link copper artefacts from northwestern Botswana to the Copperbelt of Katanga Province, Congo. *Journal of Archaeological Science*, *117*, pp.105-124.

Stos-Gale, Z.A. and Gale, N.H., 2009. Metal provenancing using isotopes and the Oxford archaeological lead isotope database (OXALID). *Archaeological and Anthropological Sciences*, *1*(3), pp.195-213.

Stos-Gale ZA. 1992. Application of lead isotope analysis to provenance studies in Archaeology. Michaelmas: Doctoral Dissertation University of Oxford.

Stos-Gale, Z. A., Maliotis, G., Gale, N. H., and Annetts, N., 1997, Lead isotope characteristics of the Cyprus copper ore deposits applied to provenance studies of copper oxhide ingots, *Archaeometry*, 39, (1), pp83–123.

Stos-Gale, Z.,and Gale, N.H. 2009. Metal provenancing using Isotopes and Oxford archaeological lead isotope database (OXALID). *Archaeological Anthropological Science* 1, (3), pp 199-213.

Summers, R. 1969. Ancient Mining in Rhodesia and Adjacent Areas. *Museum memoir* No 3. Salisbury. Mardon Printers.

Summers, R., Robinson, K. R., and Whitty, A. 1961. Zimbabwe excavations, 1958. *Occasional Papers of the National Museums and Monuments of Southern Rhodesia, Series A, Human Sciences* 3, pp 226–333.

Swan, L. 2002. Excavations At Copper Queen Mine, Northwestern Zimbabwe. *South African Archaeological Bulletin* 57, (176), pp 64-79.

Swan, L. M. 2007. Economic and ideological roles of copper ingots in prehistoric Zimbabwe. *Antiquity* 81, (314), pp999–1012.

Swan., L. 2008. *Minerals and Managers: Production contexts as evidence for social organization in Zimbabwean Prehistory*. Studies in Global Archaeology Series 12. Uppsala: Societas Archaeologica Uppsaliensis.

Taringa, N. 2006. "How Environmental is African Traditional Religion?" *Exchange* 35, (2),pp 191-214.

Taylor, C.D., Schulz, K.J., Doebrich, J.L., Orris, G.J., Denning, P.D. and Kirschbaum, M.J., 2005. *Geology and nonfuel mineral deposits of Africa and the Middle East*. US Geological Survey.

Thondhlana, T.P. 2007. *An investigation of fabrication technology and composition of copper and copper alloy beads from second millennium AD archaeological sites in Northern Zimbabwe.* Unpublished Master's Thesis. University College London.

Thondhlana, T. P. 2012. *Metalworkers and Smelting Precincts: Technological Reconstructions of Second Millennium Copper Production around Phalaborwa, Northern Lowveld of South Africa*, PhD dissertation, University College London, London.

Thondhlana, T.P. and Martinón-Torres M. 2009. Small Size, High Value: Composition and

Manufacture of Second Millennium AD Copper-Based Beads from Northern Zimbabwe. *Journal of African Archaeology*. 7, pp. 79-97.

Thondhlana, T.P., Martinón-Torres, M. and Chirikure, S., 2016. The archaeometallurgical reconstruction of early second-millennium AD metal production activities at Shankare Hill, northern Lowveld, South Africa. *Azania: Archaeological Research in Africa*, 51, (3), pp.327-361.

Tomczyk, C., Costa, K., Giosa, A., Brun, P. and Petit, C., 2021. Provenance studies using lead isotopy: contribution of the consideration of geological contexts in archaeological databases. *BSGF-Earth Sciences Bulletin*, *192*, (1), pp2-11.

Trumbull, R.B., 1995. Tin mineralization in the Archean Sinceni rare element pegmatite field, Kaapvaal Craton, Swaziland. *Economic Geology*, 90, (3), pp.648-657.

Tucker, R.F., Viljoen, R.P. and Viljoen, M.J., 2016. A review of the Witwatersrand Basin–The world's greatest goldfield. *Episodes*, 39, (2), pp.105-133.

Tyndale-Biscoe, R. 1951. The Geology of The Bikita Tin-Field, Southern *Rhodesia. South African Journal of Geology*, 54, (1), pp 11-25.

Vanhaecke, F. and Degryse, P. eds., 2012. *Isotopic analysis: fundamentals and applications using ICP-MS*. John Wiley & Sons.

VanWaarden, C. 2012. Butua and the End of an Era. The effect of the collapse of the Kalanga state on ordinary citizens. An analysis of behaviour under stress, *Cambridge Monographs in African Archaeology 82, BAR International Series 2420*. Oxford: Archaeopress.

Van Waarden, C. 2014. Prehistoric Copper Mining in Botswana. *Encyclopaedia of the History of Science, Technology, and Medicine in Non-Western Cultures*, Springer Dordrecht, pp.1-13.

Wilson, J.F. and Nutt, T.H.C., 1990. The nature and occurrence of mineralisation in the early Precambrian crust of Zimbabwe. In *Developments in Precambrian Geology*. 8, (1), pp. 555-591.

Wilson, J.F., Nesbitt, R.W. and Fanning, C.M., 1995. Zircon geochronology of Archaean felsic sequences in the Zimbabwe craton: a revision of greenstone stratigraphy and a model for crustal growth. *Geological Society, London, Special Publications*, 95, (1), pp.109-126.

Wilson, J.G., 1979. The major controls of tin mineralisation in the Bushveld Igneous Complex, South Africa. *Geological Society of Malaysia Bulletin*, 11, pp. 239-251.

Woldai, T., Pistocchi., A. and Master., S. 2006. Validation and sensitivity analysis of a mineral potential model using favourability functions. *Applied GIS*, 2, (1), pp 2-19.

Yener, K.A., Sayre, E.V., Joel, E.C., Özbal, H., Barnes, I.L. and Brill, R.H., 1991. Stable lead isotope studies of Central Taurus ore sources and related artifacts from Eastern Mediterranean Chalcolithic and Bronze Age sites. *Journal of Archaeological Science*, 18, (5), pp.541-577.

Appendices

Appendix 1. Inventory of documented metallurgical material culture from USTM and Wall 55 TP 1

Context	Object type	Material	Qnty	Length mm	Width/ diameter /Thickness /	Wt (mg)	Macroscopic description	State	Photo number Folder 100
USTM L1 0-20cm	Arrowhead	Fe	1	153.26	17	72	The head was broad and was blunt suggesting other uses rather than hunting	Partially good	8238-39
USTM L1 0-20c	Piece of a hoe blade	Fe	1	106.8	13	24	It is broken piece of a hoe blade	Bad	8240-41
USTM L1	Hematite	Ore	1	16.99	2.06	10	Reddish possible Fe ore	Good	8241-42
USTM L 1	Flexible cuprous wire	Cuprous	2			4	Pieces of coiled wire	partially stable with evidence of patina	8572-74
USTM L1	Slag	Slag	1	12.36	9.31	20000	Blackish slag	Good	8563
USTM L1	Flexible Cu wire	Cuprous?	1	155	1.18	71	Coiled Cu wire, greyish in color with greenish patina developing	Partially good (stable)	8391-97
USTM L2 20-40cm	bangle	Fe	1	73.30	3.44	8	Small circular bangle possibly for a child	Good	8433-40
USTM L2	Flexible wire fragments	Cuprous	4			22	Fragmented Cuprous wound bangles	Good	8505
USTM L2	BANGLE	Fe	1	122	1.63	14	Complete bangle but very small in	Partially good evidence	8506-7

							circumference	of corrosion	
USTM L2	Flexible bangle fragment	Cuprous	1	70.56	3.15	16	Wound on a vegetable core, the wire seems to have flat edges	Unstable deteriorating	8441-47
USTM L2	Flexible wound wire	Cuprous possibly Cu-Sn alloy	3			15	Small fragmented pieces of copper wound wire	Partially stable	8574-75
USTM L3 40-60CM	Flexible Cu wire	Cuprous	1	129.39	2.87	37	Flexible coiled wire possible a necklace fragment	Partially good	8448-51
USTM L 3	Slag		1	26.44	6.67 Thickness	10000	The slag is blackish in color	Good	8543-47
USTM L4	Slag		1	17.95		30 000	The slag is brownish in color	Good	8559-61
USTM L4	Flexible wire	Cu alloys	4			57	Pieces of Cu wire	good	8600
USTM L4	Spear head	Fe	1	29.56	6	23000	A sharp Fe spear hammering marks	Partially corroded	8492-94
USTM L 5 80-100	Cuprous wire	Cuprous/ Brass ?	1	36.04	1.43	87	Coiled cuprous wire with no fiber core its is possibly brass ?	Good	8412
USTM L5	Cuprous bangle	Cuprous/Cu?	16 fragments			79	Coiled flexible wire, one possibly Bronze	Partially good	8426-30
USTM L5	Bangle	Cuprous	1	66.87	6	87	It's a C shaped cuprous bangle possible Brass	Good	8456-58

USTM L6 100-120	Wound wire	Cuprous	1 full & 2 fragments	23.41	1.13	88	Wound cuprous wire which is very fragile associated with fragments	Unstable (bad)	8377-79
USTM L6	Flexible wire	Cuprous	1	41.15	1.32	78	Wound on a vegetable core	Good	8421-25
USTM L6	Small ball	Fe	1		58.83	47	Fe ball developing a bit of corrosion	Partially good	8517-21
USTM L6	Slag		5			19	Small pieces of slag	Good	8553-58
USTML7 120-140cm	wound	Cu	1	`10.7mm	2	77	Bangle fragment on fibre	Good	8178-79
USTM L7	Slag	Fe	1	21.74	9.23	4000	Greyish Fe slag	good	8578
USTM L7 120-140cm	Wound	Cu	6			58	Fragmented wires wound on a fiber core	Good – evidence of rust	8184-86
USTM L7	Bangle	Cuprous	1	200	3.47	40	Flexible coiled wire with greenish patina development and a darkish grey color	Unstable	8188
USTM L8 140-160 cm	Ore	Mineral rock	1	31.60	11.61	20 000	Black and shiny and its possibly a lithium ore	Good	8224-31
USTM L8	Crucible	Ceramic	1	140	63.52	35 000	Triangular shaped crucible with a coarse quartz dominated interior and evidence of gold nodules	Bad	8318-8326
USTM L8	Crucible	Ceramic	1	52.97	10.59	29 000	Smooth exterior and a glassy interior with silver traces	Good	8327-31
USTM L8	Skimmer	Ceramic	1	10.35	14	70000	It's a broken crucible piece with a glassy interior and exterior	Good	8332-38
USTM L8	Crucible	Ceramic	1	36.84	26.41	12 000	Burnt interior, no evidence of any	Partially good	8343-55

							metallic traces		
USTM L8	Skimmer	Ceramic	1	47.46	29.95	18 000	Its burnt, glassy interior and exterior	Partially good	
USTM L8	Bangle fragment	Cuprous	1	137.39	2.13	57.33	Wound on vegetable core is greyish in color	Good	8470-74
UTSM L 8	Flexible cuprous wire	Cuprous possibly Cu ?	1	103	1.37	98.02	The flexible cuprous wire seems as if it was in sits initial stages of sample analysis	Good	8479-81
USTM L 9	Flexible cuprous bangle fragment	Cuprous possibly Cu-Sn alloy	1	98	13	40	Fragmented Cu wires wound on vegetable core	Good	8478
USTM L9 180-200cm	Hollow wire	Fe		33.65	6.01	20	It seems to have been wiredrawn like Cu	Very fragile due to rusting	8187
USTM L9 180-200CM	Wound	Cu	1	127.67	3.51		Wound on fiber	Fragile-rust	8180-84
USTM L9	Slag		2	51.01	6.47	98.22	Possibly Fe smelting residue	Good	8508-10
USTM L9	Crucible	Ceramic	1	35.58	21.16	14	No visible evidence of metallic nodules	Good	8511-13
USTM Level 9	Vitrified Slag	Mixture of dross, soil& ceramic	1	34.24	28mm	22g	Predominantly greenish with burnt black exterior	Good	8191-94
USTM Level 9	Slag		1	54.18	17	70 000	Very small circular in nature possibly flow slag	Good	8195
USTM L 9	Arrowhead	Fe	1	147.15		20 000	It’s a small arrow head that’s well pointed	Good	

USTM L9	Crucible	Ceramic	1	19.90	7.76	24	Fine grained crucible with gold residues	Very good	8236-37
USTM L9	Cuprous bangle	Cu alloy	1	225	3.91		Flat wire wound on vegetable, possibly was folded	Good	8407-10
USTM L9	Cuprous	Cu alloy	1	149	2.43		Coiled cuprous wire possibly copper	Partially good	8419-20
USTM L9	Vitrified slag	Glass	1	15.21	10.02	55 000	Glass and vitrified with a dark color in the exterior	Good	8205-07
USTM L9	Bangle	Cuprous – bronze/ brass?	1	21.09	0.96	5	Flexible Cuprous wire wound on a vegetable it is not Cu because of its color	Partially good- with corroding ends	8244
USTM L9	Flexible coiled wire	Cu alloy	8	67.51	1.25	9	Flexible copper wires joined to a single Cu wire	Good	8247
USTM L9	Crucible	Ceramic	1	176	12.08	48	Ceramic crucible with gold fragments	Good	8525-27
USTM L9	Mold fragment	Ceramic	1	50.72	12.30	20	Possible mold fragment with hollow		
USTM L 10 100-120cm	Crucible Fragment	Thin ceramic	1	45.71	10.39		Crucible fragments with gold nodules possibly a recycled potsherd	Good	8253-54
USTM L10 100-120cm	Circular object	Fe	1	31.51	9	7	Fragmented Fe circular bangle	Partially good	8242-43
USTM L10	Crucible	Ceramic	1	35.56	34.97	31	Very smooth exterior, with a burnt edge and greenish traces	Good	8302-09
USTM L11 210-230	Flexible wire bangle	Cu alloy	1	54.83	1.88	40	Possible bangle/necklace coiled	Partially good	8400-8404
USTM L11	Flexible wire bangle	Cu alloy	1	76.81	1.90	59	Wound on a vegetable core	Good	8407-10

USTM L12 230-250cm	Flexible bangle fragment	Cuprous	1	58.61	3.28	66	Thick flexible cuprous wire		8486
	Flexible wire fragment	Cuprous	1	22	1,91	32	Flexible cuprous wire with evidence of greenish patina possibly copper	Partially stable	8654
USTM Under rock	Wound wire	Cu alloy	1	34.23	3	21	Cuprous bangle fused with a lot of wires	Good	8452-55
USTM L 13 230-270	Cu bead	Copper	1	150	3,39	0.8	Cu bead	Good	8650-53
Wall 55 TP 1 L1	Coiled	Cu	1	88.89	4.65	7.65	Possible Cu coiled specimen	Bad deteriorating	8208-20
Wall 55 TP 1 L1	Flexible wire	Cuprous	1					Good	
Wall 55 TP L 2		Cuprous	1				Flexible wound on a vegetable core	Good	8723
Wall 55 TP 1 BC	Wound Bangle	Fe?	1	9724	3.51	4g	Possible Fe wound on a vegetable core	Very bad, deteriorated	8221-24
Wall 55 TP 1 L 2	Wound bangle fragment	Cu	1	88.90	10.24	1	Flexible wound vegetable which is greenish in color	Partially good	8685-87
Wall 55 TP L3	Cu Lump	Cu			7.41	1200	Greenish Cu lump circular in nature	Stable	8659-62
Wall 55 TP 1 L3	Flexible wire fragment	Cuprous	1	35.15	2.63	14	Flexible wound Bangle fragment with vegetable core	Unstable	8690
Wall 55 TP 1 L4	Coiled wire fragment	Cu	1	22.6	3,56	12	Flexible cuprous wire	Good	8688

Wall 55 TP -T3	Crucible	Ceramic	1	60.20	8.87	36	Ceramic crucible with traces of gold visible	Good with a chipped edge	8716
Wall TP1 L5	Ore	Fe	1	26.77	11.30	5000	Possibly Fe ore	Good	8712-15
Wall 55 TP L 6	Crucible	Ceramic	1	27	10	4500	Ceramic crucible with greenish metallic traces and a smooth surface with decoration possibly a broken domestic potsherd converted into a crucible	Partially good	

Appendix 2. Table of SEM-EDS results normalized to 100 wt.%

Sample name	Context	Fe	Cu	Zn	As	Ag	Sn	Pb	Total
Wall 55 TP L1	Area 1	0.79	88.88	bdl	bdl	bdl	10.32	bdl	100
	Area 2	0.59	99.41	bdl	bdl	bdl	0	bdl	100
	Area 3	4.49	88.01	bdl	bdl	bdl	7.5	bdl	100
	Mean	1.96	92.1	bdl	bdl	bdl	5.94	bdl	100
Wall 55 TP 1 L 4	Area 1	0	100	bdl	bdl	bdl	0	bdl	100
	Area 2	0	100	bdl	bdl	bdl	0	bdl	100
	Area 3	0	100	bdl	bdl	bdl	0	bdl	100
	Area 4	0	94.94	bdl	bdl	bdl	5.06	bdl	100
	Area 5	4.64	74.81	0	7.13	0	13.42	bdl	100
	Area 6	0	91.55	0	0	0	4.22	4.23	100
	Mean	0.77	93.55	0	1.19	0	3.78	0.7	100
Wall 55 TP L5	Area 1	1.20	95.42		2.68	0	1	bdl	100
	Area 2	0.80	98		0	0	1.20	bdl	100
	Area 3	O	100		0	0	0	bdl	100
	Area 4	0	96.20		1	0	1.80	bdl	100
	Mean	0.50	97.58		0.92	0	1	bdl	100

Wall 55 TP UC-T3	Area 1	0	99.32	0	0	0	0.68	0	100
	Area 2	11.91	86.14	0	0.97	0	0.61	0.37	100
	Area 3	0.35	96.19	0	2.34	0	1.12	0	100
	Area 4	0.63	89.01	0	5.44	0	4.92	0	100
	Mean	3.22	92.66	0	2.19	0	1.83	0.09	100
Wall 55 TP UC 1	Area 1	0.12	97.84	0	0	0	2.04	0	100
	Area 2	0.87	98.81	0	0	0	0.32	0	100
	Area 3	0.17	99.47	0	O	0	0.36	0	100
	Area 4	0	99.2	0	0.8	0	0	0	100
	Mean	0.29	99.01	0	0.02	0	O.68	0	100
Wall 55 TP 1 L4 b	Area 1	1.2	95.15	0	1.26	0	2.05	0.34	100
	Area 2	0	97.22	0	0	0	2	0.78	100
	Area 3	1	96.50	0	1	0	0.90	0.6	100
	Area 4	0	85.33	0	2.50	0	10.17	1.99	100
	Mean	0.55	93.55	0	1.19	0	3.78	0.93	100
Wall 55 ST.TP L14	Area 1	0	92.88	0	0	0	7.12	0	100
	Area 2	0	90.55	0	0	0	9.45	0	100

	Area 3	0	89.55	0	0	0	10.45	0	100
	Area 4	0	96.45	0	0	0	3.55	0	100
	Area 5	0	96.47	0	0	0	3.53	0	100
	Mean	0	93.18	0	0	0	6.82	0	100
USTM L 1	Area 1	0	92.13	0	0	0	7.87	0	100
	Area 2	0	90.56	0	0	0	9.50	0	100
	Area 3	0	91.88	0	0	0	8.12	0	100
	Area 4	0	88.63	0	0	0	11.37	0	100
	Mean	0	90.8	0	0	0	9.2	0	100
USTM L3	Area 1	0.80	92.11	0	0	2.75	2.31	2.03	100
	Area 2	0	94.98	0	0	0	5	0	100
	Area 3	2.50	93.36	0	0.15	2	0.80	1.19	100
	Area 4	1.5	91.11	0	0.25	2.45	1.50	3.19	100
	Mean	1.20	92.89	0	0.10	1.80	3.21	0.80	100
USTM L3a	Area 1	2.01	93.35	0	1.99	0	2.65	0	100
	Area 2	1.55	94.99	0	0	0	3.46	0	100
	Area 3	0.55	95.11	0	0	0	4.34	0	100
	Area 4	0	95.55	0	1.21	0	3.24	0	100
	Mean	1.02	94.75	0	0.80	0	3.43	0	100
USTM L6	Area 1	0	96.50	0	0	0	2.55	0	100
	Area 2	2.55	98	0	0	0	0.98	0	100

	Area 3	0	94	0	0	0	6	0	100
	Area 4	0.97	95.50	0	0	0	2.50	0	100
	Mean	0.88	96	0	0	0	3.10	0	100
USTM L7	Area 1	0	96.98	0	0	0	3.02	0	100
	Area 2	0	96.65	0	0	0	3.35	0	100
	Area 3	0.72	96.09	0	0	0	3.18	0	100
	Area 4	0	97.51	0	0	0	2.49	0	100
	Mean	0.18	96.81	0	0	0	3.01	0	100
USTM L7b	Area 1	0	91.18	0	0	0	8.82	0	100
	Area 2	5.89	85.6	0	2.30	0	6.21	0	100
	Area 3	2.90	89.92	0	0	0	7.18	0	100
	Area 4	2.33	88.50	0	2.06	0	7.11	0	100
	Mean	2.78	88.8	0	1.09	0	7.33	0	100
USTM L7c	Area 1	0.47	93	0	0	0	6.53	0	100
	Area 2	0	91	0	0	0	9	0	100
	Area 3	2.87	84.56	0	0	0	12.57	0	100
	Area 4	0	92.12	0	0	0	7.88	0	100
	Mean	0.83	90.17	0	0	0	9	0	100
USTM L 8	Area 1	0	98.23	0	0	0	1.7	0	100
	Area 2	0	96.50	0	0	0	3.5	0	100
	Area 3	0	93.42	0	0	0	6.66	0	100

	Area 4	0	94.25	0	0	0	5.75	0	100
	Mean	0	95.6	0	0.	0	4.4	0	100
USTM L8b	Area 1	1.78	95.45	0	0	0	2.77	0	100
	Area 2	2.45	94.89	0	0	0	2.66	0	100
	Area 3	2.47	92.03	0	0	0	5.5	0	100
	Area 4	3.50	91.91	0	0	0	4.59	0	100
	Mean	2.55	93.57	0	0	0	3.88	0	100
USTM L8c	Area 1	1.01	93.5	0	0	0	5.49	0	100
	Area 2	1.29	92.98	0	0	0	5.73	0	100
	Area 3	0.90	95	0	0	0	4.10	0	100
	Area 4	0	92.48	0	0.12	0	7.4	0	100
	Mean	0.80	93.49	0	0.03	0	5.68	0	100
USTM L8 d	Area 1	0	92.25	0	0	0	7.75	0	100
	Area 2	0	93.45	0	0	0	6.55	0	100
	Area 3	0	87.08	0	0	0	9.99	2.94	100
	Area 4	0	93.71	0	0	0	0	6.29	100
	Area 5	0	100	0	0	0	0	0	100
	Area 6	1.44	98.56	0	0	0	0	0	100
	Area 7	0	70.14	0	0	0	29.86	0	100
	Area 8	0	98.81	0	0	0	0	1.19	100

	Area 9	0	97.15	0	0	0	2.85	0	100
	Area 10	0	98.56	0	0	0	1.44	0	100
	Area 11	0	93.45	0	0	0	6.55	0	100
	Mean	0.13	93.01	0	0	0	5.91	0.95	100
USTM L9	Area 1	2.99	90.47		0		6.54	0	100
	Area 2	3.50	89.50		0.18	1	6	0.82	100
	Area 3	4	90		0		5	1	100
	Area 4	2	77.83		0.30	3	11.54	1.46	100
	Mean	3.10	86.95	0	0.12	1	7.02	0.82	100
USTM 9b	Area 1	0	92	0	0	0	4	3.02	100
	Area 2	2.79	93.22	0	0	0	2.35	1.48	100
	Area 3	3.50	90.52	O	0	0	2.50	2.52	100
	Area 4	1.71	94.62	0	0	0	3.67	0	100
	Mean	2	92.59	0	0	0	3.13	1.80	100
USTM L 9c	Area 1	0.52	96.47	0	0	0	3	0	100
	Area 2	0	91.99	0	0	0	8	0	100
	Area 3	2	93.98	0	0	0	4.02	0	100
	Area 4	4.50	88.2	0	0	0	7.48	0	100
	Mean	1.80	92.4	0	0	0	5.80	0	100
USTM L 10	Area 1	0,76	98.24	0	0		0	1	100
	Area 2	0,6	93.86	0,61	0		4	0.93	100

	Area 3	3,77	93.28	0	3		0	0	100
	Area 4	3,86	84.86	0	5.37		5,91	0	100
	Mean	2.25	92.56	0.12	2.09	0	2.48	0.33	100
USTM L10b	Area 1	0	98.50	0	0	0	1.50	0	100
	Area 2	0	96	0	0	0	4	0	100
	Area 3	0	96.25	0	0	0	3.75	0	100
	Area 4	1.96	90.13	0	0	0	7.91	0	100
	Mean	0.49	95.22	0	0	0	4.29	0	100
USTM L11	Area 1	0.45	95.54	0	0	0	4.01	0	100
	Area 2	2.42	93.02	0	0	0	4.56	0	100
	Area 3	8.7	85.93	0	0	0	5.37	0	100
	Area 4	7.99	89.92	0	0	0	2.09	0	100
	Mean	4.89	91.10	0	0	0	4.01	0	100
USTM L12	Area 1	1.33	98	0	0	0	0.67	0	100
	Area 2	0.72	95.69	0	0	0		0	100
	Area 3	0.83	96.27	0	0	0		0	100
	Area 4	0	94.09	0	0	0		0	100
	Mean	0.72	96.01	0	0	0	3.15	0	100
USTM L13	Area 1	0	100	0	0	0	0	0	100
	Area 2	0	100	0	0	0	0	0	100
	Area 3	0	96,65	0	0	0	0	3,35	100

Area 4	0	95,42	0	0	0	0	4,58	100
Area 5	0	96,19	0	0	0	3,81	0	100
Area 6	6,04	75,25	0	0	0	18,71	0	100
Mean	1,01	93,92	0	0		3,75	1,32	100

Legend.

0= below instrument detection limit

SEM-EDS = Scanning Electron Microscope with Energy Dispersive Spectrometer USTM

USTM= Upper Southern Terrace Midden

Wall 55 TP= Wall 55 Test Pit Fe= Iron

Zn=Zinc

As=Arsenic Sn= Tin

Pb= Lead

Appendix 3. Southern African Pb Metalliferous Database Link

NB. The database was attached as part of additional material

https://onlinelibrary.wiley.com/action/downloadSupplement?doi=10.1111%2Farcm.12573&file=arcm12573-sup-0001-LIA+Regional+Databases.xlsx

Appendix 4. Recalculated model ages for Southern African metalliferous deposits

Country	Tectonic Zone	District	Class	Deposit Name	Sample Number	Code	$^{206}Pb/^{204}Pb$	207Pb/204Pb	208Pb/204Pb	mu	kappa	T (x10^6)	± T (x10^6)
Zim	Zimbabwe Craton	Bulawayan Greenstone Belt	1	Kadoma	A1	1	14.08	14.95	33.57	11.19771	3.62305054	2730.18	10.3
	Zimbabwe Craton	Bulawayan Greenstone Belt	1	Kadoma	A2	1	13.6	14.85	33.34	13. 9749	3.977060	3045.80	17.5
	Zimbabwe Craton	Bulawayan Greenstone Belt	1	Kadoma	A2	1	13.59	14.85	33.32	13.2256	3.959890	3065. 58	17.8
	Zimbabwe Craton	Bulawayan Greenstone Belt	1	Kadoma	A3	1	13.65	14.79	33.28	11.41106	3.773842	2908.49	10.75
	Zimbabwe Craton	Bulawayan Greenstone Belt	1	Kadoma	A4	1	13.68	14.86	33.4	12.39010	3.944588	2973.79	15.07
	Zimbabwe Craton	Sebakwian Group	1	Kadoma	A6	1	14.28	15.33	33.63	15.18846	3.538912	2975.63	24.87
	Zimbabwe Craton	Sebakwian Group	1	Kadoma	A6	1	14.25	15.32	33.71	15.31122	3.68453	2990.63	25.07

Zimbabwe Craton	Bulawayan Greenstone Belt	1	Kwekwe	B1	2	18.03	15.75	38.6	10.3340	4.419282	742.57	9.97
Zimbabwe Craton	Sebakwian Group	1	Kwekwe	B2	2	13.35	14.85	32.83	18.24901	3.473525	3320.77	28.3
Zimbabwe Craton	Sebakwian Group	1	Kwekwe	B4	2	13.27	14.64	32.65	12.74813	3.20249	3127.39	15.63
Zimbabwe Craton	Sebakwian Group	1	Kwekwe	B7	2	13.56	14.97	33.37	17.17453	4.13334	3242.08	27.03
Zimbabwe Craton	Sebakwian Group	1	Kwekwe	B9	2	13.63	14.96	33.44	15.39900	4.126092	3156. 593	23.8
Zimbabwe Craton	Sebakwian Group	1	Kwekwe	B10	2	14.33	15.27	33.71	13.69288	3.572926	2863. 78	20.9
Zimbabwe Craton	Sebakwian Group	1	Kwekwe	B12	2	14.7	15.51	33.71	14.62724	3.209722	2823.44	2.45
Zimbabwe Craton	Sebakwian Group	1	Kwekwe	B12	2	14.72	15.6	33.96	15.89693	3.505189	2901.95	2.75
Zimbabwe Craton	Bulawayan Greenstone Belt	1	Bulawayo	C1	3	13.76	14.8	33.43	10.72258	3.84566	2804.41	7.22
Zimbabwe Craton	Bulawayan Greenstone Belt	1	Bulawayo	C2	3	13.77	14.75	33.39	9.978254	3.751458	2719.07	2.39
Zimbabwe Craton	Bulawayan Greenstone Belt	1	Bulawayo	C3	3	13.8	14.83	33.46	10.88551	3.838561	2804.93	8.20

Zimbabwe Craton	Bulawayan Greenstone Belt	1	Bulawayo	C5	3	13.83	14.89	33.52	11.57342	3.902580	2857.85	11.80
Zimbabwe Craton	Bulawayan Greenstone Belt	1	Bulawayo	C6	3	13.79	14.82	33.44	10.80865	3.819740	2801.14	7.75
Zimbabwe Craton	Bulawayan Greenstone Belt	1	Bulawayo	C7	3	13.65	14.69	33.37	9.889502	3.89557	2759.69	17.2
Zimbabwe Craton	Bulawayan Greenstone Belt	1	Bulawayo	C8	3	13.81	14.78	33.35	10.13968	3.635695	2721.13	3.56
Zimbabwe Craton	Bulawayan Greenstone Belt	1	Filabusi	D1	4	13.78	14.85	33.42	11.33023	3.811874	2854.34	10.5
Zimbabwe Craton	Bulawayan Greenstone Belt	1	Filabusi	D2	4	13.87	14.93	33.65	11.89529	4.052655	2871.38	13.35
Zimbabwe Craton	Bulawayan Greenstone Belt	1	Filabusi	D3	4	13.84	14.85	33.59	10.90485	3.985009	2791.52	8.35
Zimbabwe Craton	Sebakwian Group	1	Filabusi	D4	4	13.46	14.75	33.32	12.66546	4.169885	3062.91	15.68
Zimbabwe Craton	Sebakwian Group	1	Filabusi	D5	4	13.37	14.78	33.44	14.99378	4.58194	3206.62	22.27

Zimbabwe Craton	Sebakwian Group	1	Filabusi	D6	4	13.38	14.73	33.27	13.34564	4.229034	3126.42	17.83
Zimbabwe Craton	Bulawayan Greenstone Belt	1	Gwanda	E1	5	13.56	14.68	33.03	10.35483	3.459647	2846.35	48.1
Zimbabwe Craton	Bulawayan Greenstone Belt	1	Gwanda	E2	5	13.72	14.78	33.23	10.70580	3.578407	2818.03	7.08
Zimbabwe Craton	Bulawayan Greenstone Belt	1	Gwanda	E2	5	13.75	14.81	33.43	10.93985	3.864572	2829.30	8.44
Zimbabwe Craton	Bulawayan Greenstone Belt	1	Gwanda	E3	5	13.73	14.84	33.58	11.56887	4.150398	2893.13	11.6
Zimbabwe Craton	Bulawayan Greenstone Belt	1	Gwanda	E4	5	13.71	14.77	33.24	10.62821	3.607252	2814.21	6.61
Zimbabwe Craton	Bulawayan Greenstone Belt	1	Gwanda	E5	5	13.89	14.94	33.66	11.89717	4.038684	2864.59	13.4
Zimbabwe Craton	Bulawayan Greenstone Belt	1	Gwanda	E6	5	13.77	14.93	33.67	12.80029	4.252901	2973.44	16.8

Zimbabwe Craton	Bulawayan Greenstone Belt	2	Gwanda	E7	5	13.73	14.93	33.61	13.23647	4.225633	3014.65	18.1
Zimbabwe Craton	Bulawayan Greenstone Belt	2	Mberengwa	F1	6	13.65	14.78	33.31	11.12427	3.821524	2894.16	9.91
Zimbabwe Craton	Bulawayan Greenstone Belt	2	Mberengwa	F2	6	13.63	14.8	33.35	11.76911	3.9298391	2944. 46	12.4
Zimbabwe Craton	Bulawayan Greenstone Belt	2	Mberengwa	F3	6	13.28	14.61	32.99	11.85663	3.849202	3070.49	12.21
Zimbabwe Craton	Bulawayan Greenstone Belt	2	Mberengwa	F4	6	13.71	14.87	33.53	12.27612	4.111873	2955.63	14.67
Zimbabwe Craton	Bulawayan Greenstone Belt	2	Mberengwa	F5	6	13.3	14.64	33.06	12.8915	3.956848	3091.12	13.99
Zimbabwe Craton	Bulawayan Greenstone Belt	2	Mberengwa	F6	6	13.73	14.83	33.48	11.40469	3.984293	2879.09	10.83
Zimbabwe Craton	Bulawayan Greenstone Belt	2	Mberengwa	F7	6	13.26	14.67	33.18	13.77688	4.285843	3182.97	1.88
Zimbabwe Craton	Sebakwian Group	2	Mberengwa	F8	6	14.17	15.27	34.08	15.191164	4.303501	3005.17	24.60

Zimbabwe Craton	Sebakwian Group	2	Mberengwa	F9	6	14.48	15.51	34.89	16.57978	4.963609	3000.36	28.25
Zimbabwe Craton	Sebakwian Group	2	Mberengwa	F10	6	15.73	16.17	34.7	17.24547	3.426785	2734.44	32.90
Zimbabwe Craton	Sebakwian Group	2	Mashava	G1	7	13.09	14.64	33.51	17.23100	5.393228	3349.42	26.06
Zimbabwe Craton	Sebakwian Group	2	Mashava	G2	7	13.1	14.67	33.38	18.4940	5.093132	3378.57	27.99
Zimbabwe Craton	Sebakwian Group	2	Mashava	G3	7	13.72	14.97	33.67	14.24469	4.3553839	3076.31	21.17
Zimbabwe Craton	Sebakwian Group	2	Mashava	G3	7	13.7	14.9	33.62	12.96333	4.28745	3006.40	17.21
Zimbabwe Craton	Sebakwian Group	2	Mashava	G4	7	14.18	15.16	33.84	13.12042	3.923713	2867.08	18.77
Zimbabwe Craton	Sebakwian Group	2	Mashava	G5	7	14.22	15.2	33.84	13.44439	3.877439	2879.62	19.94
Zimbabwe Craton	Sebakwian Group	2	Mashava	G6	7	16.6	16.07	35.75	13.36523	3.606995	2092.57	26.30
Zimbabwe Craton	Sebakwian Group	2	Mashava	G7	7	14.7	15.57	34.46	15.56577	4.123811	2886.71	26.80
Zimbabwe Craton	Sebakwian Group	2	Mashava	G7	7	14.79	15.66	34.69	16.30918	4.301470	2908.66	28.57
Zimbabwe Craton	Sebakwian Group	2	Mashava	G8	7	13.33	14.68	33.2	12.83770	4.374689	3112.78	16.05
Zimbabwe Craton	Sebakwian Group	2	Mutare	H1	8	14.14	15.26	34.02	15.33007	4.262246	3020.70	24.85

Zimbabwe Craton	Sebakwian Group	2	Mutare	H2	8	14.18	15.21	34.06	13.95699	4.244728	2929.70	21.42
Zimbabwe Craton	Sebakwian Group	2	Mutare	H3	8	14.16	15.14	33.82	12.95956	3.919090	2860.99	18.16
Zimbabwe Craton	Sebakwian Group	2	Mutare	H4	8	14.1	15.09	33.66	12.63621	3.763854	2854.76	16.84
Zimbabwe Craton	Sebakwian Group	2	Mutare	H5	8	14.15	15.1	33.68	12.42183	3.725960	2820.44	16.10
Zimbabwe Craton	Sebakwian Group	2	Mutare	H6	8	13.41	14.81	33.37	15.11888	4.380570	3201.39	22.65
Zimbabwe Craton	Mangondi	2	Copper Queen	CQ1	9	15.245	15.314	34.865	10.4517	3.874212	2151.88	7.05
Zimbabwe Craton	MangondiMangondi	2	Copper Queen	CQ2	9	15.209	15.305	34.828	10.46089	3.872815	2168.95	7.06
Zimbabwe Craton	Mangondi	2	Copper Queen	CQ3	9	15.139	15.261	34.704	10.27364	3.808898	2166.50	5.51
Zimbabwe Craton	Mangondi	2	Copper Queen	CQ4	9	15.148	15.266	34.717	10.292273	3.814013	2165.91	5.67
Zimbabwe Craton	Mangondi	2	Copper Queen	CQ5	9	15.159	15.3	34.819	10.53035	3.91663	2209.64	7.53
Zimbabwe Craton	Bulawayan Greenstone Belt	2	Empress Mine	EM-S-3	10	15.2398024700139	14.7515126729185	36.9480811477958	7.086945	5.715778	1195.41	4.74
Zimbabwe Craton	Bulawayan Greenstone Belt	2	Empress Mine	EM-76-3	10	16.9913446503682	15.3757136121426	36.8186851786336	9.101256	3.896511	866.86	8.99

Zimbabwe Craton	Bulawayan Greenstone Belt	2	Empress Mine	EM-76-4	10	16.774931255509	15.3477765278328	36.6852725015555	9.071706	3.97890	988.11	9.11
Zimbabwe Craton	Bulawayan Greenstone Belt	2	Empress Mine	EM-76-5	10	18.2637123919385	15.6291924948097	38.684409069734	9.759207	4.152432	363.39	1.76
Zimbabwe Craton	Bulawayan Greenstone Belt	2	Empress Mine	EM-S-1	10	17.0382069452798	15.3106134222569	36.9574410157499	8.799167	3.929275	707.38	1.52
Zimbabwe Craton	Bulawayan Greenstone Belt	2	Empress Mine	EM-S-2	10	17.2129964734549	15.271448191138	36.9754645595005	8.579399	3.790457	484.20	2.10
Zimbabwe Craton		2	OO	OO-76-3	10	18.0285719159642	15.6777027109607	38.0646234720593	10.002633	3.991424	621.90	5.81
Zimbabwe Craton		2	OO	OO-76-5	10	21.1371007584247	15.9045718622618	45.9885860732242	10.40878	5.418228	-1213338	20.32
Zimbabwe Craton	Shamva Greenstone belt	2	Mazowe (Jumbo mine)	JM 1	11	14.146	15.007	33.905	11.17514	4.024159	2702.84	10.62
Zimbabwe Craton	Shamva Greenstone belt	2	Mazowe (Jumbo mine)	JM2	11	14.195	15.031	33.859	11.21284	3.896141	2.688323	10.53

South Africa	Limpopo sedimentary basins	Griqualand West Subbasin	3	Pering mine	PR6a	12	13.53	14.582	33.301	9.164551	3.952193	2725.305	4.05
	Limpopo sedimentary basins	Griqualand West Subbasin	3	Pering mine	PR12	12	13.43	14.537	33.236	9.160954	4.005460	2770.792	4.01
	Limpopo sedimentary basins	Griqualand West Subbasin	3	Pering mine	PR13	12	13.534	14.675	33.627	10.47614	4.547399	2868.505	5.54
	Limpopo sedimentary basins	Griqualand West Subbasin	3	Bushy Park	PR10	12	13.815	14.667	33.464	8.804968	3.772988	2538.14	7.81
	Limpopo sedimentary basins	Griqualand West Subbasin	3	Bushy Park	PR11	12	13.878	14.669	33.472	8.592793	3.690336	2471.49	10.24
	Limpopo sedimentary basins	Griqualand West Subbasin	3	Bushy Park	PR14	12	14.3	14.98	34.13	10.17051	4.09923	2517.88	4.07
	Limpopo sedimentary basins	Griqualand West Subbasin	3	Banghoek		12	14.18	14.78	33.43	8.680561	3.260099	2332.06	9.80
	Limpopo sedimentary basins	Griqualand West Subbasin	3	Geelbek Dam		12	13.59	14.81	34.01	12.372283	5.142531	3002.04	14.83

	Limpopo sedimentary basins	Griqualand West Subbasin	3	Kalkfontein		12	14.03	14.88	33.9	10.22503	4.157160	2639.48	4.28
	Limpopo sedimentary basins	Griqualand West Subbasin	3	Langrug		12	14.2	14.88	33.9	9.534453	3.902981	2468.82	10.87
	Limpopo sedimentary basins	Griqualand West Subbasin	3	Balloch		12	14.15	14.96	34.13	10.58639	4.319373	2634.36	6.80
S.A.	Limpopo fold belt	Limpopo Belt	3	Parfuri Nickel Prospect	OVB 37	13	16.37	15.64	38.18	10.89317	5.601187	1737.73	12.21
	Limpopo fold belt	Limpopo Belt	3	Campbell Mine	OVB 36. 67	13	18.58	16.34	41.46	12.77774	5.649915	1224.79	31.6
	Limpopo fold belt	Limpopo Belt	3	Campbell Mine	OVB 35	13	17.38	15.93	38.8	11.54430	5.050142	1437.71	19.6
	Limpopo fold belt	Limpopo Belt	3	Messina	OVB 41	13	17.36	15.85	39.23	11.14713	5.322549	1344.07	16.56
	Limpopo fold belt	Limpopo Belt	3	Messina	OVB 44	13	17.63	16.11	41.73	12.29323	6.71716	1505.79	25.11
	Limpopo fold belt	Limpopo Belt	3	Messina	OVB 54	13	18.6	16.47	40.13	13.41313	4.949460	1341.31	34.47
	Limpopo fold belt	Limpopo Belt	3	Messina	OVB 55	13	18.78	16.38	41.57	12.85212	5.54553	1159.83	32.87
S.A.	Limpopo sedimentary basins	Transvaal subbasin	3	Buffelshoek	PR8a	14	14.778	15.048	34.156	9.413699	3.549769	2173.31	2.40

Limpopo sedimentary basins	Transvaal subbasin	3	Buffelshoek	PR15	14	14.78	15.072	34.316	9.594577	3.736233	2207.14	6.20
Limpopo sedimentary basins	Transvaal subbasin	3	Buffelshoek	BK1	14	14.77	14.978	33.955	8.913459	3.311387	2072.81	8.00
Limpopo sedimentary basins	Transvaal subbasin	3	Buffelshoek	BK2	14	14.843	15.048	34.124	9.282082	3.443937	2114.58	3.83
Limpopo sedimentary basins	Transvaal subbasin	3	Kafferskraal		14	14.53	15.17	34.55	11.25249	4.363608	2564.95	11.2
Limpopo sedimentary basins	Transvaal subbasin	3	Witkop		14	15	15.17	34.48	9.874504	3.698338	2156.18	2.01
Limpopo sedimentary basins	Transvaal subbasin	3	Strydfontein		14	14.72	15.38	34.97	12.77189	4.659157	2661.74	18.7
Limpopo sedimentary basins	Transvaal subbasin	3	Bokkraal		14	15.03	15.28	34.72	10.67436	3.951606	2282.28	8.40
Limpopo sedimentary basins	Transvaal subbasin	3	Doornhoek		14	15.19	15.5	35.28	12.15611	4.411522	2429.62	17.20

Limpopo sedimentary basins	Transvaal subbasin	3	Rhenosterhoek	PR1	14	14.809	15.029	34.1	9.208784	3.447912	2116.39	4.60
Limpopo sedimentary basins	Transvaal subbasin	3	Rhenosterhoek	PR2	14	14.831	15.027	34.04	9.152240	3.357125	2093.31	5.26
Limpopo sedimentary basins	Transvaal subbasin	3		PR16	14	14.303	14.835	33.91	8.821604	3.761873	2295.72	8.36
Limpopo sedimentary basins	Transvaal subbasin	3	Doornrandje	PR9D	14	14.411	14.858	33.801	8.566884	3.623357	2187.52	11.6
Limpopo sedimentary basins	Transvaal subbasin	3	Broederstroom		14	15.11	15.33	34.84	10.88682	4.001124	2282.43	9.97
Limpopo sedimentary basins	Transvaal subbasin	3	Knoppieslaagte		14	14.66	15.1	34.25	10.12829	3.808894	2354.89	3.98
Limpopo sedimentary basins	Transvaal subbasin	3	Leeuwenkloof		14	14.92	15.06	34.21	9.224907	3.461717	2063.68	4.52
Limpopo sedimentary basins	Transvaal subbasin	3	Western Deep Levels	PR5a	14	14.818	15.05	34.043	9.346210	3.39777	2140.17	3.13

Limpopo sedimentary basins	Transvaal subbasin	3	Western Deep Levels	PR14	14	14.884	15.161	34.367	10.06058	3.699650	2243.42	3.57
Limpopo sedimentary basins	Transvaal subbasin	3	Elandsfontein	MY546	14	14.961	15.083	34.145	9.314228	3.355509	2062.19	3.56
Limpopo sedimentary basins	Transvaal subbasin	3	Elandsfontein	MY547	14	14.778	15.016	33.963	9.173771	3.322021	2124.73	4.96
Limpopo sedimentary basins	Transvaal subbasin	3	Leeuwbosch	PR3	14	15.096	15.237	34.783	10.1862	3.932261	2169.15	4.72
Limpopo sedimentary basins	Transvaal subbasin	3	Leeuwbosch	PR7	14	15.144	15.295	34.943	10.52472	4.060806	2208.52	7.47
Limpopo sedimentary basins	Transvaal subbasin	3	Vogelstruisdraai		14	15.14	15.42	35.21	11.57812	4.378382	2372.24	14.18
Limpopo sedimentary basins	Transvaal subbasin	3	Genadendal		14	16.14	15.96	36.76	13.50893	4.813434	2269.58	2.53
Limpopo sedimentary basins	Transvaal subbasin	3	Spitzkop		14	16.93	15.73	36.4	10.85298	3.758998	1469.18	13.0

	Limpopo sedimentary basins	Transvaal subbasin	3	Boschkop		14	16.2	15.8	36.23	12.16910	4.271014	2053.46	1..98
	Limpopo sedimentary basins	Transvaal subbasin	3	Hendrina	PR4a	14	17.236	15.629	36.791	10.14363	3.76907	1108.05	6.42
	Limpopo sedimentary basins	Transvaal subbasin	3	Groenvlei		14	16.28	15.91	36.39	12.281228	4.351358	2124.50	2.30
S.A.	Kaapvaal Craton	Murchison Greenstone Belt	4	Malati Pump Mine	Pyr 2 Aut	15	13.117	14.346	32.905	8.50267	3.917630	2840.58	9.61
	Kaapvaal Craton	Murchison Greenstone Belt	4	Malati Pump Mine	Pyr 2 ter Aut	15	16.504	15.089	36.083	8.036913	3.674783	714.90	3.11
	Kaapvaal Craton	Murchison Greenstone Belt	4	Malati Pump Mine	Pyr 3 TV	15	14.163	14.56	34.623	7.055392	4.819807	1952.17	3.68
	Kaapvaal Craton	Murchison Greenstone Belt	4	Malati Pump Mine	Pyr 2 bis	15	14.961	14.776	36.238	7.420811	5.470928	1532.05	3.50
	Kaapvaal Craton	Murchison Greenstone Belt	4	Malati Pump Mine	Pyr 1	15	16.846	15.165	37.638	8.208203	4.308713	555.11	2.88

Namaqualand Complex	Namaqualand Complex	4	Prieska	31	16	16.697	15.53	36.472	9.994027	3.941505	1346.34	4.14
Namaqualand Complex	Namaqualand Complex	4	Prieska	32	16	16.697	15.526	36.456	9.973757	3.98754	1340.28	3.90
Namaqualand Complex	Namaqualand Complex	4	Prieska	43	16	16.701	15.528	36.491	9.981065	3.951370	1340.37	3.99
Namaqualand Complex	Namaqualand Complex	4	Prieska	42	16	16.691	15.524	36.483	9.967858	3.952744	1341.66	3.84
Namaqualand Complex	Namaqualand Complex	4	Aggenys	1	16	16.839	15.648	36.882	10.489499	4.150254	1417.70	9.62
Namaqualand Complex	Namaqualand Complex	4	Aggenys	44	16	16.81	15.636	36.858	10.45497	4.15447	1421.10	9.18
Namaqualand Complex	Namaqualand Complex	4	Aggenys	33	16	16.771	15.561	36.603	10.09883	3.983406	1338.10	5.40
Namaqualand Complex	Namaqualand Complex	4	Aggenys	34	16	16.773	15.566	36.607	10.12275	3.98605	1345.04	5.67
Namaqualand Complex	Namaqualand Complex	4	Aggenys	3	16	16.728	15.566	36.631	10.15523	4.041030	1377.70	5.98
Namaqualand Complex	Namaqualand Complex	4	Aggenys	2	16	16.758	15.622	36.784	10.42253	4.142034	1437.83	8.78
Namaqualand Complex	Namaqualand Complex	4	Aggenys	7	16	16.736	15.581	36.656	10.222641	4.05657	1394.07	6.75
Namaqualand Complex	Namaqualand Complex	4	Aggenys	5	16	16.744	15.577	36.657	11.24325	4.102388	1649.03	15.68
Namaqualand Complex	Namaqualand Complex	4	Aggenys	6	16	16.789	15.638	36.878	10.48184	4.187455	1438.73	9.41

Namaqualand Complex	Namaqualand Complex	4	Aggenys	8	16	16.743	15.601	36.693	10.32465	4.083189	1418.25	7.78
Namaqualand Complex	Namaqualand Complex	4	Aggenys	10	16	16.765	15.569	36.63	10.14369	4.010061	1355.35	5.89
Namaqualand Complex	Namaqualand Complex	4	Aggenys	46	16	16.755	15.565	36.633	10.13050	4.019425	1356.61	5.74
Namaqualand Complex	Namaqualand Complex	4	Aggenys	4	16	16.77	15.617	36.804	10.38703	4.144649	1422.11	8.45
Namaqualand Complex	Namaqualand Complex	4	Aggenys	25	16	16.75	15.575	36.659	10.18519	4.04523	1375.10	6.33
Namaqualand Complex	Namaqualand Complex	4	Aggenys	26	16	16.739	15.582	36.676	9.954736	4.052910	1312.40	3.71
Namaqualand Complex	Namaqualand Complex	4	Aggenys	81	16	16.703	15.575	36.643	10.22036	4.0736267	1409.09	6.65
Namaqualand Complex	Namaqualand Complex	4	Aggenys	82	16	16.709	15.578	36.648	10.23133	4.072994	1409.16	6.77
Namaqualand Complex	Namaqualand Complex	4	Gamsberg	30	17	16.779	15.584	36.676	10.21006	4.035637	1367.48	6.63
Namaqualand Complex	Namaqualand Complex	4	Gamsberg	24	17	16.781	15.554	36.58	10.05656	3.95667	1321.17	4.93
Namaqualand Complex	Namaqualand Complex	4	Gamsberg	29	17	16.768	15.567	36.613	10.13138	3.994795	1315.02	5.76
Namaqualand Complex	Namaqualand Complex	4	Gamsberg	40	17	16.768	15.568	36.66	10.013646	4.028762	1315.66	5.82
Namaqualand Complex	Namaqualand Complex	4	Gamsberg	39	17	16.809	15.598	36.746	10.25978	4.064483	1366.65	7.20

	Namaqualand Complex	Namaqualand Complex	4	Gamsberg	89	17	16.847	15.633	36.845	10.41130	4.112904	1390.50	8.81
	Namaqualand Complex	Namaqualand Complex	4	Gamsberg	90	17	16.838	15.63	36.791	10.40257	4.081339	1392.54	8.71
	Namaqualand Complex	Namaqualand Complex	4	Rozynenbosch	20	17	16.955	15.547	36.614	9.911266	3.839128	1183.19	3.33
	Namaqualand Complex	Namaqualand Complex	4	Rozynenbosch	21	17	16.947	15.535	36.559	9.858219	3.803986	1170.16	2.65
	Namaqualand Complex	Namaqualand Complex	4	Rozynenbosch	17	17	17.009	15.604	36.801	10.15531	3.941519	1232.04	6.30
	Namaqualand Complex	Namaqualand Complex	4	O'Okiep	85	17	17.193	15.609	37.97	10.07256	4.572841	1107.66	5.52
	Namaqualand Complex	Namaqualand Complex	4	O'Okiep	86	17	17.199	15.618	37.979	10.11180	4.576490	1117.40	6.00
	Namaqualand Complex	Namaqualand Complex	4	Haib Copper Prospect	78	17	15.167	15.285	35.008	10.39728	4.099022	2176.19	6.52
South Africa	Gariep Belt	Gariep Belt	5	Rosh Pinah	13	18	17.126	15.593	37.377	10.03356	9.119435	1130.87	4.98
	Gariep Belt	Gariep Belt	5	Rosh Pinah	14	18	17.165	15.59	37.403	9.998127	4.215921	1097.97	4.57
	Gariep Belt	Gariep Belt	5	Rosh Pinah	15	18	17.174	15.602	37.421	10.04982	4.22197	1110.36	5.22
	Gariep Belt	Gariep Belt	5	Rosh Pinah	16	18	17.13	15.595	37.37	10.04083	4.224689	1131.12	5.07

Gariep Belt	Gariep Belt	5	Rosh Pinah	53	18	17.131	15.589	37.386	10.01184	4.232625	1120.10	4.72
Gariep Belt	Gariep Belt	5	Rosh Pinah	54	18	17.145	15.603	37.433	10.07049	4.256669	1132.80	5.45
Gariep Belt	Gariep Belt	5	Rosh Pinah	55	18	17.134	15.623	37.5	10.1722	4.317008	1171.59	6.64
Gariep Belt	Gariep Belt	5	Rosh Pinah	56	18	17.166	15.601	37.452	10.04945	4.251067	1145.55	5.21
Gariep Belt	Gariep Belt	5	Rosh Pinah	57	18	17.209	15.61	37.494	10.06866	4.245874	1097.73	5.49
Gariep Belt	Gariep Belt	5	Rosh Pinah	58	18	17.132	15.6	34.42	10.06348	2.256565	1137.75	5.35
Gariep Belt	Gariep Belt	5	Rosh Pinah Mine	RP1	18	17.174	15.60976	37.45704	10.08651	4.250520	1122.49	5.67
Gariep Belt	Gariep Belt	5	Rosh Pinah Mine	RP2	18	17.18453	15.61861	37.48084	10.12265	4.260294	1128.70	6.12
Phalaborwa Complex	Phalaborwa Complex	5	Phalaborwa	Pal4	19	18.7553922666584	16.0257822237858	38.2761149082536	11.26151	3.739425	694.33	2.20
Phalaborwa Complex	Phalaborwa Complex	5	Phalaborwa	Pal122-4a	19	18.3398842962588	15.9624849954497	38.2409595957965	11.14408	3.963802	865.80	1.95
Phalaborwa Complex	Phalaborwa Complex	5	Phalaborwa	Pal122-5b	19	19.7628740022702	16.2878766274264	39.8842198335347	12.04657	4.001996	466.28	3.31

	Phalaborwa Complex	Phalaborwa Complex	5	Phalaborwa	Pal1225a	19	22.8962000536751	16.6255939771729	45.5890337096511	12.83675	4.567910	-8529	6.29
	Rooiberg Complex	Rooiberg	5	Rooiberg Blaauwbank	BBD M1	20	17.3863289687386	15.5712190098468	38.6768857102014	9.805048	4.83977	963.55	2.13
	Rooiberg Complex	Rooiberg	5	Rooiberg Vellefontein	VEL M1	20	15.46471529595	15.310004994402	35.4852994727907	10.03166	4.242188	1969.09	3.68
	Rooiberg Complex	Rooiberg	5	Rooiberg Blaauwbank	BBD M3	20	17.7581983953984	15.6184447878812	39.2954122086591	9.865800	4.899952	714.90	3.21
South Africa	Kaapvaal Craton	Witwatersrand sequence	6	Durban Roodepoort Deep Central Rand	42		26.478	19.56	34.82	23.72378	9.892687	902.68	8.58
	Kaapvaal Craton	Witwatersrand sequence	6	Free State Geduld Mines	25	21	12.503	14.095	32.3	11.46665	3.816473	331.10	9.48
	Kaapvaal Craton	Witwatersrand sequence	6	Free State Geduld Mines	25	21	17.8	15.52	37.48	9.437598	3.761828	506.48	3.89
	Kaapvaal Craton	Witwatersrand sequence	6	Free State Geduld Mines	1	21	33.21	19.02	35.44	20.64478	7.024487	-2056480	19.05
	Kaapvaal Craton	Witwatersrand sequence	6	Free State Geduld Mines	2	21	16.369	15.216	36.02	8.664889	3.785429	1080.96	1.56

Kaapvaal Craton	Witwatersrand sequence	6	Free State Geduld Mines	2	21	17.453	15.546	37.27	9.665597	3.890799	814.35	8.63
Kaapvaal Craton	Witwatersrand sequence	6	Free State Geduld Mines	202f	21	15.38	15.02	34.93	8.370481	3.713559	1587.81	1.76
Kaapvaal Craton	Witwatersrand sequence	6	Free State Geduld Mines	302	21	23.042	16.424	33.91	12.11696	8.704438	-1369398	5.99
Kaapvaal Craton	Witwatersrand sequence	6	Free State Geduld Mines	123	21	14.396	14.684	32.82	7.520405	2.230383	1936.93	2.85
Kaapvaal Craton	Witwatersrand sequence	6	Free State Geduld Mines	3.1	21	27.339	19.062	34.34	21.35856	7.930736	2386.23	9.90
Kaapvaal Craton	Witwatersrand sequence	6	Free State Geduld Mines	3.2	21	29.81	19.43	34.77	22.33900	7.610265	-258549	12.02
Kaapvaal Craton	Witwatersrand sequence	6	Free State Geduld Mines	3.4	21	26.27	18.96	34.31	21.21691	8.517361	514.10	8.98
Kaapvaal Craton	Witwatersrand sequence	6	Free State Geduld Mines	3.6	21	28.52	19.21	34.44	21.70496	7.526671	-2899265	10.93
Kaapvaal Craton	Witwatersrand sequence	6	St. Helena Gold Mine	74	22	29.5	19.2	36.8	21.5207	1.188195	-3769956	12.11
Kaapvaal Craton	Witwatersrand sequence	6	St. Helena Gold Mine	75	22	22.7	18	34.8	18.38118	1.307066	990.70	6.66
Kaapvaal Craton	Witwatersrand sequence	6	St. Helena Gold Mine	St.H.2	22	34.8	22	35.3	3.135632	7.040538	276.30	1.23

Kaapvaal Craton	Witwatersrand sequence	6	St. Helena Gold Mine	St.H.4	22	31.7	20.8	35.1	27.28471	7.715437	278.22	1.51
Kaapvaal Craton	Witwatersrand sequence	6	St. Helena Gold Mine	St.H.70	22	18	16.3	34.2	12.99673	1.882038	1509.64	3.00
Kaapvaal Craton	Witwatersrand sequence	6	Dominion Reefs Gold Mine	D-1	23	22.21	18.17	37.77	19.47722	2.479874	1319.38	6.31
Kaapvaal Craton	Witwatersrand sequence	6	Dominion Reefs Gold Mine	D-2	23	23.48	18.71	37.87	21.32221	2.255154	1268.07	6.97
Kaapvaal Craton	Witwatersrand sequence	6	Dominion Reefs Gold Mine	D-3	23	25.02	19.27	37.79	23.10849	1.973182	1153.90	7.71
Kaapvaal Craton	Witwatersrand sequence	6	Dominion Reefs Gold Mine	D-4	23	25.58	19.5	37.73	26.92672	2.472483	2042.15	6.20
Kaapvaal Craton	Witwatersrand sequence	6	Dominion Reefs Gold Mine	D-5	23	24.94	19.43	38.31	23.93720	2.150752	1283.90	7.56
Kaapvaal Craton	Witwatersrand sequence	6	Dominion Reefs Gold Mine	D-5a	23	21.13	17.67	36.36	17.70604	2.171237	1337.14	5.65
Kaapvaal Craton	Witwatersrand sequence	6	Dominion Reefs Gold Mine	D-6	23	21.03	17.46	35.84	16.73268	1.964848	1923.35	5.53
Kaapvaal Craton	Witwatersrand sequence	6	Dominion Reefs Gold Mine	D-7	23	21.32	17.75	36.44	17.97741	2.162269	1327.03	5.77
Kaapvaal Craton	Witwatersrand sequence	6	Dominion Reefs Gold Mine	D-9	23	25.78	19.44	37.31	23.50239	1.728688	1033.32	8.15
Kaapvaal Craton	Witwatersrand sequence	6	Dominion Reefs Gold Mine	D-10	23	25.95	19.63	38.02	24.30136	1.909320	1108.10	8.12
Kaapvaal Craton	Witwatersrand sequence	6	Dominion Reefs Gold Mine	D-11	23	15.53	15.56	34.4	11.73723	3.204525	2244.40	1.60

	Kaapvaal Craton	Witwatersrand sequence	6	Dominion Reefs Gold Mine	D-12	23	18.12	16.55	34.84	14.28218	2.246835	1711.12	3.52
South Africa	Kaapvaal Craton	Witwatersrand sequence	6	Afrikander Lesses Mine	D-13	23	33.42	22.38	37.17	3.335403	1.101597	791.50	1.07
	Kaapvaal Craton	Witwatersrand sequence	6	Vaal Reef	105	23	16.88	15.97	33.55	12.27028	1.80563	1805.50	2.24
	Kaapvaal Craton	Witwatersrand sequence	6	West Driefontein Gold Mine	106	23	19.31	16.56	34.01	13.41330	1.459944	1803.11	3.80
	Kaapvaal Craton	Witwatersrand sequence	6	Stilfontein Gold Mine	163	23	23.32	18.21	36.23	19.04864	1.708480	934.90	7.05
	Kaapvaal Craton	Witwatersrand sequence	6	Stilfontein Gold Mine	164	23	19.72	16.96	34.96	15.10537	1.856175	1309.69	4.52
	Kaapvaal Craton	Witwatersrand sequence	6	Stilfontein Gold Mine	165	23	21.05	17.31	35.36	16.1227	1.752024	1039.93	5.47
	Kaapvaal Craton	Witwatersrand sequence	6	Lorraine Gold Mine	166	23	14.84	15.31	33.9	11.50981	3.2552681	2478.17	13.2
	Kaapvaal Craton	Witwatersrand sequence	6	South Roodepoort	G-1	23	16.39	15.4	32.21	9.552775	9.000505	1376.47	1.31
	Kaapvaal Craton	Witwatersrand sequence	6	Sub-Nigel Gold Mine	G-2	23	29.9	18.8	38.8	20.03824	1.525197	-97619	13.65
	Kaapvaal Craton	Witwatersrand sequence	6	East Geduld Gold Mine	G-3	23	18.35	16.34	34.48	12.93076	1.936680	1355.74	3.12
	Kaapvaal Craton	Witwatersrand sequence	6	Vaal Reef	30	23	15.853	15.246	33.98	9.176998	2.530612	1558.11	6.06

Kaapvaal Craton	Witwatersrand sequence	6	Vaal Reef	30	23	22.875	17.014	36.63	14.26105	1.8108812	-1974394	6.70
Kaapvaal Craton	Witwatersrand sequence	6	East Champ D'Or Gold Mine	33	23	14.53	14.92	33.02	8.964803	2.419036	2207.86	7.05
Kaapvaal Craton	Witwatersrand sequence	6	East Champ D'Or Gold Mine	34	23	14.35	14.7	32.18	7.70082	1.454804	2015.68	2.48
Kaapvaal Craton	Witwatersrand sequence	6	East Champ D'Or Gold Mine	35	23	14.2	14.8	32.54	8.798548	2.035790	2343.95	8.46
Kaapvaal Craton	Witwatersrand sequence	6	South Roodepoort	36	23	19.94	16.92	33.48	14.77194	1.119344	1161.02	4.58
Kaapvaal Craton	Witwatersrand sequence	6	Consolidated Main Reef Mine	43	23	17.14	15.81	33.11	11.10540	1.400868	1435.86	1.56
Kaapvaal Craton	Witwatersrand sequence	6	Van Dyk Consoolidated Mine	66	23	15.01	15.13	34.31	9.560235	3.495316	2089.46	9.91
Kaapvaal Craton	Witwatersrand sequence	6	Van Dyk Consoolidated Mine	67	23	14.95	15.2	34.75	10.21772	4.055962	2241.09	4.90
Kaapvaal Craton	Witwatersrand sequence	6	Government Gold Mine	73a	23	24.7	18.5	35	19.77933	1.158084	672.90	8.00
Kaapvaal Craton	Witwatersrand sequence	6	Government Gold Mine	73b	23	24.2	18.4	34.7	19.52811	11.15995	769.09	7.65

Kaapvaal Craton	Barberton Greenstone Belt	7	Rosetta		24	12.522	14.126	32.35	12.28448	3.923997	3338.77	12.72
Kaapvaal Craton	Barberton Greenstone Belt	7	Rosetta		24	12.527	14.119	32.41	13.91577	4.199	3319.73	1.83
Kaapvaal Craton	Barberton Greenstone Belt	7	Amo		24	12.794	14.357	32.67	13.6524	4.098	3299.20	1.79
Kaapvaal Craton	Barberton Greenstone Belt	7	Amo		24	12.805	14.345	32.64	13.8604	3.7905	3315.19	7.75
Kaapvaal Craton	Barberton Greenstone Belt	7	Gypsy Queen		24	12.796	14.348	32.54	11.12790	3.791647	3075.68	8.67
Kaapvaal Craton	Barberton Greenstone Belt	7	Eagles Nest	B6	24	13.125	14.488	32.83	9.415291	2.742053	2304.40	2.28
Kaapvaal Craton	Barberton Greenstone Belt	7	Eagles Nest	EN	24	14.508	14.969	33.26	7.553944	2.727955	1638.10	3.12
Kaapvaal Craton	Barberton Greenstone Belt	7	Sheba Queen	29B	24	14.873	14.786	33.56	7.529871	2.6657228	1698.19	3.10

Kaapvaal Craton	Barberton Greenstone Belt	7	Sheba Queen	29B*	24	14.77	14.763	33.43	9.059461	3.772639	838.54	9.80
Kaapvaal Craton	Barberton Greenstone Belt	7	Sheba Queen	29B*	24	17.01	15.368	36.66	9.023435	3.331986	2822.83	5.11
Kaapvaal Craton	Barberton Greenstone Belt	7	Sheba Queen	SG29	24	13.281	14.458	32.75	7.836287	2.917701	1838.10	2.42
Kaapvaal Craton	Barberton Greenstone Belt	7	Sheba Queen	SG29	24	14.7	14.8	33.59	7.74787	4.078916	2473.92	2.03
Kaapvaal Craton	Barberton Greenstone Belt	7	Ivanhoe	B24	24	13.59	14.48	33.46	7.747871	4.079816	2473.91	2.03
Kaapvaal Craton	Barberton Greenstone Belt	7	Ivanhoe	B24	24	13.026	14.298	32.91	8.467556	4.111904	2.878617	9.98
Kaapvaal Craton	Barberton Greenstone Belt	7	Daisy	7	24	16.77	15.45	37.01	9.552789	4.239901	1165.95	1.42
Kaapvaal Craton	Barberton Greenstone Belt	7	Daisy	8	24	14.251	14.88	33.87	9.416406	3.793498	2426.34	2.88

Kaapvaal Craton	Barberton Greenstone Belt	7	Daisy	8	24	14.228	14.878	34.12	9.472621	4.161816	2446.15	4.28
Kaapvaal Craton	Barberton Greenstone Belt	7	Daisy	8	24	16.16	15.257	36.49	9.003761	4.362054	1329.93	9.44
Kaapvaal Craton	Barberton Greenstone Belt	7	Comstock	B7	24	12.746	14.147	32.51	8.622481	3.778842	3028.6	7.31
Kaapvaal Craton	Barberton Greenstone Belt	7	Contractors	SG97	24	13.312	14.472	33.06	9.136362	3.882349	2821.76	1.89
Kaapvaal Craton	Barberton Greenstone Belt	7	Middle Marker	B17	24	13.576	14.746	33.43	11.421784	4.147435	2935.94	1.27
Kaapvaal Craton	Barberton Greenstone Belt	7	Middle Marker	B17	24	15.561	15.194	35.94	9.195677	4.521933	1722.21	9.16
Kaapvaal Craton	Barberton Greenstone Belt	7	Consort Bar	C3	24	13.62	14.4	32.74	7.013954	2.809627	2298.72	1.4
Kaapvaal Craton	Barberton Greenstone Belt	7	Agnes	B20	24	13.597	14.644	32.94	9.68614	3.241956	2758.98	2.80

Kaapvaal Craton	Barberton Greenstone Belt	7	Rochfort	SG86	24	12.762	14.319	32.61	13.658101	4.059545	3319.36	7.94
Kaapvaal Craton	Barberton Greenstone Belt	7	Unity	SG27	24	14.01	14.673	33.08	8.28255781	2.941885	2344.98	4.65
Kaapvaal Craton	Barberton Greenstone Belt	7	Rosetta		24	12.58	14.18	32.59	13.4137369836207	4.47744298927608	3362.38	1.46
Kaapvaal Craton	Barberton Greenstone Belt	7	Daylight		24	12.62	14.21	32.77	13.4209695775989	4.87093162501692	3351.21	1.26
Kaapvaal Craton	Barberton Greenstone Belt	7	Consort Bar		24	12.52	14.22	32.86	20.8596722800862	5.51140729701017	3533.75	3.73
Kaapvaal Craton	Barberton Greenstone Belt	7	French Bobs		24	12.51	14.21	32.89	20.6810966733454	5.63888752401975	3532.20	3.71
Kaapvaal Craton	Barberton Greenstone Belt	7	Alfstrom		24	12.78	14.49	33.25	27.0637146585045	5.72554431886862	3559.45	4.75
Kaapvaal Craton	Barberton Greenstone Belt	7	Amo		24	13.03	14.55	33	15.3695929482868	4.39728880878179	3307.74	6.71

Kaapvaal Craton	Barberton Greenstone Belt	7	Mica	24	13.12	14.53	32.01	12.5037065582759	2.071027	3161.05	7.06
Kaapvaal Craton	Barberton Greenstone Belt	7	Swaziland	24	13.55	14.73	33.45	11.3812152852821	4.225933	2942.01	1.44
Kaapvaal Craton	Barberton Greenstone Belt	7	Swaziland	24	14.03	15.1	33.6	13.4600317459824	3.778579	2938.07	1.33
Kaapvaal Craton	Barberton Greenstone Belt	7	Fairview	24	14.44	15.01	33.53	10.0181639425118	3.156478	2434.83	3.50
Kaapvaal Craton	Barberton Greenstone Belt	7	Rosetta	24	12.636	14.264	32.774	15.9253480024132	4.852017	3420.10	8.80
Kaapvaal Craton	Barberton Greenstone Belt	7	Daylight	24	12.544	14.217	32.678	18.199926	4.873798	3487.80	2.44
Kaapvaal Craton	Barberton Greenstone Belt	7	French Bobs	24	12.559	14.226	32.711	17.868996	4.920883	3478.72	2.23
Kaapvaal Craton	Barberton Greenstone Belt	7	Alfstrom	24	12.681	14.324	32.846	17.73022	4.926256	3450.22	1.70

Kaapvaal Craton	Barberton Greenstone Belt	7	Mica		24	13.032	14.419	33.006	11.004486	4.359477	3101.00	2.60
Kaapvaal Craton	Murchison Greenstone Belt	8	Old Star	OS1	25	12.233	13.891	32.28	12.043556	4.599828	3420.85	8.51
Kaapvaal Craton	Murchison Greenstone Belt	8	Old Star	OS2	25	12.228	13.877	32.23	11.373499	4.427653	3399.46	2.46
Kaapvaal Craton	Murchison Greenstone Belt	8	Old Star	OS3	25	12.196	13.814	32.05	9.270496	3.843025	3318.35	7.83
Kaapvaal Craton	Murchison Greenstone Belt	8	Old Star	OS3'	25	12.2	13.824	32.08	9.604943	3.947024	3334.14	9.30
Kaapvaal Craton	Murchison Greenstone Belt	8	Monarch East	M7	25	13.63	14.43	33.19	7.241533	3.547107	2345.44	4.71
Kaapvaal Craton	Murchison Greenstone Belt	8	Monarch East	M7	25	13.78	14.54	33.53	7.775503	3.891361	2371.03	8.70
Kaapvaal Craton	Murchison Greenstone Belt	8	Monarch East	M7	25	17.33	15.38	36.71	9.003707	3.575149	609.59	1.20

Kaapvaal Craton	Murchison Greenstone Belt	8	Monarch East	M7*	25	13.805	14.458	33.25	7.03957077412758	3.391806	2185.28	4.10
Kaapvaal Craton	Murchison Greenstone Belt	8	Monarch East	M7*	25	14.415	14.602	34.15	7.026022	3.841289	1769.87	1.65
Kaapvaal Craton	Murchison Greenstone Belt	8	Letaba	Le6	25	12.676	14.115	32.58	8.814576	4.1346453	3078.27	1.76
Kaapvaal Craton	Murchison Greenstone Belt	8	Letaba	Le2	25	12.668	14.072	32.45	7.982274	3.788478	3002.20	4.52
Kaapvaal Craton	Murchison Greenstone Belt	8	Letaba	Le4	25	12.668	14.067	32.47	7.883128	3.840124	2991.51	3.7
Kaapvaal Craton	Murchison Greenstone Belt	8	Letaba	Le4	25	12.707	14.103	32.54	8.168688	3.9382098	3002.26	4.52
Kaapvaal Craton	Murchison Greenstone Belt	8	Romotshidi	RML-06	25	12.625	14.071	32.64	8.491792	4.427464	3074.10	1.61
Kaapvaal Craton	Murchison Greenstone Belt	8	Romotshidi	RML-09	25	12.63	14.071	32.61	8.424249	4.429405	3065.00	1.40

Kaapvaal Craton	Murchison Greenstone Belt	8	Romotshidi	RMA-033	25	13.025	14.186	32.703	7.145557	3.621559	2680 .09	1.73
Kaapvaal Craton	Murchison Greenstone Belt	8	Romotshidi	RMB-030	25	12.949	14.192	32.67	7.573987	3.722617	2803 .12	7.80
Kaapvaal Craton	Murchison Greenstone Belt	8	Maranda J	MJA-049	25	12.883	14.07	32.607	6.374430	3.662738	2642 .17	1.01
Kaapvaal Craton	Murchison Greenstone Belt	8	Maranda J	MJL-21	25	12.932	14.223	32.661	8.176469	3.740228	2891 .77	5.13
Kaapvaal Craton	Murchison Greenstone Belt	8	Maranda J	MJL-27	25	13.023	14.334	32.69	9.287950	3.650617	2970 .84	2.32
Kaapvaal Craton	Murchison Greenstone Belt	8	Maranda J	MJL-28	25	12.881	14.151	32.606	7.446811	3.69826	2823 .17	1.22
Kaapvaal Craton	Murchison Greenstone Belt	8	Maranda J	MJL-32	25	13.045	14.284	32.614	8.252477	3.433643	2845 .21	1.90
Kaapvaal Craton	Murchison Greenstone Belt	8	Mon Desir	MMD-3-4	25	13.002	14.222	32.83	7.646575	3.964144	2800 .02	5.08

Kaapvaal Craton	Murchison Greenstone Belt	8	Mon Desir	MMD-3-6	25	12.984	14.209	32.817	7.581733	3.971173	2788.04	5.15
Kaapvaal Craton	Murchison Greenstone Belt	8	Mon Desir	MMD-9-5	25	13.067	14.328	33.124	8.776568	4.494866	2895.21	5.50
Kaapvaal Craton	Murchison Greenstone Belt	8	Solomons	MSOL-1-60	25	13.181	14.36	33.023	8.413946	4.034226	2796.80	6.60
Kaapvaal Craton	Murchison Greenstone Belt	8	Solomons	MSOL-3-14	25	13.206	14.494	33.166	10.441680	4.31938055110295	2996.55	4.01
Kaapvaal Craton	Murchison Greenstone Belt	8	Solomons	MSOL-1-50	25	13.155	14.334	32.961	8.228707	3.952601	2783.19	4.98
Kaapvaal Craton	Murchison Greenstone Belt	8	Solomons	MSOL-5-22	25	13.156	14.308	32.893	7.862474	3.801284	2801.55	3.56
Kaapvaal Craton	Murchison Greenstone Belt	8	LCZ	MPL-2-19	25	13.008	14.223	32.832	7.621850	3.955367	2778.69	4.36
Kaapvaal Craton	Murchison Greenstone Belt	8	LCZ	MPL-2-15	25	13.107	14.281	32.92	7.795852	3.94930602372138	2750.13	2.21

	Kaapvaal Craton	Murchison Greenstone Belt	8	LCZ	LCZ-12	25	12.603	14.099	32.229	9.569566	3.35330714671009	3168.40	7.96
	Kaapvaal Craton	Murchison Greenstone Belt	8	LCZ	LCZ-14	25	12.607	14.09	32.214	9.253782	3.298614	3144.35	5.30
Zambia	Damaran-Lufilian fold belt	Zambezi Belt	9	Nampundwe	151	26	19.335	15.738	38.862	9.977218	3.605374	-2169973	6.65
	Damaran-Lufilian fold belt	Zambezi Belt	9	Nampundwe	327/A	26	18.841	15.689	38.972	9.871113	3.934273	510.83	4.11
	Damaran-Lufilian fold belt	Zambezi Belt	9	Nampundwe	141	26	19.12	15.717	38.869	9.939475	3.723994	-9995989	5.49
	Damaran-Lufilian fold belt	Zambezi Belt	9	Nampundwe	17	26	17.893	15.689	37.852	10.12115	3.968446	737.88	6.97
	Damaran-Lufilian fold belt	Zambezi Belt	9	Nampundwe	247	26	18.155	15.7	37.617	10.8018	3.662371	570.31	6.75
	Damaran-Lufilian fold belt	Damaran-Lufilian Fold Belt	9	Kabwe	880/72	27	17.992	15.707	38.393	10.16321	4.214952	697.93	7.68

Damaran-Lufilian fold belt	Damaran-Lufilian Fold Belt	9	Kabwe	910/12	27	17.978	15.688	38.329	10.08687	4.182270	675.76	6.61
Damaran-Lufilian fold belt	Damaran-Lufilian Fold Belt	9	Kabwe	910cd13	27	17.983	15.694	38.338	10.011075	4.185746	682.38	6.95
Damaran-Lufilian fold belt	Damaran-Lufilian Fold Belt	9	Kabwe	910cd14	27	18	15.719	38.428	10.021186	4.233060	712.36	8.33
Damaran-Lufilian fold belt	Damaran-Lufilian Fold Belt	9	Kabwe	910/1	27	18.006	15.726	38.453	10.23981	4.24523	719.80	8.72
Damaran-Lufilian fold belt	Damaran-Lufilian Fold Belt	9	Kabwe	910/2	27	18.007	15.728	38.458	10.24805	4.24805	722.40	8.83
Damaran-Lufilian fold belt	Damaran-Lufilian Fold Belt	9	Kabwe	910/5	27	18.003	15.723	38.441	10.22789	4.239603	716.90	8.56
Damaran-Lufilian fold belt	Damaran-Lufilian Fold Belt	9	Kabwe	302	27	18.003	15.72	38.433	10.21332	4.230302	708.41	8.37
Damaran-Lufilian fold belt	Damaran-Lufilian Fold Belt	9	Kabwe	312	27	18.008	15.723	38.448	10.22620	4.239884	713.40	8.54

	Damaran-Lufilian fold belt	Damaran-Lufilian Fold Belt		Kabwe	313	27	18.007	15.723	38.441	10.22656	4.236623	714.10	8.54
	Damaran-Lufilian fold belt	Damaran-Lufilian Fold Belt		Kabwe	315	27	17.983	15.692	38.343	10.01022	4.187943	679.15	6.83
DRC	Damaran-Lufilian fold belt	Kundelungu Plateau	Group 10	Kikonkula	03/08-Da	28	18.264	15.722	38.782	10.13902	4.238410	513.11	7.75
	Damaran-Lufilian fold belt	Kundelungu Plateau	10	Kikonkula	06/99	28	18.314	15.734	38.862	10.17412	4.250053	516.58	8.33
	Damaran-Lufilian fold belt	Kundelungu Plateau	10	Kibila	03/05-Da	28	19.987	15.86	39.566	10.34612	3.607775	-4422707	14.87
	Damaran-Lufilian fold belt	Kundelungu Plateau	10	Kibila	06/111	28	21.047	15.858	38.347	10.20105	2.666998	-1261814	16.52
	Damaran-Lufilian fold belt	Kundelungu Plateau	10	Luemba	03/09-Da	28	21.917	15.901	38.33	10.36146	2.385724	-1865584	23.00
	Damaran-Lufilian fold belt	Kundelungu Plateau	10	Mwitapile	03/27-Da	28	26.901	16.261	45.207	13.62942	3.045928	-2919066	13.07

Damaran-Lufilian fold belt	Kundelungu Plateau	10	Dikulushi mine	03/13-Da	28	18.269	15.711	38.633	10.09199	4.149561	508.26	7.07
Damaran-Lufilian fold belt	Kundelungu Plateau	10	Dikulushi mine	03/16	28	18.07	15.685	38.33	9.629779	4.080036	424.66	5.33
Damaran-Lufilian fold belt	Kundelungu Plateau	10	Dikulushi mine	03/40-Da	28	18.268	15.702	38.602	10.05512	4.130251	493.10	6.53
Damaran-Lufilian fold belt	Kundelungu Plateau	10	Dikulushi mine	06/122	28	18.215	15.698	38.551	10.05387	4.138500	523.96	6.44
Damaran-Lufilian fold belt	Kundelungu Plateau	10	Dikulushi mine	06/123	28	18.36	15.712	38.764	10.07068	4.156653	450.31	6.88
Damaran-Lufilian fold belt	Kundelungu Plateau	10	Dikulushi mine	06/124	28	18.356	15.712	38.779	10.07177	4.167544	448.10	6.89
Damaran-Lufilian fold belt	Kundelungu Plateau	10	Dikulushi mine	06/125	28	18.352	15.711	38.777	10.06876	4.168942	448.97	6.84
Damaran-Lufilian fold belt	Kundelungu Plateau	10	Dikulushi mine	03/16-Da	28	18.144	15.701	38.424	10.08776	4.119756	579.99	6.84

Damaran-Lufilian fold belt	Kundelungu Plateau	10	Dikulushi mine	06/89	28	18.489	15.728	38.855	10.10195	4.120982	381.52	7.54
Damaran-Lufilian fold belt	Kundelungu Plateau	10	Dikulushi mine	06/122	28	18.391	15.72	38.855	10.09502	4.186446	437.16	7.29
Damaran-Lufilian fold belt	Kundelungu Plateau	10	Dikulushi mine	03/11-Da	28	18.98	15.729	38.795	10.00023	3.775516	278.02	6.58
Damaran-Lufilian fold belt	Kundelungu Plateau	10	Dikulushi mine	04/03	28	21.334	15.872	39.094	10.28496	2.833587	-1458204	18.42
Damaran-Lufilian fold belt	Kundelungu Plateau	10	Dikulushi mine	04/05	28	21.684	15.897	39.377	10.35616	2.810093	-1679239	21.69
Damaran-Lufilian fold belt	Kundelungu Plateau	10	Dikulushi mine	04/12	28	22.832	15.994	40.012	10.65252	2.651093	-2376860	36.34
Damaran-Lufilian fold belt	Kundelungu Plateau	10	Dikulushi mine	04/55	28	18.821	15.726	38.792	10.001886	3.870395	138.25	6.68
Damaran-Lufilian fold belt	Kundelungu Plateau	10	Dikulushi mine	04/63	28	18.657	15.723	38.759	10.04181	3.957126	251.56	6.84

Damaran-Lufilian fold belt	Kundelungu Plateau	10	Dikulushi mine	06/11	28	19.124	15.734	38.837	9.994559	3.681353	-683005	6.67
Damaran-Lufilian fold belt	Kundelungu Plateau	10	Dikulushi mine	06/12	28	18.894	15.744	38.772	10.07465	3.821485	119.80	7.72
Damaran-Lufilian fold belt	Kundelungu Plateau	10	Dikulushi mine	06/025	28	23.652	16.024	40.174	10.73967	2.456195	-303713	4.65
Damaran-Lufilian fold belt	Kundelungu Plateau	10	Dikulushi mine	06/025/2	28	22.418	15.945	39.936	10.49652	2.748082	-216662	2.93
Damaran-Lufilian fold belt	Kundelungu Plateau	10	Dikulushi mine	06/69	28	21.722	15.896	39.172	10.35127	2.727209	-171412	2.17
Damaran-Lufilian fold belt	Kundelungu Plateau	10	Dikulushi mine	06/084	28	18.783	15.725	38.568	10.02266	3.78143	163.99	6.70
Damaran-Lufilian fold belt	Kundelungu Plateau	10	Dikulushi mine	06/103	28	19.947	15.795	39.007	10.11253	3.369237	-554756	10.39
Damaran-Lufilian fold belt	Kundelungu Plateau	10	Dikulushi mine	06/104	28	18.803	15.723	38.691	10.01075	3.830089	145.59	6.52

	Damaran-Lufilian fold belt	Kundelungu Plateau	10	Dikulushi mine	06/131	28	19.217	15.767	38.947	10.10510	3.721740	-702754	8.79
DRC	Damaran-Lufilian fold belt	Damaran-Lufilian Fold Belt	Group 11	Kipushi	K1	29	18.01	15.6	37.9	9.70780	3.885465	497.21	8.17
	Damaran-Lufilian fold belt	Damaran-Lufilian Fold Belt	11	Kipushi	K2	29	18.05	15.6	37.92	9.696566	3.869314	467.52	6.32
	Damaran-Lufilian fold belt	Damaran-Lufilian Fold Belt	11	Kipushi	K3	29	18.1	15.61	38.01	9.723846	3.888944	448.91	1.11
	Damaran-Lufilian fold belt	Damaran-Lufilian Fold Belt	11	Kipushi	k3	29	18.076	15.636	37.678	9.837586	3.727685	514.06	2.98
	Damaran-Lufilian fold belt	Damaran-Lufilian Fold Belt	11	Kipushi	k4	29	18.018	15.635	37.666	9.850600	3.758826	554.64	3.15
	Damaran-Lufilian fold belt	Damaran-Lufilian Fold Belt	11	Kipushi	k5	29	18.032	15.625	37.648	9.804856	3.736212	526.45	2.43
	Damaran-Lufilian fold belt	Damaran-Lufilian Fold Belt	11	Kipushi	KI 1270/128	29	18.008	15.634	37.692	6.045070	1.244770	379.85	4.99

Damaran-Lufilian fold belt	Damaran-Lufilian Fold Belt	11	Kipushi	KI 1270/135	29	18.011	15.638	37.688	9.865241	3.776918	565.09	3.37
Damaran-Lufilian fold belt	Damaran-Lufilian Fold Belt	11	Kipushi	KI 787/12	29	18.017	15.63	37.667	9.830077	3.758478	546.43	2.82
Damaran-Lufilian fold belt	Damaran-Lufilian Fold Belt	11	Kipushi	KI 787/13	29	18.038	15.637	37.711	9.852920	3.771647	543.62	3.19
Damaran-Lufilian fold belt	Damaran-Lufilian Fold Belt	11	Kipushi	KI 787/14	29	17.989	15.646	37.775	9.905558	3.843087	595.23	3.98
Damaran-Lufilian fold belt	Damaran-Lufilian Fold Belt	11	Kipushi	KI 787/17	29	17.987	15.64	37.734	9.881014	3.819867	586.10	3.60
Damaran-Lufilian fold belt	Damaran-Lufilian Fold Belt	11	Kipushi	1132/11/U+36/-80/SE 3	29	17.905	15.496	37.252	9.311054	3.552419	379.62	6.42
Damaran-Lufilian fold belt	Damaran-Lufilian Fold Belt	11	Kipushi	1132/19/-80/SE 184	29	18.017	15.628	37.654	9.821756	9.821756	542.84	2.69
Damaran-Lufilian fold belt	Damaran-Lufilian Fold Belt	11	Kipushi	1150/19/22 30	29	18.096	15.718	37.963	10.17472	3.900329	643.68	7.99

Damaran-Lufilian fold belt	Damaran-Lufilian Fold Belt	11	Kipushi	1243/15/HZ /NW 90 30	29	17.964	15.582	37.533	9.646648	3.702133	498.32	2.29
Damaran-Lufilian fold belt	Damaran-Lufilian Fold Belt	11	Kipushi	1132/2/-75/SE I	29	17.721	15.584	37.462	9.731273	3.826884	682.17	1.14
Damaran-Lufilian fold belt	Damaran-Lufilian Fold Belt	11	Kipushi	992/D7/03 sphal	29	17.99	15.581	37.519	9.635185	3.676759	477.05	4.30
Damaran-Lufilian fold belt	Damaran-Lufilian Fold Belt	11	Kipushi	KH 1200 sphal	29	17.977	15.594	37.611	9.692491	3.741789	510.70	5.53
Damaran-Lufilian fold belt	Damaran-Lufilian Fold Belt	11	Kipushi	KH 600	29	17.97	15.564	37.463	9.953744	3.681203	626.65	4.69
Damaran-Lufilian fold belt	Damaran-Lufilian Fold Belt	11	Kipushi	1132/2/-75/SE 1	29	17.985	15.656	37.849	9.781399	3.748044	544.74	2.02
Damaran-Lufilian fold belt	Damaran-Lufilian Fold Belt	11	Kipushi	1132/[11/U +36/-80/SE 3	29	18.001	15.616	37.619	9.776642	3.806701	532.97	1.95
Damaran-Lufilian fold belt	Damaran-Lufilian Fold Belt	11	Kipushi	1132/11/-80/187 30	29	18.1	15.61	37.741	9.723846	3.738908	489.91	1.10

Damaran-Lufilian fold belt	Damaran-Lufilian Fold Belt	11	Kipushi	1132/11/-80/SE 187 30	29	18.176	15.634	37.885	9.801451	3.760178	437.07	2.44
Damaran-Lufilian fold belt	Damaran-Lufilian Fold Belt	11	Kipushi	1132/13/V-80/SE/100 90	29	18.221	15.643	37.961	9.826180	3.791942	420.57	2.88
Damaran-Lufilian fold belt	Damaran-Lufilian Fold Belt	11	Kipushi	1132/13/V-80/SE/226 90	29	18.187	15.653	37.944	9.876243	3.808194	463.74	3.67
Damaran-Lufilian fold belt	Damaran-Lufilian Fold Belt	11	Kipushi	1132/9/183 70	29	18.165	15.652	37.906	9.878245	3.801391	477.97	3.69
Damaran-Lufilian fold belt	Damaran-Lufilian Fold Belt	11	Kipushi	1130/19/I80 7	29	18.011	15.31	37.581	8.560864	3.601637	-1090 893	2.59
Damaran-Lufilian fold belt	Damaran-Lufilian Fold Belt	11	Kipushi	1150/19/28 52	29	18.006	15.596	37.533	9.692443	3.679016	492.83	5.56
Damaran-Lufilian fold belt	Damaran-Lufilian Fold Belt	11	Kipushi	1243/15/HZ /NW 90 30	29	18	15.618	37.641	9.785245	3.751214	537.32	2.95
Damaran-Lufilian fold belt	Damaran-Lufilian Fold Belt	11	Kipushi	15/HA/NW/ 128 90	29	18.013	15.611	37.594	9.75240	3.713737	515.07	1.56

Damaran-Lufilian fold belt	Damaran-Lufilian Fold Belt	11	Kipushi	3283	29	18.021	15.61	37.575	9.745950	3.697419	507.35	1.46
Damaran-Lufilian fold belt	Damaran-Lufilian Fold Belt	11	Kipushi	KH 600	29	18.176	15.651	37.893	9.871074	3.786641	468.13	3.58
Damaran-Lufilian fold belt	Damaran-Lufilian Fold Belt	11	Kipushi	1005/4	29	18.012	15.596	37.512	9.690744	3.663221	488.38	5.28
Damaran-Lufilian fold belt	Damaran-Lufilian Fold Belt	11	Kipushi	KH70	29	18.01	15.604	37.54	9.724320	3.682902	504.53	1.09
Damaran-Lufilian fold belt	Damaran-Lufilian Fold Belt	11	Kipushi	KM11	29	17.988	15.569	37.388	9.586478	3.599954	456.18	1.29
Damaran-Lufilian fold belt	Damaran-Lufilian Fold Belt	11	Kipushi	992/D7/19	29	17.981	15.572	37.402	9.600709	3.613343	467.04	1.03
Damaran-Lufilian fold belt	Damaran-Lufilian Fold Belt	11	Kipushi	1150/MA8	29	18.004	15.635	37.752	9.854851	3.817030	564.85	3.21
Damaran-Lufilian fold belt	Damaran-Lufilian Fold Belt	11	Kipushi	925/MA4	29	17.994	15.628	37.392	9.828680	3.616656	559.67	2.78

DRC	Damaran-Lufilian fold belt	Zambia copperbelt	12	Musoshi ore deposit	350W-1240[BB]-L3	30	20.153	15.818	44.309	10.17536	5.467840	-6.592417	1.21
	Damaran-Lufilian fold belt	Zambia copperbelt	12	Musoshi ore deposit	350W-1240[BB]-R	30	18.63	15.724	40.64	10.05189	4.943411	272.92	6.96
	Damaran-Lufilian fold belt	Zambia copperbelt	12	Musoshi ore deposit	350W-1240[MM]-T	30	23.639	16.016	52.598	10.703827	5.795467	-3065,424	5.76
	Damaran-Lufilian fold belt	Zambia copperbelt	12	Musoshi ore deposit	350W-1240[MM]-L1	30	24.523	16.084	54.789	10.9207918108591	5.829187	-3690,89	5.79
	Damaran-Lufilian fold belt	Zambia copperbelt	12	Musoshi ore deposit	350W-1240[MM]-L2	30	24.35	16.063	53.515	10.852623	5.598943	-3598,32	6.76
	Damaran-Lufilian fold belt	Zambia copperbelt	12	Musoshi ore deposit	350W-1240[MM]-L3	30	27.569	16.303	61.088	11.629176	5.454574	-6277,82	14.56
	Damaran-Lufilian fold belt	Zambia copperbelt	12	Musoshi ore deposit	350W-1240[MM]-R	30	23.507	16.02	51.809	10.728783	5.675367	-2922,81	21.4
	Damaran-Lufilian fold belt	Zambia copperbelt	12	Musoshi ore deposit	350W-1229[R]-T	30	20.382	15.802	43.925	10.29354	5.121539	-876,99	12.23

	Damaran-Lufilian fold belt	Zambia copperbelt	12	Musoshi ore deposit	350W-1229[R]--L1	30	20.749	15.819	44.402	10.127359	5.155186	-1126,47	6.44
	Damaran-Lufilian fold belt	Zambia copperbelt	12	Musoshi ore deposit	350W-1229[R]-L2	30	21.47	15.866	46.02	10.2530784	5.183172	-1592,07	22.4
	Damaran-Lufilian fold belt	Zambia copperbelt	12	Musoshi ore deposit	350W-1229[R]-L3	30	21.657	15.914	47.222	10.409621	5.482895	-1613,54	2.53
	Damaran-Lufilian fold belt	Zambia copperbelt	12	Musoshi ore deposit	350W-1229[R]-R	30	19.948	15.81	43.197	10.162439	5.1469667	-524,79	3.29
	Damaran-Lufilian fold belt	Zambia copperbelt	12	Musoshi ore deposit	350W-1243[S]-T	30	21.91	15.896	46.374	10.338069	5.017366	-1880,32	4.28
	Damaran-Lufilian fold belt	Zambia copperbelt	12	Musoshi ore deposit	350W-1243[S]-L3	30	22.227	15.931	47.448	10.446792	5.1797732	-2049,54	14.11
	Damaran-Lufilian fold belt	Zambia copperbelt	12	Musoshi ore deposit	350W-1243[S]-R	30	22.07	15.924	47.195	10.427811	5.197568	-1934,53	6.45
Namibia	Damaran-Lufilian fold belt	Damaran-Lufilian Fold Belt	13	Tsumeb	TSU5	31	18.110432	15.69752427	38.34844464	10.081635	4.100136	596.95	1.51

Damaran-Lufilian fold belt	Damaran-Lufilian Fold Belt	13	Tsumeb	TSU7	31	18.1100709	15.68932621	38.3225401	10.047607	4.083152	583.09	1.94
Damaran-Lufilian fold belt	Damaran-Lufilian Fold Belt	13	Tsumeb	Tsu1	31	18.139457209064	15.661835028589	38.2951923638365	9.935147	4.037931	513.82	5.96
Damaran-Lufilian fold belt	Damaran-Lufilian Fold Belt	13	Tsumeb	Tsu4	31	18.1607960489616	15.6638295842404	38.3410900148504	9.935113	4.0491029	501.89	7.11
Damaran-Lufilian fold belt	Damaran-Lufilian Fold Belt	13	Tsumeb	Tsu19	31	18.0995386298696	15.6635798894474	38.2559546391207	9.945097	4.044728	545.8	3.64
Damaran-Lufilian fold belt	Damaran-Lufilian Fold Belt	13	Tsumeb	Tsu16	31	18.048168235874	15.664317287569	38.226728288766	9.962835	4.065013	584.19	1.9
Damaran-Lufilian fold belt	Damaran-Lufilian Fold Belt	13	Tsumeb	28/T1	31	18.104	15.669	38.257	9.965162	4.043972	552.09	3.28
Damaran-Lufilian fold belt	Damaran-Lufilian Fold Belt	13	Tsumeb	28/T2	31	18.094	15.671	38.248	9.976472	4.046655	562.8	2.75
Damaran-Lufilian fold belt	Damaran-Lufilian Fold Belt	13	Tsumeb	28/T3	31	18.144	15.688	38.345	10.131697	4.071214	556.51	3.05

	Damaran-Lufilian fold belt	Damaran-Lufilian Fold Belt	13	Tsumeb	28/T4	31	18.104	15.667	38.255	9.956892	4.0421851	548.59	3.47
Botswana	Limpopo sedimentary basins	Bushman District	14	Mapanipani North	B-89-57	32	17.61	15.75	37.43	10.510448	3.936449	1031.05	1.25
	Limpopo sedimentary basins	Bushman District	14	Mapanipani North	B-89-59	32	17.46	15.71	37.11	10.402277	3.834031	1074.15	4.22
	Limpopo sedimentary basins	Bushman District	14	Mapanipani North	B-89-60	32	17.71	15.84	37.73	10.875375	4.072542	1096.26	12.2
	Limpopo sedimentary basins	Bushman District	14	Mapanipani North	B-89-62	32	17.76	15.83	37.6	10.8029771857011	3.954848	1048.40	7.50
	Limpopo sedimentary basins	Bushman District	14	Mapanipani North	B-89-63	32	17.55	15.72	37.33	10.4026658914967	3.909548	1027.91	6.96
	Limpopo sedimentary basins	Bushman District	14	Mapanipani North	B-90-25	32	18.39	15.76	37.38	10.2558063550176	3.408076	507.10	6.23
	Limpopo sedimentary basins	Bushman District	14	Mapanipani North	B-90-54	32	17.36	15.67	36.86	10.268836528651	3.735542	1083.20	6.74

Limpopo sedimentary basins	Bushman District	14	Mapanipani North	B-90-46	32	18.82	15.75	37.15	10.1098120075721	3.057574	183.07	2.31
Limpopo sedimentary basins	Bushman District	14	Mapanipani North	B-90-48	32	18.44	15.73	37.64	10.1198336246872	3.509504	418.80	2.16
Limpopo sedimentary basins	Bushman District	14	Mapanipani North	B-90-80	32	18.57	15.77	38.13	10.2473762100219	3.701588	397.46	2.80
Limpopo sedimentary basins	Bushman District	14	Bushman	B-89-61	32	17.81	15.84	37.75	10.8238666707527	4.011979	1029.69	10.31
Limpopo sedimentary basins	Bushman District	14	Bushman	B-90-62	32	18.2	15.74	37.92	10.230529714539	3.813490	605.88	12.78
Limpopo sedimentary basins	Matsitama Belt	14	Dihudi	BCL 3142	33	14.78	15.16	34.56	10.345555	4.040489	2337.01	3.81
Limpopo sedimentary basins	Matsitama Belt	14	Dihudi	BCL 3143	33	14.77	15.15	34.53	10.287277	4.015686	2332.05	3.36
Limpopo sedimentary basins	Matsitama Belt	14	Dihudi	BCL 3144	33	14.86	15.24	34.67	10.816367	4.088309	2375.19	9.56

	Limpopo sedimentary basins	Matsitama Belt	14	Dihudi	BCL 3145	33	14.77	15.15	34.43	10.287276	3.900704	2333.1	3.36
	Limpopo sedimentary basins	Matsitama Belt	14	Thakadu	BCL 3134	33	14.82	15.26	34.67	11.122029	4.143439	2434.77	3.43
	Limpopo sedimentary basins	Matsitama Belt	14	Thakadu	BCL 3135	33	14.98	15.26	34.73	10.657521	4.015743	2300.78	1.45
	Limpopo sedimentary basins	Matsitama Belt	14	Thakadu	BCL 3136	33	14.96	15.25	34.75	10.626028	4.058557	2304.27	1.60
	Limpopo sedimentary basins	Matsitama Belt	14	Thakadu	BCL 3137	33	14.84	15.23	34.71	10.786374	4.155616	2379.02	10.40
	Limpopo fold belt	Limpopo Belt	14	Magogophate	OVB 131	33	17.77	15.74	39.18	10.390888	4.866447	905.45	9.5
	Limpopo fold belt	Limpopo Belt	14	Torome	BCL 134	33	14.62	15.18	34.53	11.039763	4.217909	2503.13	12.20
South Africa	Limpopo sedimentary basins	Johannesburg area	15		GGMA73a	34	24.7	18.5	35	19.691367	1.157101	654.90	4.76
	Limpopo sedimentary basins	Johannesburg area	15		GGMA73b	34	24.2	18.4	34.7	19.44176	1.115086	751.89	3.89

	Limpopo sedimentary basins	Sabie area	15	Olifantsgeraamte		34	15.19	15.04	34.45	8.717598	8.71759712085554	1797.34	3.44
	Limpopo sedimentary basins	Sudwala Area	15	Rietvallei		34	17.18	15.38	35.65	9.054799	9.05479801229198	728.93	3.01
	Limpopo sedimentary basins	Sudwala Area	15	Sudwalaskraal		34	16.08	15.27	35.01	9.1284109	9.12841087115654	1416.41	3.25
DRC	Damaran-Lufilian fold belt	Damaran-Lufilian Fold Belt	16	Kolwezi	MA8	35	18.034	15.617	37.664	9.77153	3.741419	511.00	6.25
	Damaran-Lufilian fold belt	Damaran-Lufilian Fold Belt	16	Kolwezi	KZI2	35	18.59	15.704	38.077	9.979257	3.64145	263.52	1.13
	Damaran-Lufilian fold belt	Damaran-Lufilian Fold Belt	16	Kolwezi	KZI1	35	19.207	15.779	38.39	10.148547	3.468486	-4121,44	1.15
	Damaran-Lufilian fold belt	Damaran-Lufilian Fold Belt	16	Lombe	Lo8	35	18.059	15.593	37.504	9.666499	3.627549	448.50	1.49
	Damaran-Lufilian fold belt	Damaran-Lufilian Fold Belt	16	Lombe	Lo 28 b2	35	18.626	15.619	37.793	9.64042	3.447342	720.01	5.41

Damaran-Lufilian fold belt	Damaran-Lufilian Fold Belt	16	Lombe	Lo 38 sphal	35	18.044	15.612	37.703	9.748162	3.755208	494.25	7.93
Damaran-Lufilian fold belt	Damaran-Lufilian Fold Belt	16	Kengere	Ke 22 sphal	35	18.017	15.62	37.71	9.788824	3.779684	528.57	4.77
Damaran-Lufilian fold belt	Damaran-Lufilian Fold Belt	16	Kengere	Ke 9 sphal	35	18.052	15.591	37.511	9.660274	3.635337	449.86	1.46
Damaran-Lufilian fold belt	Damaran-Lufilian Fold Belt	16	Kinsenda	Maz 22 cpy	35	17.796	15.337	36.583	8.711552	3.185224	140.80	3.24
Damaran-Lufilian fold belt	Damaran-Lufilian Fold Belt	16	Kinsenda	Maz 22 cpy + tm	35	17.642	15.637	37.849	9.990213	4.134509	830.24	9.17
Damaran-Lufilian fold belt	Damaran-Lufilian Fold Belt	16	Kinsenda	KINS 13	35	17.644	15.655	37.831	10.06832	4.127847	858.32	4.57